

Cracking Behavior of Reinforced Concrete Structures Subjected to Service Load: Experimental and Numerical Investigation

by

Chavin Nilanga Naotunna

Thesis submitted in fulfilment of
the requirements for the degree of
PHILOSOPHIAE DOCTOR
(PhD)



Faculty of Science and Technology
Department of Mechanical and Structural Engineering and Materials Science
2021

University of Stavanger

NO-4036 Stavanger

NORWAY

www.uis.no

©2021 Chavin Nilanga Naotunna

ISBN: 978-82-8439-029-1

ISSN: 1890-1387

PhD: Thesis UiS No. 606

Abstract

Cracks in reinforced concrete (RC) structures are controlled to enhance the service life, for a better aesthetic appearance, and to avoid leakages in liquid retaining structures. The most widely used crack controlling method at the structural design stage is to limit the calculated crack width to an allowable crack width limit. With an understanding of the economic and social benefits, there is a trend to build RC structures with a long service life. To enhance the durability of these structures, large concrete cover thicknesses are required to protect the embedded reinforcement from corrosion. These enhanced concrete cover thicknesses are larger than the limitations of existing crack width calculation models. From a literature survey and a parametric study conducted with the results from recent experiments in the literature, it can be identified that the existing crack width calculation models require improvement, to predict the crack widths in RC specimens with large concrete cover thicknesses.

The next objective is to study the different theoretical approaches discussed in the literature regarding the approaches to cracking and to identify the most relevant method for the actual cracking behavior in RC members subjected to service load. To achieve this objective, an experimental program was conducted to test large-scale RC specimens in axial tension. Then it was identified that the actual cracking behavior in RC members with ribbed reinforcement is more related to the 'no-slip approach' (perfect bond between reinforcement and concrete) than the classical bond-slip approach. This finding has been further confirmed with a literature survey focused on the previous experimental studies that measured the slip between the reinforcement-concrete interface.

After studying the 'no-slip approach', an experimental program was conducted to investigate the governing parameters for crack spacing. From the experimental program, it was identified that both concrete cover thickness and the clear distance between bars have an influence on

crack spacings and therefore on the crack widths in RC specimens. Then, with the results of the conducted experiments and the results of a series of calibrated 3D non-linear finite element method simulations, an improved crack spacing model was developed, to predict the crack spacings in RC members with multiple bars that are subjected to axial tension. The crack width variation along the large concrete cover thickness has been studied by means of an experimental program. From this study, it was found that the effect of shear lag has an influence on the surface crack widths of RC members. Based on the findings, an improved crack width calculation model has been proposed, and its predictions gave good agreement with the experimental results in recent literature.

Keywords: reinforced concrete, cracks, crack width, crack spacing, prediction models, durability, serviceability limit state, concrete cover thickness, reinforcement, axial tension, flexure, clear distance between bars, experiments, non-linear FEM, large-scale specimens.

Preface and Acknowledgements

This doctoral thesis is submitted as a partial requirement for the degree of Doctor of Philosophy (PhD) at the University of Stavanger (UiS), Norway. The research work has been carried out at the Department of Mechanical and Structural Engineering and Material Science, Faculty of Science and Technology, UiS, during the period from February 2018 to August 2021. During this period, the author also performed several duties in the department. The author was the lecturer in the ‘Concrete Structures’ subject during the spring semesters in 2020 and 2021, as well as supervising several Bachelor/Master theses during the contract period. The PhD project was mainly funded by the Norwegian Ministry of Education and Research. The laboratory experiments were funded by Statens Vegvesen via the Ferry free E39 project.

First and foremost, I would like to convey my gratitude to my main supervisor, Associate Professor Samindi Samarakoon, for the immense support, constant guidance and encouragement, and for sharing her enormous knowledge with me throughout the doctoral study. I am highly grateful to have her as my supervisor, and I should specially mention the support she has given my family and me during this period, even apart from the PhD-related works. I would also like to thank my co-supervisor, Professor Kjell Tore Fosså, for the continuous guidance and support and for sharing his immense knowledge and experience with me for the successful completion of the PhD.

I am very thankful to Professor R.M. Chandima Ratnayake for his valuable advice and support, given to me from the beginning to the end of my PhD period. Further, I would like to thank Professor Sudhira De Silva for the various advice and support given to me. Special thank goes to Mathias Eidem and Kjersti Dunham from the Statens Vegvesen Ferry Free E39 project for the financial support given to conduct the experiments. I would like to take this opportunity to thank Dr. Reignard

Tan in Multiconsult AS for the research-related discussions and for sharing his valuable experimental data with me. I am also grateful to the UiS laboratory staff, Mr. John C. Grønli, Mr. Samdar Kakay, Mr. Jarle Berge, Mr. Jørgen Grønsund, Mr. Emil Kristiansen, and Mrs. Caroline Einvik, for the variety of support provided during the laboratory experiments.

I would like to thank my father, Mr. Sunanda Naotunna, and my mother, Mrs. Kishanthi Naotunna, for the support and encouragement given to me throughout my whole life. I appreciate all the support and courage I received from my brother, Dulshan, sister, Chulandi, and my brother-in-law, Buddhika. Further, I would like to thank my current and previous colleagues, Dr. Jithin Jose, Dr. Ashish Aeran, Dr. Kiyam Parham, Mr. Nicolo Daniotti, Mr. Payam Zadeh, and Mr. Mostafa Atteya for the variety of support given to me during the PhD period.

Last, but not least, I would like to thank my wife, Pavithra, who experienced all the good and bad times with me during the past years. I always appreciate her patience and encouragement. Also, I would like to mention my two sons, Thejaka and Abeetha, for being a part of this journey.

List of Appended Papers

- Paper 1 Naotunna, C.N., Samarakoon, S.M.S.M.K., and Fosså, K.T. (2019). Comparison of the behavior of crack width governing parameters with existing models. *International Conference on Sustainable Materials, Systems and Structures (SMSS 2019)*. Rovinj: pp. 124-131, ISBN: 978-2-35158-226-8, ISSN: 1333-9095.
- Paper 2 Naotunna, C.N., Samarakoon, S.M.S.M.K., and Fosså, K.T. (2021). Applicability of existing crack controlling criteria for structures with large concrete cover thickness. *The Journal of Nordic Concrete Research*, pp. 69-91, DOI: 10.2478/ncr-2021-0002.
- Paper 3 Naotunna, C.N., Samarakoon, S.M.S.M.K., and Fosså, K.T. (2020). Experimental and theoretical behavior of crack spacing of specimens subjected to axial tension and bending. *The Journal of Structural Concrete*, pp. 775-791, DOI: 10.1002/suco.201900587.
- Paper 4 Naotunna, C.N., Samarakoon, S.M.S.M.K., and Fosså, K.T. (2020). Identification of the influence of concrete cover thickness and \emptyset/ρ parameter on crack spacing. *The 15th International Conference on Durability of Building Materials and Components (DBMC 2020)*. Barcelona: pp.1797-1804, ISBN: 978-84-121101-8-0.

- Paper 5 Naotunna, C.N., Samarakoon, S.M.S.M.K., and Fosså, K.T. (2021). Influence of concrete cover thickness and clear distance between tensile bars on crack spacing behavior: Experimental and numerical investigation. (Submitted to journal).
- Paper 6 Naotunna, C.N., Samarakoon, S.M.S.M.K., and Fosså, K.T. (2021). A new crack spacing model for reinforced concrete specimens with multiple bars subjected to axial tension using 3D non-linear FEM simulations. *The Journal of Structural Concrete* (Accepted to publish).
- Paper 7 Naotunna, C.N., Samarakoon, S.M.S.M.K., and Fosså, K.T. (2021). Experimental investigation of crack width variation along the concrete cover depth in reinforced concrete specimens with ribbed bars and smooth bars. *The Journal of Case Studies in Construction Materials*. DOI: 10.1016/j.cscm.2021.e00593.

List of Notations

a	Distance to the gradient changing point of the crack widths from the reinforcement surface
A_c	Sectional area
A_s	Reinforcement area
c	Concrete cover thickness
E_c	Young's modulus of concrete
E_s	Young's modulus of steel
f_{cm}	Mean compressive strength of concrete
f_{ct}	Tensile strength of concrete
f_{ctm}	Mean tensile strength of concrete
G_f	Tensile fracture energy of concrete
m_r	Mean value of the sample
s	Clear distance between tensile reinforcements
S_r	Standard deviation of the sample
$S_{r,max}$	Maximum crack spacing
$S_{r,mean}$	Mean crack spacing
w_k / w	Calculated crack width
ε_{ij}	Total strain tensor
ε_{ij}^e	Elastic strain component
ε_{ij}^f	Fracture strain component
ε_{ij}^p	Plastic strain component
F_k^f	Rankine failure criterion
\emptyset	Reinforcement diameter
α_e	Modular ratio
ε_{cm}	Mean concrete strain
ε_{sm}	Mean reinforcement strain
ρ	Effective reinforcement ratio

σ_s	Steel stress
σ_{sr}	Maximum steel stress at the crack formation stage
τ_m	Mean bond stress between reinforcement and concrete

Table of Contents

- Abstract i
- Preface and Acknowledgements iii
- List of Appended Papers v
- List of Notations vii
- Table of Contents ix
- Part I: Thesis Summary 1
- 1 Introduction 3
 - 1.1 General Overview 3
 - 1.2 Research Motivation 4
 - 1.3 Research Objectives 4
 - 1.4 Research Delimitations 5
 - 1.5 Outline of the Thesis 5
- 2 Research Methodology 7
 - 2.1 Part 1: Identification of the research question 7
 - 2.2 Part 2: Development of the research plan 8
- 3 Discussion and Conclusion 10
 - 3.1 The Work Seen in Context 10
 - 3.2 Overview of Appended Papers 10
- 4 Research Contributions 20
- 5 Suggestions for Future Research 22
- 6 References 24
- Part II: Papers 28
- Appendices 158

Part I: Thesis Summary

1 Introduction

1.1 General Overview

Crack controlling is one of the main serviceability limit state requirements when designing reinforced concrete (RC) structures. These cracks in concrete occur when the applied tensile stress in concrete exceeds the tensile strength of concrete (Leonhardt, 1988). Based on the applied tensile load on the RC structure, cracks can be classified into three categories: tensile stresses induced by service loads, imposed deformations, and environmentally induced loads. These cracks in reinforced concrete (RC) structures create many adverse effects on the durability, aesthetic appearance, and liquid or gas tightness of the structure (FIB, 2013). To mitigate these adverse effects, repairing the cracks in RC structures involves high costs (Makhlouf and Malhas, 1996). Therefore, it is preferable to control these cracks at the structural design stage.

The current method for controlling cracks at the structural design stage is to limit the calculated crack width to a prescribed allowable crack width limit. Both the crack width calculation models and the allowable crack width limits in codes of practice differ from region to region. Crack width calculation models are based on empirical, analytical or semi-analytical methods (Borosnyói and Balázs, 2005). Allowable crack width limits for the different exposure classes are based on the environmental conditions in the region such as airborne chloride content, freeze and thaw effect, etc. (West et al., 1999).

1.2 Research Motivation

Increasing the concrete cover thickness is a main measure taken to improve the durability of an RC structure. It has been identified experimentally that the crack width increases with the concrete cover thickness (Pérez Caldentey et al., 2013, Tan et al., 2018). Similarly, the crack width prediction models in codes of practice consider the same way that the crack width increases with the increase in concrete cover thickness (CEN, 2004, FIB, 2013). As a result, the measures taken to enhance the durability of an RC structure contradict each other. On the other hand, when limiting the crack widths of structures with larger concrete covers to the current allowable limits, it requires additional tensile reinforcement, resulting in an increase in construction cost.

According to the Norwegian Public Road Administration guidelines (Statens Vegvesen, 2009), the current requirement for concrete cover thickness, can be as high as 120 mm. However, the governing crack width calculation models in Europe have limitations for the concrete cover thickness parameter. For example, the crack width calculation model in Model Code 2010 limits its validity up to 75 mm of concrete cover thickness. This shows the necessity to improve the existing crack controlling criteria, especially for RC structures with large concrete cover thicknesses.

1.3 Research Objectives

The main objective is to identify a crack width calculation model to predict the cracks in RC members with large cover thickness. It is planned that this will be achieved through the following steps.

1. Investigation of the backgrounds of existing crack width calculation methods and crack width governing parameters. – Literature survey.

2. Identification of the actual cracking behavior of RC specimens subjected to service load. – Experimental investigation.

3. Investigation of the crack governing parameters, based on the identified cracking behavior. – Experimental and numerical investigation.

4. Proposal of new models to predict crack spacings and crack widths in RC specimens subjected to service load.

1.4 Research Delimitations

The work in this study is limited to those cracks which occur due to axial tensile and flexural loads. Cracks which occur due to other service loads, such as shear, torsion, vibration, and dynamic loads, are not focused on during this study.

Cracks which it is not possible to control at the structural design stage are not covered in this study. Those are the cracks which occur due to shrinkage, temperature variation, freeze and thaw, chemical reactions, sub grade settlement, formwork movement, etc.

To improve the allowable crack width limits to effectively control the cracks in RC members with large concrete cover thickness, the necessary future studies have been identified. This study has not focused on the allowable crack width limits of liquid retaining structures.

1.5 Outline of the Thesis

The thesis is written based on seven papers, five of which are journal papers (four have been accepted or published, and one has been submitted to a journal), and two have been published in conference proceedings. The thesis is divided into two main sections, with Section 1 consisting of a summary of the content of the aforementioned seven

papers in Section 2. Section 1 has been divided into six chapters, the first of which describes the overview, motivation, objectives and limitations of the conducted research. The second chapter of Section 1 describes the research methodologies used to conduct the studies of the papers in Section 2. The third chapter of Section 1 contains summaries of the appended papers. Chapters 4 and 5 of Section 1 discuss the research contributions and suggestions for future research, respectively. Section 2 consists of the seven papers which comprise the main findings of this research.

2 Research Methodology

The conducted research is divided into two main parts, as shown in Figure 1. In Part I, the research question is identified. In Part 2, a research plan is developed, to investigate the research question. The conducted research methods in each part are described in the sections below.

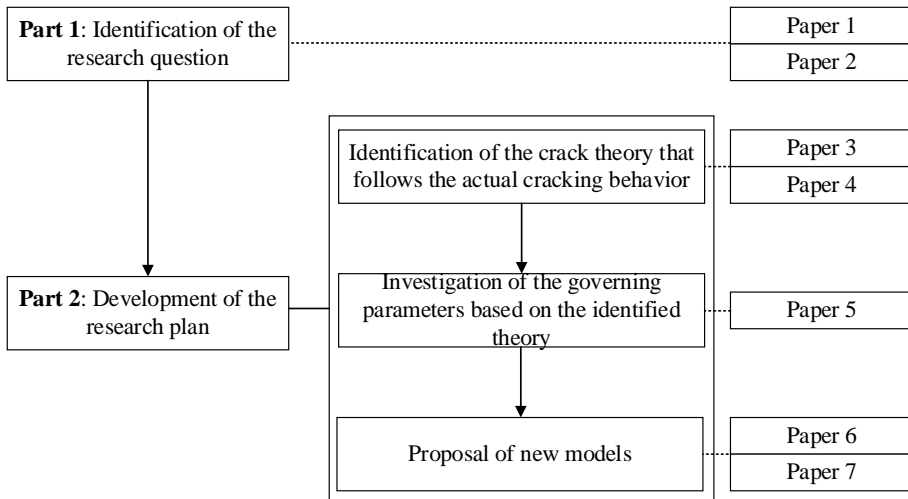


Figure 1 Research plan.

2.1 Part 1: Identification of the research question

Part 1 consists of the methods by which the research question was identified. Conducting a parametric study identified that the existing crack width calculation methods need to be improved to predict the crack widths of RC specimens with large cover thicknesses. Paper 1 illustrates the conducted parametric study and identified findings. Conducting an extensive literature survey identified the limitations of existing crack width controlling methods and the future research required to improve

the crack controlling criteria. Paper 2 discusses the identified findings related to the literature survey.

2.2 Part 2: Development of the research plan

After identifying the research question, the next task was to identify a research method to answer the research question. In science, the main research methods are considered to be quantitative, qualitative, and mixed methods (Eyisi, 2016). Qualitative methods are used to openly explore specific topics; the main research tools of this method are survey research, case studies, and so on. The quantitative method is mainly concerned with conducting experiments to investigate a specific hypothesis and identify the relationships between variables. According to this method, the research tools can be identified as statistical analysis of experimental measurements, numerical modeling, theoretical derivations, curve fitting, optimization techniques, and so on (Thiel, 2014). Therefore, among the aforementioned research methods, the quantitative research method has been selected.

There are several theories/approaches available to describe the cracking behavior in RC specimens. Such theories can be named as ‘bond-slip’ theory, ‘no-slip’ theory and ‘combined’ theory. The next objective was to investigate the cracking theory that is more related to the actual cracking behavior in RC specimens subjected to service load. An experimental program was conducted to examine this; it is presented in Paper 3. To further verify this identified cracking approach, a literature survey was carried out, and that study is reported in Paper 4.

Next, an experimental program was conducted to investigate the crack governing parameters in RC specimens, based on the identified crack theory. The details of this conducted experimental program are documented in Paper 5. From the results of the conducted experiments and the results from the calibrated numerical simulation model, a new

crack spacing model has been introduced. Several research tools like statistical analysis, optimization techniques, and so on were used to introduce this model. The details of this study are reported in Paper 6.

Finally, another experimental program was conducted to examine the crack width variation along the concrete cover thickness. After using several research tools, such as theoretical derivations, curve fitting, etc., a new crack width calculation model has been introduced. The details of this study are reported in Paper 7.

3 Discussion and Conclusion

3.1 The Work Seen in Context

Figure 1 in Chapter 2 shows the steps taken to reach the final objective of this research. The findings of each step are reported in five journal papers and two conference proceedings. The first two papers identify the research question and the possible measures that are necessary to improve the crack controlling criteria in RC members. Papers 3 and 4 illustrate how the cracking approach that can represent the actual cracking behavior in RC members was identified. Then, the crack governing parameters were experimentally distinguished, based on the identified approach; this study is reported in Paper 5. Papers 6 and 7 introduce improved crack spacing and crack width calculation models, which were the final objectives of this PhD study.

3.2 Overview of Appended Papers

3.2.1 Paper 1: Comparison of the behavior of crack width governing parameters with existing models

The main objective of the study mentioned in this paper is to investigate the research question. An investigation was carried out to identify the governing crack width calculation models in Europe, which are provided in Eurocode 2 (CEN, 2004) and Model Code 2010 (FIB, 2013). A literature survey was carried out to identify the physical behavior of crack governing parameters in the aforementioned two crack width calculation models. Next, a parametric study was conducted to compare the predicted behaviors of the two code models with the actual behavior. In order to do that, the results of the recent experimental programs in Tan et al. (2018) and Pérez Caldentey et al. (2013) were used. From this study, parameters like the ' σ/ρ ' ratio (the ratio of the bar diameter to the

effective steel area) were identified as having less influence on the cracking behavior. Further, these codes were seen to have limitations regarding parameters like concrete cover thickness (i.e., Model Code 2010 limits the concrete cover thickness to 75 mm). The current requirement of concrete cover thickness is above this limitation (Basteskår et al., 2019, Statens Vegvesen, 2009). Therefore, from this study, the necessity of improving the existing crack width calculation models could be seen.

3.2.2 Paper 2: Applicability of existing crack controlling criteria for structures with large concrete cover thickness

From Paper 1, it could be seen that the existing crack width calculation models required improvement. Therefore, this paper made a thorough investigation of the previous literature, to identify the theoretical background of the crack width calculation models. This investigation was conducted for the crack width calculation models in Eurocode 2 (EC2), Model Code 2010 (MC 2010), Japanese code (JSCE, 2007), American code (ACI, 1995) and British code (BS, 1985). It could be seen that both the empirically based models in American Concrete Institute (ACI) and British Standard (BS) codes used the results of RC specimens up to 84 mm and 89 mm cover thicknesses, respectively, to develop their models (Gergely and Lutz, 1968, Beeby, 1970). Based on a study comparing the experimental results with the model predictions, it has been found that the EC2 model predictions are more conservative, and both ACI and BS code model predictions demonstrated good agreement with the experimental crack widths of the specimens with concrete cover thickness above 60 mm.

Crack widths increase with the increase in concrete cover thickness. Consequently, when the crack widths of RC specimens with large cover thickness are limited to existing limits, additional tensile reinforcement is required to limit the crack widths. Therefore, an extensive literature

survey was carried out to investigate the backgrounds of the existing allowable crack width limits. Considering the durability aspect, from the long-term results of the study conducted by Schiessl (1975b), it can be seen that the allowable crack width limits can be increased with the increase in concrete cover thickness, similar to the Japanese code guidelines. When considering the aesthetic aspect, the authors suggest categorizing the structures based on their prestige level and deciding the allowable crack widths accordingly. The paper proposes potential solutions for future research on how to improve both crack width calculation methods and allowable crack width limits to be used effectively in structures with large cover thickness.

3.2.3 Paper 3: Experimental and theoretical behavior of crack spacing of specimens subjected to axial tension and bending

After thorough investigation of the research question, the next objective was to identify the actual cracking behavior of RC specimens. There are three main cracking theories/approaches, named ‘bond-slip’, ‘no-slip’ and ‘combined’ theory. Concrete cover thickness is the governing parameter in the ‘no-slip’ theory (Broms, 1965), while the bond (σ/ρ) is the governing parameter according to the slip theory (Saliger, 1936), and both concrete cover thickness and bond are the governing parameters for the combined theory (Borges, 1965). The stochastic nature of the cracking behavior in RC specimens causes several disagreements among researchers regarding the effect of certain parameters (Beeby et al., 2005). Therefore, an experimental program was planned to obtain a large sample of data to investigate the crack spacing behavior. This paper describes the details and the identified findings of this experimental study.

The experimental specimens were tested in both axial tension and bending. The tested RC specimens were relatively large in size and reinforced with larger bar diameters (ϕ 32 mm). Since a large sample size

of data was obtained, the mean and average crack spacing values were obtained after statistical analysis. The obtained test results and those from similar studies in the literature, were compared with the prediction models, which were selected from Eurocode, Model Code 2010, The German code (DIN, 2011), Beeby’s model (Beeby and Scott, 2005) and JSCE code (Japanese code), as they cover the aforementioned three main cracking theories. As shown in the Table 1, it could be seen that the crack spacing behavior in RC specimens subjected to axial tension gives a good agreement with the predictions of Japanese code model, which is based on the ‘no-slip’ approach.

Table 1. Experimental and predicted crack spacing values of selected axial tensile experiments considered in Paper 3.

Study	Exp. crack spacing (mm)		Predicted max crack spacing (mm)					Error ^a %				
	Mean	Max	EC2	MC 2010	JSCE	Beeby	DIN	EC2	MC 2010	JSCE	Beeby	DIN
Conducted Test	133	202	254	181	199	214	111	-26	10	1	-6	45
Tan et al. (2018)	163	250	569	434	209	244	354	-128	-74	16	2	-42
	178	240	407	301	201	244	221	-70	-25	16	-2	8
	217	290	739	534	375	549	354	-155	-84	-29	-89	-22
	266	320	577	401	367	549	221	-80	-25	-15	-72	31
Barre et al. (2016)	200	330	654	590	390	397	446	-98	-79	-18	-20	-35
	174	288	534	434	268	275	348	-85	-51	7	5	-21
Rimkus & Gribniak (2017)	100	146	203	143	127	183	82	-39	2	13	-25	44
	92	133	203	143	122	183	83	-53	-8	8	-38	37
	73	103	224	159	131	183	99	-117	-54	-27	-78	4
	100	127	276	202	168	183	144	-117	-59	-32	-44	-13
	86	148	305	226	165	183	167	-106	-53	-11	-24	-13
	113	143	346	259	173	183	198	-142	-81	-21	-28	-39

^a Error = (Experimental Value - Predicted Value)/Experimental Value

3.2.4 Paper 4: Identification of the influence of concrete cover thickness and \emptyset/ρ parameter on crack spacing

From the conducted experimental program mentioned in Paper 4, it could be seen that the ‘no-slip’ theory can be more related to the actual cracking behavior of RC specimens. On the other hand, several studies claim that the ‘ \emptyset/ρ ’ parameter (which appears in the ‘bond-slip theory’) has a negligible influence on the cracking behavior of RC specimens (Rimkus and Gribniak, 2017, Beeby et al., 2005). Therefore, this paper investigates the actual ‘bond-slip’ behavior of RC specimens subjected to axial tension.

Very limited experimental investigations are reported in the literature that has investigated the bond-slip behavior in RC specimens subjected to axial tension. Those studies are reported in Doerr (1978) and Beconcini et al. (2008). According to the findings from these studies, specimens are subjected to a negligible amount of ‘slip’, when they are subjected to axial tension. These findings have been further confirmed by the recent study mentioned in Bado et al. (2021) (this study had not been published at the time of Paper 4’s publication). This paper, which is based on a literature survey, has further confirmed the applicability of the ‘no-slip’ approach (perfect bond conditions) for the cracking behavior of RC specimens.

3.2.5 Paper 5: Influence of concrete cover thickness and clear distance between tensile bars on crack spacing behavior: Experimental and numerical investigation

Many studies in the literature have identified that the crack width is governed by the crack spacing parameter rather than by the mean strain difference between concrete and reinforcement (Wang et al., 2017). From the previous findings (Papers 1 to 4), it could be observed that the ‘no-slip theory’ has a considerable influence on cracking behavior.

Concrete cover thickness and the clear distance between tensile bars are the governing crack spacing parameters, according to the ‘no-slip’ theory. The parameter ‘clear distance between tensile bars’ has not been considered in the crack width calculation models in either Eurocode 2 or Model Code 2010. However, this parameter is included in the current Japanese code and in the CEB-FIP Model Code 1978 (CEB-FIP, 1978).

An experimental program was conducted using large-scale RC specimens to investigate the influence of concrete cover thickness (RC specimens with 35-mm, 60-mm and 85-mm cover thicknesses) and clear distance between tensile bars (RC specimens with 66-mm, 116-mm and 166-mm clear distance between bars) on crack spacings. Figure 2 shows the set-up of the conducted experiments. For the further verification of results, these experiments were numerically simulated with 3D non-linear finite element models, using ATENA software. The results shown in Figure 3 shows that, both concrete cover thickness and ‘clear distance between tensile bars’ have an influence on crack spacing behavior.

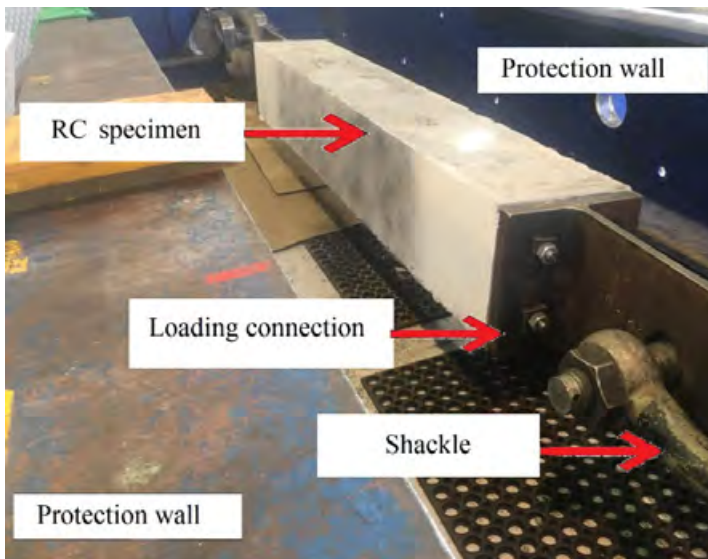


Figure 2. Experimental set-up of axial tensile test.

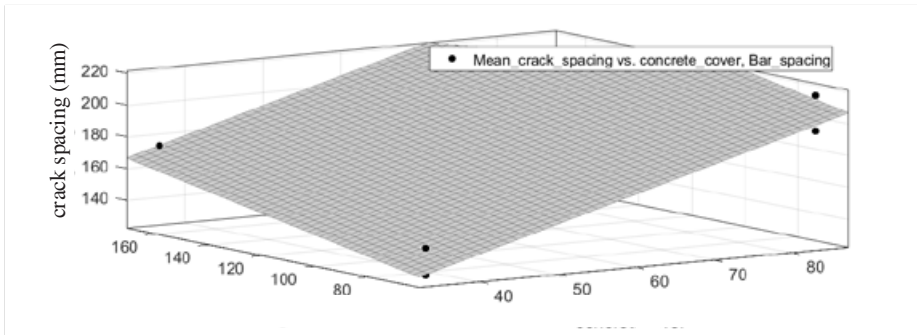


Figure 3. Mean crack spacing behavior of the tested specimens.

3.2.6 Paper 6: A new crack spacing model for reinforced concrete specimens with multiple bars subjected to axial tension using 3D non-linear FEM simulations

From the experimental program reported in Paper 5, ‘concrete cover thickness’ and ‘clear distance between tensile bars’ could be identified as crack spacing governing parameters. By using the results of these conducted experiments and similar experiments reported in Barre et al. (2016), a calibrated and validated 3D FEM simulation model was developed, using ATENA software (Cervenka, 2002). The numerical model was developed using the perfect bond criteria to represent the no-slip theory. The purpose of this 3D FEM simulation model is to conduct several numerical simulations, as the physical experiments consume a considerable amount of time, cost and labor.

After conducting a series of 3D non-linear finite element method simulations with the calibrated model, an equation was developed to predict the average crack spacings, using multiple linear regression analysis. To develop this model, the results of around 30 numerical experiments were considered. The validity of the proposed model has been checked with the recent experimental results in the literature. The

proposed crack spacing model in the Equation 1, gives good agreement with the experimental results reported in the literature.

$$S_{r,\text{mean}} = 66 + 0.51 c + 0.6 s^{n/2} \quad \text{Equation 1}$$

where ‘ $S_{r,\text{mean}}$ ’ is the mean crack spacing, ‘ c ’ is the concrete cover thickness, ‘ s ’ is the clear distance between tensile reinforcements and ‘ n ’ is the number of bars close to the specimen surface and all the units of these values are in mm.

3.2.7 Paper 7: Experimental investigation of crack width variation along the concrete cover depth in reinforced concrete specimens with ribbed bars and smooth bars

After introducing a reliable crack spacing model, the next objective was to introduce a crack width calculation model. To do that, an experimental program was conducted to investigate the crack width variation along the concrete cover thickness. In order to achieve the aforementioned main objective, it was necessary to investigate the ‘shear-lag’ effect along the concrete cover thickness, which is reported in Tammo and Thelandersson (2009), Walraven (2010), etc. Further, for this experimental program, concrete prisms reinforced with smooth bars were included, to further clarify the behavior of ‘slip’ between the reinforcement and concrete.

An experimental program was conducted, to study the crack width variation along the cover depth in concrete prisms reinforced with a central ribbed bar and smooth bar, by varying the concrete cover thicknesses (cover thicknesses vary from 20 mm to 80 mm). Crack widths along the concrete cover thickness were obtained by sealing the crack with a high strength and low viscosity epoxy and observing the crack after cutting the RC specimen. Figure 4 shows the crack width variation along the concrete cover depth in specimens with 40-mm cover

in both specimens with ribbed bars and specimens with smooth bars. In both specimens with smooth bars and specimens with ribbed bars, crack width is larger on the concrete surface than at the steel bar surface. In the specimens with smooth bars, significant slip was identified at the reinforcement and concrete interface, whereas negligible slip was observed in the specimens with ribbed bars. A surface crack width calculation model was developed, considering both the strain difference and the ‘shear-lag’ effect along the concrete cover thickness. Its predictions gave good agreement with the experimental surface crack widths from the conducted study and with the results from experiments in the literature, as shown in Figure 5.

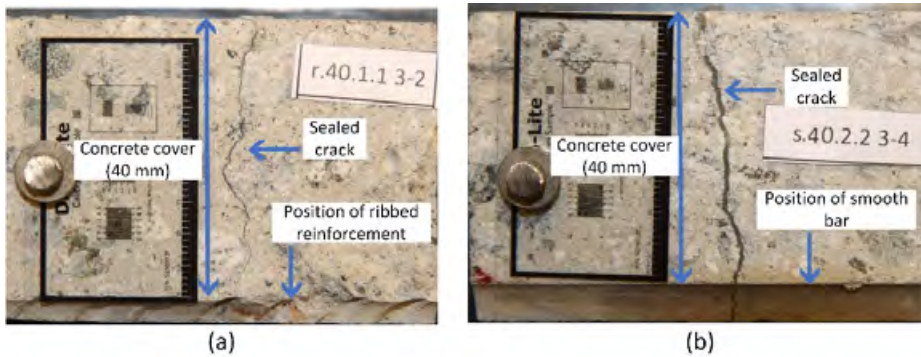


Figure 4. Crack width variation along the concrete cover depth in specimens with 40-mm cover (a) with ribbed bars; (b) with smooth bars.

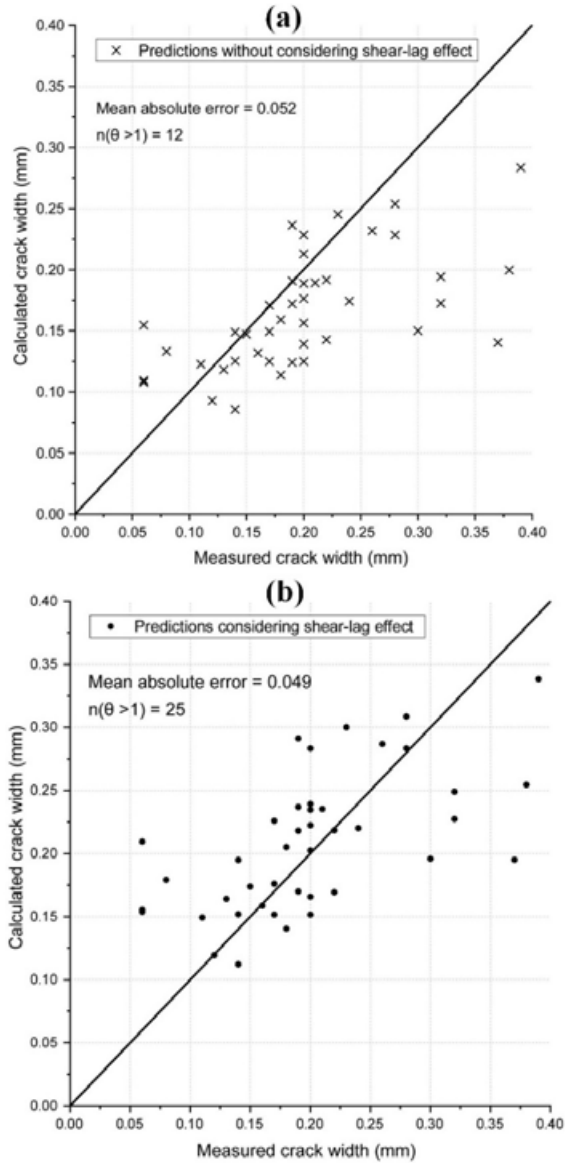


Figure 5. Comparison of the measured surface crack widths in Gribniak et al. (2020) with the predictions of equations (a) without considering, and (b) with considering shear-lag effect. ‘ $n(\theta > 1)$ ’ notation represent the number of conservative predictions out of 42 cases, where calculated crack width is greater than the measured crack width.

4 Research Contributions

In general, this study contributes to the field of civil and structural engineering. This study addresses one of the main requirements in Serviceability Limit State Design, which controls the cracks in RC structures. Studies which have been conducted on the cracks in RC members have been reported in the literature for more than a century. However, the inhomogeneous nature of concrete and the advancement of material in RC structures have made understanding cracking behavior quite complicated. The contribution of each paper is given below.

1. Paper 1 shows the reasons why the existing crack width calculation models in Eurocode and Model Code 2010 need to be improved. It identifies that the use of parameters like bond parameter (σ/ρ) in the existing prediction models need to be reconsidered.
2. Paper 2 shows the future studies necessary to improve the existing crack controlling criteria to effectively control the cracks in RC specimens with large concrete cover thicknesses. This study, which is based on a literature survey, was conducted in two main parts. The first part identifies the necessary improvements for the crack width calculation models, while the second part identifies the necessary future studies to improve the existing allowable crack width limits.
3. One of the main identifications from the study reported in Paper 3 is that of a suitable theoretical approach to the cracking behavior in RC specimens. This identified approach was further confirmed by studying the previous literature, as described in Paper 4. The next identification of Paper 3 is that the ratio of maximum to mean crack spacing values of RC members subjected to axial tension varies from 1.2 to 1.7. These findings were obtained by testing large-scale

RC specimens, and the experimental results would be beneficial for potential researchers in the field.

4. The experimental program described in Paper 5 identified that ‘clear distance between bars’ is a parameter in the crack spacing of RC specimens. The effect of this parameter is not included in either the Eurocode 2 or Model Code 2010 crack spacing calculation models. Further, these experimental results would be beneficial for potential researchers in the field, since very limited similar studies are available in the literature.
5. Paper 6 introduces a new crack spacing calculation model that gives good agreement with the experimental results in recent literature (experimental results of RC specimens with up to 85 mm of concrete cover thickness). This model was developed based on the results of recent experiments on large-scale RC specimens.
6. A new crack width calculation model is introduced in Paper 7. A new parameter, ‘effect of shear-lag’, was introduced to this model, to effectively predict the surface crack widths in RC members.

5 Suggestions for Future Research

The main focus of this study is to improve the existing crack width calculation models to effectively predict the crack widths of RC specimens with large concrete cover thicknesses. Therefore, from Paper 6, an improved crack spacing model has been introduced, to predict the mean crack spacings of RC specimens subjected to axial tension. The proposed model has not considered the effect of ‘number of tensile reinforcement layers’ on crack spacing. The necessity of studying this parameter has been identified by comparing the predictions from the proposed models with the experimental results reported in Paper 6.

After developing the mean crack spacing model, the next objective is to propose the maximum crack spacing model. Widely used ‘maximum crack spacing models’ have been developed by multiplying the mean ‘crack spacing model’ with a factor that represents the ratio of maximum to mean crack spacing. EC2 and MC 2010 consider this ratio to be 1.7 (Braam, 1990, Concrete, 1985). When considering the results of several recent axial tensile experiments, including the experiments conducted during this study (which are reported in Papers 3 and 6), it can be seen that this ratio varies between 1.2 and 1.7. However, several previous studies reported in Broms and Lutz (1965) and Beeby and Scott (2005) considered this parameter to be 2. Therefore, it is necessary to conduct a study to identify a suitable value for the ratio of mean to maximum crack spacing values.

Crack width calculation models in many codes of practice have considered that the effect of curvature has an influence on crack width. As reported in Paper 2, MC 2010, ACI and BS codes suggest multiplying the calculated crack widths from their models with the ‘ $(h-x) / (d-x)$ ’ ratio, to include the curvature effect. Here, ‘h’ denotes the total depth of the cross section, ‘d’ is the effective depth, and ‘x’ is the depth of the

neutral axis. From the study reported in Paper 3, it can be observed that the effect of curvature has an influence on the crack spacings of RC specimens. The Eurocode 2 crack spacing model contains the ' k_2 ' parameter, to include the effect of curvature on crack spacings. This identified effect of curvature on the crack spacings of RC specimens subjected to flexure should be further studied, to propose a factor to predict the crack spacings of RC specimens in flexure.

Paper 2 has identified the necessary future studies to improve the 'allowable crack width limits', to effectively control the crack widths of RC specimens with relatively large cover thicknesses. Considering the durability aspect, according to the long-term study conducted by Schiessl (1975a), there is a possibility that the allowable crack width limits can be increased with the concrete cover thickness, as in the Japanese code. However, this study was conducted for specimens with 25-mm and 35-mm cover thicknesses, and it can be further developed for RC specimens with different concrete cover thicknesses, to identify a pattern.

6 References

- ACI. 1995. Building Code Requirements for Structural Concrete (ACI 318-95) and Commentary (ACI 318R-95). American Concrete Institute.
- Bado, M. F., Casas, J. R. and Kaklauskas, G. 2021. Distributed Sensing (DOFS) in reinforced concrete members for reinforcement strain monitoring, crack detection and bond-slip calculation. *Engineering Structures*, 226, 111385.
- Barre, F., Bisch, P., Chauvel, D., Cortade, J., Coste, J.-F., Dubois, J.P., Erlicher, S., Gallitre, E., Labbé, P. and Mazars, J. 2016. *Control of cracking in reinforced concrete structures*, Wiley Online Library.
- Basteskår, M., Engen, M., Kanstad, T. and Fosså, K. T. 2019. A review of literature and code requirements for the crack width limitations for design of concrete structures in serviceability limit states. *Structural Concrete*, 20, 678-688.
- Beconcini, M. L., Croce, P. and Formichi, P. 2008. Influence of bond-slip on the behaviour of reinforced concrete beam to column joints. Proceedings of International fib Symposium “Taylor Made Concrete Structures: New Solutions for our Society”, Amsterdam. 19-21.
- Beeby, A. W. 1970. An investigation of cracking in slabs spanning one way. *Cement and Concrete Association*.
- Beeby, A. W., Alander, C., Cairns, J., Eligehausen, R., Mayer, U. and Lettow, S. 2005. Discussion: The influence of the parameter ϕ/ϕ_{eff} on crack widths. *Structural Concrete*, 6(4):155-165.
- Beeby, A. W. and Scott, R. H. 2005. Cracking and deformation of axially reinforced members subjected to pure tension. *Magazine of Concrete Research*., 57, 611-621.
- Borges, J. F. 1965. *Cracking and deformability of reinforced concrete beams*, Laboratório Nacional de Engenharia Civil.
- Borosnyói, A. and Balázs, G. L. 2005. Models for flexural cracking in concrete: the state of the art. *Structural Concrete*, 6, 53-62.

- Braam, C. 1990. *Control of crack width in deep reinforced concrete beams (Ph.D. Thesis)*. Delft University.
- Broms, B. B. 1965. Crack width and crack spacing in reinforced concrete members. *ACI Journal Proceedings*, 62, 1237-1256.
- Broms, B. B. and Lutz, L. A. 1965. Effects of arrangement of reinforcement on crack width and spacing of reinforced concrete members. *ACI Journal Proceedings*, 62, 1395-1410.
- BS. 1985. 8110: Part 1, Structural use of concrete—code of practice for design and construction. London, UK: British Standard Institute.
- CEB-FIP. 1978. Model Code 1978 -Design Code; Comité Euro-International du Béton. *CEB Bulletin d'Information*. London: Thomas Telford.
- CEN 2004. EN 1992-1-1, Eurocode 2: Design of concrete structures - Part 1-1: General rules and rules for buildings. Brussels, Belgium: European Committee for Standardization.
- CEB. 1985. CEB Design manual on cracking and deformations. Lausanne, Switzerland:École Polytechnique Fédérale du Lausanne.
- Cervenka, V. 2002. Computer simulation of failure of concrete structures for practice. 1st fib Congress. 289-304.
- DIN. 2011. EN-1992-1-1/NA: 2011-01, National Annex- Nationally determined parameters- Eurocode 2: Design of concrete structures- Part 1-1: General rules and rules for buildings.
- Doerr, K. Bond behavior of ribbed reinforcement under transversal pressure. Nonlinear behavior of reinforced concrete structures; Contributions to IASS Symposium, 1978. 3-7.
- Eyisi, D. 2016. The usefulness of qualitative and quantitative approaches and methods in researching problem-solving ability in science education curriculum. *Journal of Education and Practice*, 7, 91-100.
- FIB. 2013. fib Model code for concrete structures 2010. *International Federation for Structural Concrete*. Berlin: Ernst & Sohn.
- Gergely, P. and Lutz, L. A. 1968. Maximum crack width in reinforced concrete flexural members. *ACI Special Publication*, 20, 87-117.
- JSCE. 2007. Standard Specifications for Concrete Structures-2007 "Design".

- Leonhardt, F. 1988. Cracks and crack control in concrete structures. *PCI Journal*, 33, 124-145.
- Makhlouf, H. M. and Malhas, F. A. 1996. The effect of thick concrete cover on the maximum flexural crack width under service load. *Structural Journal*, 93, 257-265.
- Pérez Caldentey, A., Corres Peiretti, H., Peset Iribarren, J. and Giraldo Soto, A. 2013. Cracking of RC members revisited: influence of cover, ϕ/ρ_s , e_f and stirrup spacing—an experimental and theoretical study. *Structural Concrete*, 14, 69-78.
- Rimkus, A. and Gribniak, V. 2017. Experimental investigation of cracking and deformations of concrete ties reinforced with multiple bars. *Construction and Building Materials*, 148, 49-61.
- Saliger, R. High grade steel in reinforced concrete. Preliminary Publication, 2nd Congress of IABSE. Berlin-Munich: IABSE Publications, 1936.
- Schiessl, P. 1975a. Admissible crack width in reinforced concrete structures. Contribution II *Preliminary reports Vol. II, Inter-Association Colloquium on the Behaviour in Service of Concrete Structures*.
- Schiessl, P. 1975b. *Admissible Crack Widths in Reinforced Concrete Structures*, Liege.
- Stattens Vegvesen. 2009. NPRA Håndbok N400 Bruprosjektering. Oslo: Vegdirektoratet.
- Tammo, k. and Thelandersson, S. 2009. Crack behavior near reinforcing bars in concrete structures. *ACI Structural Journal*, 106, 259.
- Tan, R., Eileraas, K., Opkvitne, O., Zirgulis, G., Hendriks, M. A., Geiker, M., Brekke, D. E. and Kanstad, T. 2018. Experimental and theoretical investigation of crack width calculation methods for RC ties. *Structural Concrete*, 1436 - 1447.
- Thiel, D. V. 2014. *Research Methods for Engineers*, Cambridge University Press.
- Walraven, J. 2010. *Model Code 2010-First complete draft-Volume 2: Model Code*, fib Fédération Internationale du Béton.
- Wang, j.j., Tao, M.X. and Nie, X. 2017. Fracture energy-based model for average crack spacing of reinforced concrete considering size

References

- effect and concrete strength variation. *Construction and Building Materials*, 148, 398-410.
- West, J. S., Larosche, C. J., Koester, B. D., Breen, J. E. and Kreger, M. E. 1999. State-of-the-art report about durability of post-tensioned bridge substructures. Center for Transportation Research, Bureau of Engineering Research, the University of Austin at Texas.

Part II: Paper

Paper 1: Comparison of the behavior of crack width governing parameters with existing models.

Naotunna, C.N., Samarakoon, S.M.S.M.K., and Fosså, K.T. (2019)



In: Proceedings of *International Conference on Sustainable Materials, Systems and Structures (SMSS 2019)*. Rovinj: pp. 124-131, ISBN: 978-2-35158-226-8, ISSN: 1333-9095.

This paper is not available in Brage due to the copyright.

Paper 2: Applicability of existing crack controlling criteria for structures with large concrete cover thickness.

Naotunna, C.N., Samarakoon, S.M.S.M.K., and Fosså, K.T. (2021)

In: *The Journal of Nordic Concrete Research*, pp. 69-91, DOI: 10.2478/ncr-2021-0002.

	
<p>© Article authors. This is an open access article distributed under the Creative Commons Attribution-NonCommercial-NoDerivs licens. (http://creativecommons.org/licenses/by-nc-nd/3.0/).</p>	<p>ISSN online 2545-2819 ISSN print 0800-6377</p>
<p>DOI: 10.2478/ncr-2019-0002</p>	<p>Received: March 15, 2021 Revision received: June 15, 2021 Accepted: June 16, 2021</p>

Applicability of Existing Crack Controlling Criteria for Structures with Large Concrete Cover Thickness



Chavin Nilanga Naotunna – Corresponding Author.
PhD Candidate.
University of Stavanger, Department of Mechanical and Structural Engineering and Material Science, Stavanger.
Address: Kjell Arholmsgate 41, 4036 Stavanger, Norway.
E-mail: chavin.guruge@uis.no



S.M Samindi M.K Samarakoon.
Associate Professor.
University of Stavanger, Department of Mechanical and Structural Engineering and Material Science, Stavanger.
Address: Kjell Arholmsgate 41, 4036 Stavanger, Norway.
E-mail: samindi.samarakoon@uis.no



Kjell Tore Fosså.
Adjunct Professor.
University of Stavanger, Department of IMBM.
Manager Concrete Technology.
Aker Solutions, Stavanger, NO 4020.
E-mail: kjell.t.fossa@uis.com

ABSTRACT

Widely used crack width calculation models and allowable crack width limits have changed from time to time and differ from region to region. It can be identified that some crack width calculation models consist with limitations for parameters like cover thickness. The current Norwegian requirement for cover thickness is larger than these limitations. The applicability of existing crack width calculation models and the allowable crack width limits must be verified for structures with large cover thickness. The background of crack width calculation models in Eurocode, Model Code 2010, Japanese code, American code and British code have been examined. By comparing the experimental crack widths with the predictions of the aforementioned models, the existing codes can be identified as requiring modification. Considering the durability aspect, it can be identified a long-term study proving that the allowable crack width can be increased with the increase in cover thickness. When considering the aesthetic aspect, the authors suggest

categorizing the structures based on their prestige level and deciding the allowable crack widths accordingly. The paper proposes potential solutions for future research on how to improve both crack width calculation methods and allowable crack width limits to be used effectively in structures with large cover thickness.

Keywords – reinforced concrete structures, service load, crack width, durability, aesthetic, concrete cover thickness

1. INTRODUCTION

Cracks in concrete occur when the tensile stress on concrete exceeds its tensile strength [1]. The cracks in reinforced concrete (RC) structures create many adverse effects on the durability, aesthetic view and liquid or gas tightness of the structure. To avoid the discussed adverse effects from cracks, it is necessary to repair the cracks, resulting in high repair costs [2]. Therefore, it is always preferable to limit cracks at the structural design stage. On the other hand, it is not possible to control all types of cracks at this stage. Depending on the controllability of the cracks at the structural design stage, Beeby [3] has classified cracks as controllable (load-induced cracks) and non-controllable (cracks caused by plastic shrinkage, alkali-silica reaction, freeze/thaw deterioration). To minimize the occurrence of cracks due to service load, the ‘stress of the tensile steel’ has to be limited to a low value. According to the Japanese code, for the RC structures with deformed bars, if the tensile stress due to permanent loads has limited to 120 N/mm^2 , the examination of crack widths may be omitted [4]. In order to do this, a large amount of reinforcement is required. This tends to drastically increase the cost of the structure and reduce the ease of construction. Therefore, in general, cracks due to service load are allowed to occur and are controlled by limiting crack widths.

At the design stage, the ‘calculated crack width’ is limited to an ‘allowable crack width’ [5-8]. These ‘calculated crack width’ models have changed from time to time and differ from region to region. For example, crack width calculation models have changed from CEB Model Code 78 [9] to CEB/FIP Model Code 90 [5] and similarly from Eurocode 2 (1991) [10] to the current Eurocode 2 [7]. Furthermore, crack width calculation models in different regions differ from each other, as they are based on different approaches. Empirically based crack width calculation models are found in the American Concrete Institute (ACI) code [8], British Standards (BS) code [11], Gergely and Lutz [12], Kaar and Hognestad [13], Sygula [14] and so on. Crack width calculation models based on a semi-analytical approach are in Eurocode 2 (EC2) [7], CEB/FIP Model Code 90 [5], Model Code 2010 (MC2010) [6], the Japanese Society of Civil Engineers (JSCE) code [4], the Architectural Institute of Japan (AIJ) [15], and so on. Widely used analytically based crack width calculation models can be found in Balazs [16], Tan et al. [17], Oh and Kang [18] and so on.

As mentioned, there are several crack width calculation models available in the literature. However, it is vital to study their limitations. For example, the MC2010 crack width calculation model limits concrete cover thickness to 75 mm. However, recently, the economic and social benefits over the long term of structures with a significantly long service life (200 or 300 years) have been identified [19, 20]. Concrete cover thickness is mainly increased to satisfy the durability aspect, when a long service life is required for an RC structure. The current requirement of concrete cover thickness is as high as 120 mm (Norwegian Public Road Administration guidelines [21]); as an example, Hafstrfjord Bridge in Norway is constructed with a concrete cover thickness of 90 mm [22, 23]. As mentioned, some ‘crack width calculation’ models have limitations for concrete cover thickness. Further, it is important to check the applicability of existing models, as they have not been validated for such structures with large concrete cover thickness.

Similar to the crack width calculation models, it can be seen that the ‘allowable crack width limits’ in the widely used codes of practice have changed from time to time and differ from each other. For example, CEB Model Code 78 [9] prescribes limiting the crack width in severe conditions to 0.1 mm; this value has been changed in CEB/FIP Model Code 90 [5] and MC2010 [6] to 0.3 mm. Further, in severe conditions, all the EC2, MC2010 and BS codes prefer to limit the crack width to 0.3 mm, while ACI 224 [24] and ACI

318 [8] prefer to limit the crack width to 0.15 mm and 0.33 mm, respectively. In severe conditions, these limits are mainly decided on to protect the reinforcement from corrosion [1]. When referring to previous long-term studies on crack widths and corrosion, it can be seen that the allowable crack width can be increased with the increase in concrete cover thickness [25]. The allowable crack width limits in the JSCE code are an example of such application. Apart from the durability considerations, the thickness of the concrete cover depends on the safe transmission of bond properties and is based on fire resistance. For example, according to EC2, for the safe transmission of bond forces, concrete covers can be as large as 55 mm for cases with bundled bars [7]. Therefore, even for structures which are not built-in severe exposure classes, there is the possibility to have relatively large covers. This shows the necessity to revisit the allowable crack width limits, based on aesthetic acceptance, for structures with large concrete cover thicknesses. If the crack width of a structure with a large concrete cover thickness is controlled to the allowable limits which are prescribed for lower cover thicknesses, additional tensile reinforcement tends to be required. For this reason, it is necessary to identify how the existing allowable limits are decided and what improvements need to be made for them to apply to structures with higher cover thicknesses.

This paper focuses on the applicability of existing 'crack width calculation models' and existing 'allowable crack width limits', for structures with large concrete cover thickness. The manuscript starts with a discussion of the cracking phenomenon. Then, it explains the background to why the different codes of practice suggest different models to calculate the crack width. By comparing the recent experimental results with the model predictions, this study emphasizes the necessity to improve existing crack width calculation models, to effectively predict the crack width of structures with large concrete covers. The next objective is to identify the applicability of existing 'allowable crack width limits' for structures with large concrete covers. An extensive literature survey has been carried out on how the existing limitation has been appointed, based on durability and aesthetic view. The required improvements and the further studies needed to decide the 'allowable crack width limits', to apply to structures with large concrete cover thickness, have been identified.

2. CRACKING PHENOMENON OF RC MEMBERS SUBJECTED TO SERVICE LOAD

To understand the cracking phenomenon in flexure, a reinforced concrete (RC) tie in pure tension can be considered, as it can represent the tensile region of a bending member with or without any axial force [26, 27]. Many previous researchers have identified the cracking behaviour of RC specimens subjected to pure tension [28-32]. Figure 1 represents the cracking behaviour of an RC tie subjected to pure tension, according to Beeby [33]. The stress in the rebar starts affecting the concrete surface after 'KC' ('K' is a constant and 'C' is cover) distance [34-36] from the specimen end, and it takes another S_0 distance to uniformly distribute the stress along the cross section. When the applied force increases from zero, the highest stress occurs at the concrete surface after $KC+S_0$ distance (transfer length) and beyond. This theoretical explanation matches the 'combined theory' introduced by Borges [37]. Borges considered the cracking behaviour to be in accordance with the combination of the two main theories: 'no-slip' theory [28, 38, 39] and 'bond-slip' theory [40-42]. A detailed description of these theories can be seen in Naotunna et al's study [43]. When the stress in the concrete cross section reaches the tensile strength (f_{ct}), the first crack appears. After the first crack, the stress/strain distribution rearranges, as, at the crack, the concrete can no longer withstand tensile stress perpendicular to the crack face (Figure 1 (b)). When the load is further increased, another crack occurs after the transfer length. This proceeds until the last crack occurs and then transfers to the stabilized cracking stage. At this stage, the increased strain due to the further increased load accumulates at the cracks that have already occurred.

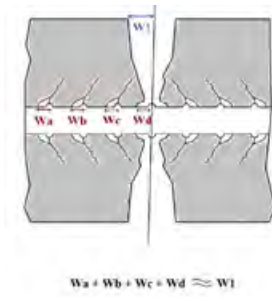
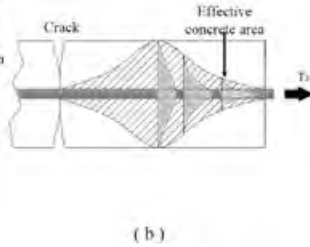
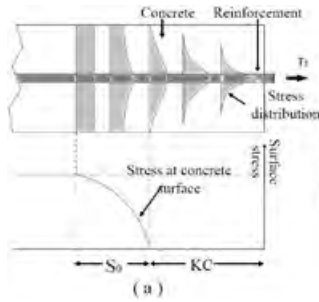


Figure 1 - (a) Internal stress distribution & surface stress variation of an RC tie before cracking, (b) Internal stress distribution of a cracked RC tie.

Figure 2 - Crack width variation along the concrete cover.

The aforementioned explanation of the cracking is a simplified approach. As shown in Figure 1(b), a strain incompatibility can be observed between reinforcement and concrete, specially at the vicinity of reinforcement [44]. In the specimens with deformed reinforcement, the strain incompatibility is accommodated in the internal cracks (secondary cracks) [26, 32, 44, 45]. Even though these cracks do not completely discontinue the concrete material, a partial discontinuity occurs [46]. This leads to a complicated stress/strain distribution throughout the specimen because concrete is an inhomogeneous material. The tensile strength of concrete is not the same, even in different samples of the same batch of concrete [47]. The variation of the tensile strength of concrete complicates the strain incompatibility. Naotunna et al. [48] have suggested including the lower and upper fractile values of concrete tensile strengths, to identify the minimum and maximum crack spacing values. The cracking phenomenon would be more complicated with conditions like effective concrete area, inhomogeneous behaviour of concrete, tension stiffening effect, internal cracking (Goto cracks) and so on.

3. CALCULATION OF CRACK WIDTHS

There are various types of crack width calculation models in the existing literature. The theoretical concept of crack width is the integration of the actual strain difference of reinforcement and concrete between two cracks [16]. The crack width at the tensile reinforcement can be calculated by using Equation (1). However, due to the nonlinear behaviour of strain variation in both concrete and reinforcement between two cracks, obtaining the crack width explicitly is a complicated process [27]. Therefore, in order to make the crack width calculation model less complicated or more user-friendly, many codes use simplified or semi-analytical approaches. Examples of such models are found in EC2 [7], MC2010 [6], JSCE [4] code and so on. On the other hand, codes like ACI [8] and BS [11] use crack width calculation models based on empirical approaches. Such models are developed by curve fitting of a considerable amount of experimental data. The ACI and BS codes were developed by the experimental investigation of Gergely and Lutz [49] and Beeby [50], respectively.

$$w = \int_0^{S_r} \epsilon_s - \epsilon_c dx \quad (1)$$

where 'w' is the crack width, 'S_r' is the crack spacing, and 'ε_s' and 'ε_c' are the strains of reinforcement and concrete in the x-direction (the direction of axial tensile load).

Semi-analytical models developed from Equation (1) predict the crack width at the tensile reinforcement surface [51]. It is assumed that the crack width propagates similarly, along with the concrete cover thickness, and therefore the same model is used to predict the crack width at the concrete surface [6, 7]. However, the experimental investigations in [51-54] have identified that the crack width at the concrete surface is two to ten times larger than the crack width at the reinforcement bar. Beeby and Scott [44]

observed that the reason for this crack width difference is the effect of shear lag, which occurs along with the concrete cover. However, Caldentey et al. [55] have proved with calculations that the effect of shear lag is considerably smaller than the aforementioned crack width difference at the reinforcement and concrete surface. The authors in [51, 55] explained that the reason for the crack width difference is the presence of Goto cracks [32] (secondary cracks). These secondary cracks are spread at the vicinity of the primary cracks [26, 32, 56]. As the strain accumulates in the secondary cracks, the width of the primary crack at the reinforcement is reduced. Therefore, as per Figure 2, it can be concluded that the predictions of semi-analytical models in [6, 7] are similar to the surface crack width.

Semi-analytical models based on Equation (1) predict the crack width by multiplying the crack spacing with the strain difference between reinforcement and concrete. Many studies have identified that it is vital to improve the 'crack spacing' model, in order to improve the crack width calculation models [57-59]. Tammo and Thelandersson [57] proved that changing the concrete properties makes no difference to the surface crack width or internal crack widths, if the crack spacing values are the same. The crack spacing models in the semi-analytical models are based on the aforementioned two main theories: 'bond-slip' and 'no-slip' theories. According to the bond-slip theory, since a 'slip' is assumed at the reinforcement-concrete interface, a bond-stress would generate. Therefore, the governing crack spacing parameters from this theory are bond parameter (σ/ρ); where ' σ ' is the bar diameter and ' ρ ' is the ratio between reinforcement area and concrete area), bond stress, etc. [26, 45]. The German National Annex of EC2 [60] proposes a model based on the bond-slip approach. According to the no-slip theory, the governing crack spacing parameters can be considered to be concrete cover thickness and the distance between tensile reinforcement (thickness of the surrounding concrete of the tensile reinforcement) [28, 61]. The crack spacing model in the Japanese code and Beeby's model in Beeby and Scott [44] are some examples of crack spacing models based on no-slip theory. The EC2 and MC2010 models are based on the combined theory, which considers the cracking behaviour to be based on the combination of the aforementioned two theories.

3.1 Crack Width Calculation Methods In Widely Used Codes Of Practice

Several widely used crack width prediction models in the codes of practice have been examined. Prediction models have been selected, as they can represent the different regions of the world. EC2 and MC2010 have been selected, as they are the governing codes of practice in Europe. Then the crack width prediction models in American code, Japanese code and British code have been considered. When examining the models proposed by codes, it can be observed that some codes mention limitations for the concrete cover thickness. MC2010 limits the applicability of the crack width calculation model to 75 mm cover thickness. Since the focus of this study is to check the applicability of existing crack controlling criteria for specimens with large concrete cover thickness, the background of these widely used crack width calculation models has been investigated and is presented, along with a detailed description of each, in Table 1. From the models proposed by the codes in Table 1, various crack width governing parameters can be identified. A detailed list of such parameters and their involvement in crack width can be identified from the literature [62].

Figure 3 categorizes all the crack width governing parameters mentioned in the aforementioned widely used crack width prediction models. The crack width governing parameters have been categorized based on the mechanical properties of concrete and reinforcement, properties of interface, cross-sectional properties of the RC member and loading conditions. From Table 1, it can be identified that the EC2, MC2010 and JSCE code models, which are based on a semi-analytical approach, consider a higher number of parameters than the empirically based ACI and BS code models. Further, it is clear that, although the mentioned models have been developed based on different approaches, the concrete cover thickness parameter is included in every model. The calculated crack width from these models causes the crack width to increase with the increase in concrete cover. The models in EC2 and MC2010 specifically mention their

applicable limitations for concrete cover thickness. The models in the JSCE, ACI and BS codes do not mention such limitations. The main reason could be that the commonly used concrete cover thickness in the period of developing the code might not be as large as the current requirement. It is important to note that the empirically based crack width calculation models developed by the ACI and BS codes have considered test specimens with concrete cover thicknesses of 84 mm and 89 mm, respectively. However, as mentioned in Section 1, there is a demand for large concrete cover thickness [21].

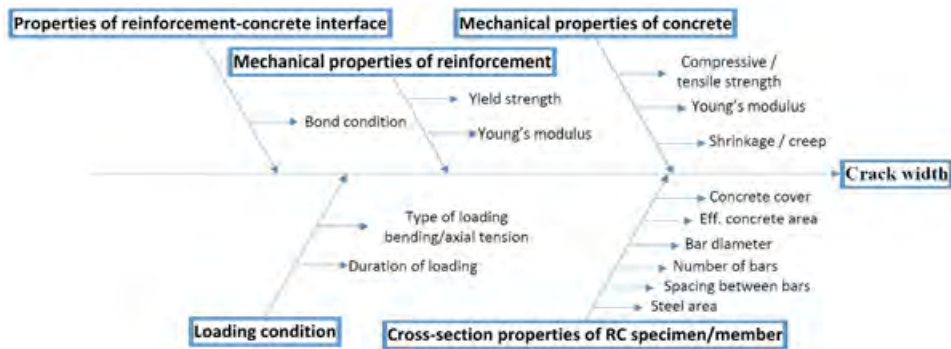


Figure 3. Cause and effect diagram for crack width.

3.2 Improvements to the existing crack width prediction models

From Table 1, it is clear that MC2010 mentions limitations for the concrete cover thickness. Further, according to the literature on recent experiments, many cases can be identified in which the experimental values deviate from the EC2 and MC2010 predictions [27, 48, 63-68]. Therefore, many improvements have been proposed for these two models, some of which are listed in Table 2. According to these suggested improvements, it can be identified that none of the improved models has compared the data with specimens having cover thickness of above 70 mm. Therefore, the applicability of the aforementioned improved models needs to be verified for concrete covers larger than 70 mm.

Identifying the crack theory which is most related to the actual cracking behaviour is vital, since the crack spacing governing parameters can be identified based on them. The recent study, published in 2021 by Bado et al. [69], has focused attention on the 'slip' values in axial tensile experiments. In this study, the slip at the reinforcement-concrete interphase is measured by optical fibre sensors. Further, these findings of Bado et al. [69] match the experimental results of previous studies conducted on the bond-slip behaviour of axial-tensile experiments by Doerr [70] and Beconcini and Croce [71]. According to the findings of these studies, the slip values in axial tension are quite negligible compared to the predictions in the widely used Eligehausen's model [72, 73]. The Eligehausen's bond-slip model is considered in MC 2010, and this model is based on the Rilem type pull-out tests [74]. Moreover, Balazs [16] has used Eligehausen's model to model the bond-slip behaviour while developing a crack width calculation model. Further, in the widely used Finite Element Modelling software like, ATENA [75], considers this Eligehausen's bond-slip model to model the cracking behaviour in RC members. However, as shown in Figure 4, the slip values in axial tension are significantly smaller than the slip values suggested by Eligehausen's bond-slip model (same bond-slip model used in MC 2010). Since it has observed a negligible amount of slip in the RC specimens in axial tension, the applicability of bond-slip law on crack spacings can be considered questionable. Furthermore, there are several experimental studies which make similar arguments, that the bond-parameter (' ϕ/ρ ' which is the dominant parameter in the bond-slip law) has little influence on crack spacings when the concrete cover is small. Such experimental studies are mentioned in Base et al. [38], Caldentey et al. [55] (for specimens with 70 mm covers), Rimkus et al. [63], and Kim et al. [76]; analytical studies are mentioned in Beeby [40], and Beeby and Scott [44]. Naotunna et al. [43, 77], have further discussed this scenario.

Table 1 - Crack width calculation models in widely used codes of practice and their significances

Model	Models	Remarks
EC2 [7] and MC2010 [6]	<p>$w_k = \text{Maximum crack spacing} \times \text{Mean strain difference of rebar and concrete}$</p> <p>Maximum crack spacing</p> <p>EC2 Model MC2010 transfer length Model</p> $s_{r, \max} = k_3 c + k_1 k_2 k_4 \phi / \rho_{p, \text{eff}} \quad s_{r, \max} = kc + (1/4)(f_{ctm}/\tau_{bms})(\phi_s/\rho_{s, \text{ef}})$ <p>where 'c' is concrete cover, '$\rho_{s, \text{ef}}$' is effective steel ratio, 'k_1' is factor for bond properties, 'k_2' is factor for distribution of strain, 'k_3' is recommended as 3.4, 'k_4' is recommended as 0.425, 'k' is empirical parameter on cover, 'τ_{bms}' is mean bond strength (steel-concrete), 'ϕ_s' is the bar diameter, and 'f_{ctm}' is the tensile strength of concrete.</p> <p>Mean strain difference of rebar and concrete</p> <p>EC2 Model MC2010 Model</p> <p>Crack Formation Stage Crack Formation Stage</p> $\varepsilon_{sm} - \varepsilon_{cm} \geq 0.6 (\sigma_s / E_s) \quad \varepsilon_{sm} - \varepsilon_{cm} = \sigma_{sr} / E_s * (1 - \beta)$ <p>Stabilized cracking stage, - $\eta_r \varepsilon_{sh}$</p> <p>Stabilized cracking stage, Stabilized cracking stage,</p> $\varepsilon_{sm} - \varepsilon_{cm} = \frac{\sigma_s - k_i (f_{ct, \text{eff}} / \rho_{p, \text{eff}}) (1 + \alpha_e \rho_{p, \text{eff}})}{E_s} \quad \varepsilon_{sm} - \varepsilon_{cm} = (\sigma_s - \beta \sigma_{sr}) / E_s$ <p>- $\eta_r \varepsilon_{sh}$</p> <p>where 'σ_s' is stress of steel at the cracked section, 'k_i' is a factor on the loading duration, 'α_e' is the modular ratio, 'σ_{sr}' is the max. steel stress at the crack formation stage, 'β' is factor on the duration of load, 'η_r' is coefficient for shrinkage strain, and 'ε_{sh}' is the shrinkage strain.</p>	<p>Semi-analytical models</p> <p>Assumptions: From the different bond stress models for reinforcement and concrete (linear, non-linear) between a crack and a no-slip location [41, 42, 78, 79], a constant mean bond stress has been assumed [80].</p> <p>Significance: EC2 uses a 'k₂' factor to take into account the variation in strain distributions (flexural or axial tension) [81], and MC2010 considers that only the 'effective concrete area' can represent the effect [82].</p> <p>Limitations for cover: MC2010 limits to 75 mm.</p> <p>Concrete cannot further increase its strain when the total number of cracks has formed (as the available length to develop stress in concrete is fixed). Therefore, when the strain of the steel is further increased (when it reaches the stabilized cracking stage), the concrete strain remains unchanged. This causes there to be different formulas for the mean strain difference between reinforcement and concrete in both cracking stages. Significance: Except for the effect of shrinkage considered in the MC2010 model, both EC2 and MC2010 use the same equation in the stabilized cracking stage.</p>
JSCE code [4]	$W = 1.1 k_1 k_2 k_3 \{4c + 0.7(c_s - \phi)\} \left[\frac{\sigma_{se}}{E_s} + \varepsilon'_{csd} \right];$ $k_2 = \frac{15}{(f'_c + 20)} + 0.7; \quad k_3 = \frac{5(n+2)}{7n+8}$ <p>where 'w' is crack width, 'k_1' is constant on the surface of rebar, 'k_2' is constant on the concrete quality, 'f'_c' is design compressive strength of concrete, 'n' is number of layers of tensile rebar, 'k_3' is constant to take account of the multiple layers of tensile bars, 'c_s' is distance of the tensile rebar, 'ϕ' is diameter of the tensile rebar, 'σ_{se}' is tensile stress increment of the bar, and 'ε'_{csd}' is compressive strain from shrinkage and creep of concrete.</p>	<p>This model is based on a semi-analytical approach. The crack spacing model (without strain components) is based on the concrete cover and the distance between tensile bars. Bar spacing has been proved to be a factor for crack spacing in [83]. The experimental findings in [84] prove that smooth bars cause large crack spacing. While both EC2 and MC2010 predict increasing crack width with concrete strength, JSCE code predicts the opposite. However, this behaviour matches the results in [66, 85, 86]. Limitations for cover: No limitations have been mentioned for concrete cover thickness.</p>
ACI code [8, 24]	$w = 2.2 \beta \varepsilon_s \sqrt{d_c A}$ <p>where 'w' is maximum crack width at the extreme tensile fibre (in), 'β' is ratio of the distance between the neutral axis and tension face to the distance between the neutral axis and centroid of reinforcing steel, 'ε_s' is strain in reinforcement due to the applied load, 'd_c' is the thickness of the cover from extreme tension fibre to the closest bar (in), and 'A' is area of concrete symmetrical with reinforcing steel divided by the number of bars (in²).</p>	<p>The empirically based equation was developed in [49], with the results of six different bending experiments. The ACI Committee 224 [24] modified the aforementioned model by using the strain, instead of the stress in the reinforcement. Limitations for concrete cover thickness: No limitations have been mentioned for concrete cover. However, the results of specimens with up to 84 mm of concrete cover were used to develop the model.</p>
BS code [11]	$w = \frac{3 c e}{1 + 2 \left(\frac{c - c_0}{d - d_n} \right)}, \quad \text{where} \quad e = \left(\text{est} - \frac{2.5 b d \cdot 10^{-6}}{A_{st}} \right) \frac{d - d_n}{d_1 - d_n}$ <p>where 'c' is the distance from the point considered to the nearest bar, 'c_0' is the concrete cover thickness, 'd' is overall depth of the member, 'd_n' is neutral axis depth calculated on the assumption that concrete has no tensile strength, 'd_1' is effective depth of a member, 'b' is breadth of the member, 'A_{st}' is area of the tensile steel, and 'est' is strain in the steel assuming concrete has no tensile strength.</p>	<p>The empirically based equation was developed based on the experiments in [50]. The derived equation in [50] has been simplified in [87] to be used in the BS code. Results show that crack width is linearly proportional for concrete covers below 40 mm, and the pattern differs when the cover increases. Limitations for concrete cover thickness: No limitations have been mentioned. The results of specimens with up to 89 mm concrete cover were used to develop the model.</p>

Table 2 - Suggested improvements for the EC2 and MC2010 crack-width calculation models

Literature	Improving Parameter	Suggestion	Remarks
Caldentey (2017) [82]	Mean strain difference	Include the shrinkage strain effect with a restraint factor (R_{ax}). $w_k = s_{r,max} \cdot (\epsilon_{sm} - \epsilon_{cm} - R_{ax} \eta_f \epsilon_{sh})$ where ' R_{ax} ' can be 1, when a member is completely restrained at edges (e.g., wall is restrained by previously cast foundation) and ' R_{ax} ' can be 0, when restrained at the ends (e.g. RC tie subjected to axial tension).	Investigating the effect of 'casting position' [88] from the experimental results of [89, 90].
Debernardi and Taliano (2016) [56] Taliano (2017) [45]	Crack spacing	$\tau_{bms} = (f_{ct} \cdot A_c) / (n_s \cdot \pi \cdot \phi_s \cdot L_s)$, where n_s is the number of tensile bars. $s_{r,max} = 2$. $L_s = 2 \cdot (1/4) (f_{ctm} / \tau_{bms}) (\phi_s / \rho_{s,ef})$. Suggest a table of values for the ' τ_{bms} / f_{ctm} ' from the suggested 'general equation' by Balazs (1993) [16].	According to this method, cover term has no influence on the crack spacing.
	Mean strain difference	To represent the reduction of tension stiffening, due to internal cracks, the ' k_i ' coefficient is considered as 0.45 (which is 0.6 for the short-term load suggested by EC2). $\epsilon_{sm} - \epsilon_{cm} = \sigma_s - 0.45 (f_{ct,eff} / \rho_{p,eff}) (1 + \alpha_e \rho_{p,eff}) / E_s$	Experimental comparison is made up to 45 mm of cover.
Rospars et al. (2014)[64] Bisch (2017) [65]	Crack spacing	After a statistical analysis of the results of 131 tests from own experiments (CEOS project France) and previous literature, an equation has been identified $s_{r,max} = 1.7 [1.37 c + 0.117 \cdot (\phi_s / \rho_{s,ef})]$	Covers of the experimental specimens are 50 mm and 70 mm.

The governing parameter of the no-slip theory is concrete cover thickness. The concrete cover thickness influences the surface crack width in two ways [57]: the first is by influencing crack spacing, and the second is by influencing through the effect of shear lag [57]. This shear-lag effect is discussed in several studies in the literature, such as those of Tammo and Thelandersson [53], Beeby et al. [91], and Walraven [92]. A quantitative relationship has been identified for this shear lag in some studies [54, 92]. According to the aforementioned literature, the influence from this shear lag becomes significant when the concrete cover thickness becomes large. Therefore, when improving the existing crack width calculation models to predict the crack widths of large cover cases, the effect of shear lag can be an influencing factor.

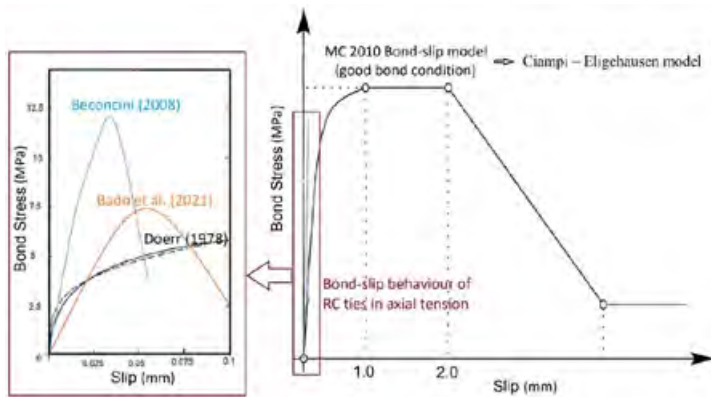


Figure 4. Predicted bond-slip behaviour in MC 2010 and the obtained bond-slip behaviour in axial tensile tests.

4. COMPARISON OF THE CRACK WIDTH CALCULATION MODEL PREDICTIONS WITH EXPERIMENTAL RESULTS

Cracking in RC structures has been studied for several decades. Consequently, a large body of experimental studies has been reported in the literature. However, in the recent past, axial tensile tests with multiple bars have become popular in studies of cracking behaviour, since they represent the tensile region of actual cracking behaviour in practical RC members [43, 63]. Therefore, such experimental studies were selected from Gribniak et al. [93], Garcia et al. [90], Dawood and Marzouk [94, 95], Bisch [65], Barre et al. [96] and Tan et al. [27]. Table 3 shows the details of the selected experiments, including the measured maximum crack widths and the predictions according to the aforementioned EC2, MC2010, ACI, JSCE and BS code predictions. As shown in Table 3, the specimens have been listed in ascending order of the concrete cover thickness. The RC specimens have been categorized into three sections, based on concrete cover thickness: Category 1 (15 mm to 39 mm), Category 2 (40 mm to 59 mm) and Category 3 (60 mm to 90 mm). It is important to mention that, in Gribniak et al. [93], the maximum crack width is obtained from the direct readings of the Digital Image Correlation system and, in Dawood and Marzouk [94], the maximum crack width above tensile reinforcement is obtained by multiplying the directly observed maximum crack spacing with a factor of 0.7, as specified in the same literature. The maximum crack widths mentioned in Tan et al. [27] are the 95 percent fractile of measured crack width at the concrete surface above tensile reinforcement. However, in both Barre et al. [96] and Garcia and Caldentey [90], only the measured average crack width is mentioned. Therefore, in order to obtain the maximum measured crack width, the average value has been multiplied by a factor of 1.7, as specified in Beeby [33].

According to Figure 5, deciding the most suitable crack width prediction model is quite complicated when concrete cover thickness becomes large. When considering the predictions of EC2, except for one case, every other prediction is on the conservative side, and, when the concrete cover increases, the overestimation also increases. Figure 5 and the error values mentioned in Table 3 note this behaviour. When one considers the MC2010 predictions, two cases in Category 3 (Cases 15 and 16) are considerably underestimated. However, it can be seen that MC2010 considers that these two cases are in the crack formation stage, as the steel stress is 200 MPa. When considering the predictions of the JSCE code, except for one case, the predictions in Category 3 are on the conservative side. However, for Case 13, the crack width has been significantly overestimated. In both ACI and BS codes, five out of seven cases in Category 3 overestimate the predictions. While considering the predictions of the models, it could be observed that the empirically based ACI and BS codes give relatively best fit for the experimental crack widths. This could be because both ACI and BS models have considered the test results of relatively large cover specimens (84 mm and 89 mm, respectively) while developing the models. However, in considering the predictions of the overall cases and based on the error percentages in Table 3, it is clear that the existing codes need to improve the models for applying RC specimens with large concrete covers.

The aforementioned study has been conducted only for the RC specimens subjected to axial tension. For the specimens subjected to bending, it is important to discuss the effect of curvature on crack width. The empirically based models which are in ACI and BS codes, considered the data from bending tests to develop their models. Furthermore, the model in ACI and BS codes use the ' β ' parameter and $(d - d_n)/(d_1 - d_n)$ factor, respectively to include the effect of curvature. Similarly, MC 2010 recommends multiplying the calculated crack width obtained from the proposed equation with $(h - x)/(d - x)$ ratio to include the curvature effect. Here, 'h' denotes the total depth of the cross section, 'd' is the effective depth and 'x' is the depth of the neutral axis. Three of these aforementioned factors in ACI, BS and MC 2010 mean the ratio of the distance between the neutral axis and tension face to the distance between the neutral axis and centroid of reinforcing steel. When consider the RC specimens with large cover thickness, the distance between the neutral axis and tension face becomes relatively larger than the distance between the neutral axis and centroid of reinforcing steel. Therefore, the aforementioned parameters in ACI, BS and

MC2010 cause to predict large surface crack widths for the specimens with large cover thickness. However, the model in JSCE code does not specifically suggest any method to consider the effect of curvature on crack width. EC2 model considers this effect of curvature would influence to crack spacings. EC2 crack spacing model consist with the 'k₂' parameter, which cause to predict lower crack spacings for the specimens subjected to bending. The study conducted in Naotunna et al. [43] shows that EC2 model predictions give a good agreement with the experimental results of specimens subjected to bending.

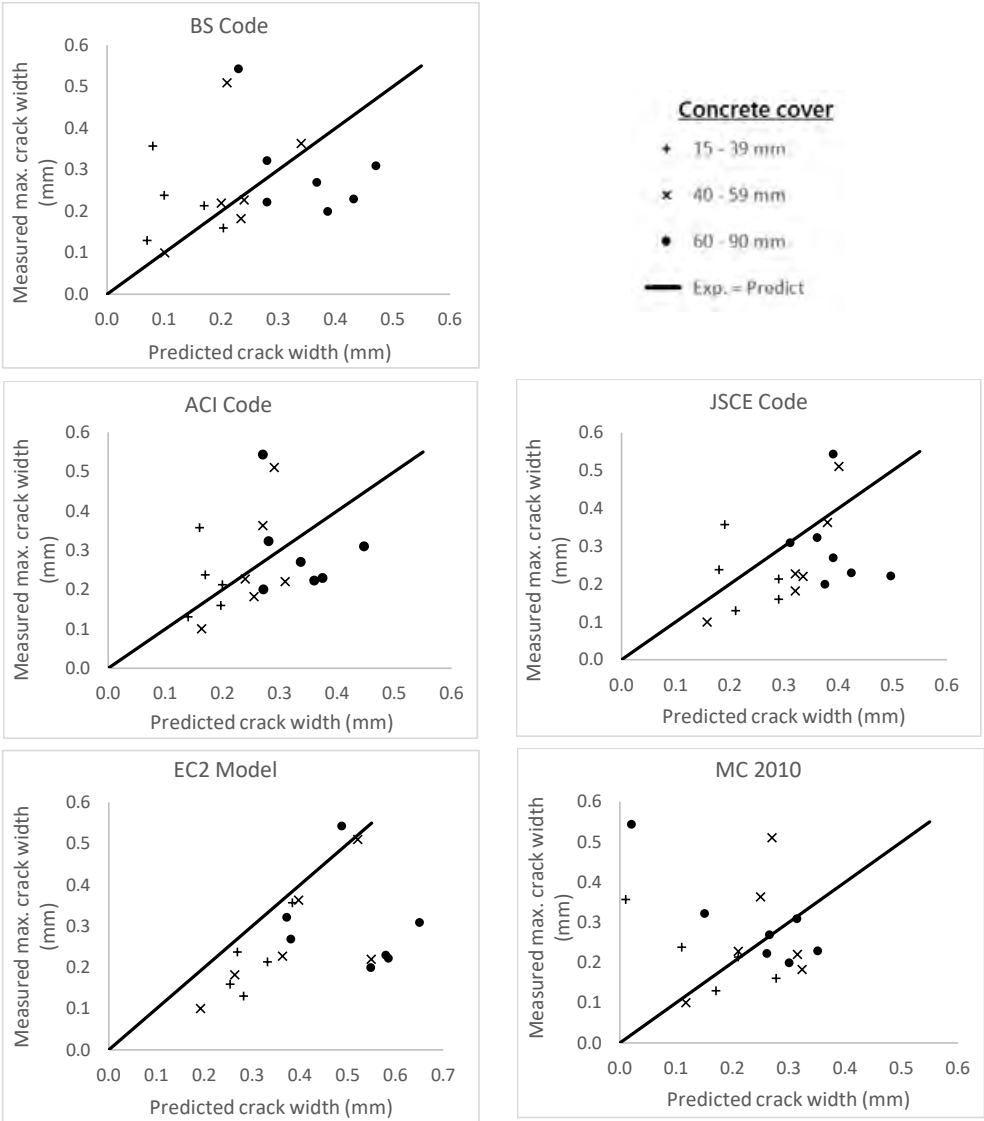


Figure 5 - Predicted versus measured maximum crack widths

Table 3 - Details of the selected RC specimens with measured and predicted maximum crack widths

Case ^a	Literature ^b	Specimen size [width × height × length] (m)	Concrete cover (mm)	Steel stress (MPa)	Concrete strength (MPa)	No. of bars	Bar dia. (mm)	Measure- d max crack width (mm)	Predicted crack width (mm)					Error ^c %				
									EC2	MC 2010	ACI	JSCB	BS	EC2	MC 2010	ACI	JSCB	BS
1	A	0.15 × 0.15 × 1.21	15	320	42.51	4	10	0.13	0.28	0.17	0.14	0.21	0.07	-118	-31	-8	-62	46
2	A	0.15 × 0.15 × 1.21	30	320	36.36	4	10	0.21	0.33	0.21	0.20	0.29	0.17	-56	1	6	-36	20
3	B	0.35 × 0.45 × 5.22	32	200	33.77	8	16	0.36	0.39	0.01	0.16	0.19	0.08	-8	97	55	47	78
4	B	0.35 × 0.45 × 5.22	32	200	41.78	8	25	0.24	0.27	0.11	0.17	0.18	0.10	-13	54	29	24	58
5	C	0.9 × 0.26 × 0.10	38	333	75.00	6	25	0.16	0.25	0.28	0.20	0.29	0.20	-59	-73	-23	-81	-28
6	A	0.15 × 0.15 × 1.2	40	320	42.51	4	10	0.23	0.36	0.21	0.24	0.32	0.24	-60	7	-6	-41	-6
7	D	0.4 × 0.4 × 2.0	40	321	74.30	8	20	0.22	0.55	0.32	0.31	0.34	0.20	-150	-43	-40	-52	9
8	D	0.4 × 0.4 × 2.2	40	157	74.30	8	32	0.10	0.19	0.12	0.16	0.16	0.10	-92	-17	-63	-58	-1
9	C	0.9 × 0.38 × 0.10	45	333	65.00	6	30	0.18	0.26	0.32	0.26	0.32	0.24	-45	-77	-40	-76	-29
10	E	0.355 × 0.355 × 3.5	45	300	40.00	8	16	0.51	0.52	0.27	0.29	0.40	0.21	-2	47	43	21	59
11	A	0.15 × 0.15 × 1.24	50	320	36.44	4	10	0.36	0.40	0.25	0.27	0.38	0.34	-9	31	26	-5	6
12	C	0.9 × 0.26 × 0.9	63	333	75.00	6	25	0.20	0.55	0.30	0.27	0.37	0.39	-174	-50	-36	-87	-93
13	E	0.355 × 0.355 × 3.6	65	254	46.30	4	25	0.22	0.58	0.26	0.36	0.50	0.28	-162	-17	-62	-123	-26
14	C	0.9 × 0.38 × 0.9	75	333	65.00	6	30	0.23	0.58	0.35	0.38	0.42	0.43	-152	-52	-63	-84	-87
15	B	0.35 × 0.45 × 5.22	82	200	32.91	8	16	0.54	0.49	0.02	0.27	0.39	0.23	10	96	50	28	58
16	B	0.35 × 0.45 × 5.22	82	200	44.39	8	25	0.32	0.37	0.15	0.28	0.36	0.28	-15	54	13	-11	13
17	D	0.4 × 0.4 × 2.1	90	293	74.30	8	20	0.31	0.65	0.31	0.45	0.31	0.47	-110	-1	-44	0	-52
18	D	0.4 × 0.4 × 2.3	90	212	74.30	8	32	0.27	0.38	0.26	0.34	0.39	0.37	-41	2	-24	-44	-36

Notes.

The specimens have been arranged in ascending order, based on cover thickness

^a Cases 1 to 5 – Category 1, Cases 6 to 11 – Category 2, Cases 12 to 18 – Category 3

^b Gribniak et al. (2020) – **A**, Garcia et al. (2020) – **B**, Dawood et al. (2011) – **C**, Tan et al. (2018) – **D**, Barre et al. (2016) – **E**

^c Error = (experimental value – predicted value)/experimental value.

5. ALLOWABLE CRACK WIDTHS IN THE EXISTING CODES

It is clear that the surface crack width increases with the increase in concrete cover thickness (Sections 3 and 4). When considering the allowable crack width limits in the discussed codes, with the exception of the JSCE code, every other code's allowable limit does not increase with the concrete cover thickness. The allowable crack width limits of an RC structure (in the absence of a water tightness requirement) have been decided for durability and aesthetic acceptance.

It can be observed that the prescribed allowable crack width limits in the codes have been changed from time to time. For example, Model Code 1978 [9] and MC 90 [5] recommend 0.1 mm and 0.3 mm crack widths, respectively, for severe exposure classes. Further, the allowable limits in each code differ from each other. For structures exposed to adverse environmental conditions, EC2, MC2010 and BS codes recommend limiting the crack widths to 0.3 mm (Table 7.1 N in EC2, Cl. 7.6.4.1.4 in MC2010 and Cl. 3.2.4 in BS codes). The allowable crack width limit of the JSCE code is shown in Table 4. Moreover, for severe exposure conditions, the ACI 318 code recommends limiting the crack width to 0.33 mm (Cl. 10.6.4), while the ACI 224 report recommends limiting it to 0.15 mm (Table 4.1 in ACI 224R [24]). However, the Norwegian National Annex [97] follows slightly different criteria than EC2. It has introduced a k_c coefficient ($k_c = c_{nom} / c_{min,dur} \leq 1.3$) and allows the EC2-specified crack width limit to be multiplied by the k_c coefficient.

To compare the applicability of allowable crack width limits, the discussed experimental results in Table 3 have been considered. According to the ACI code [8], the limitation of the steel stress at the serviceability limit state is considered as 2/3 of the yield strength of the reinforcement. Therefore, to match this requirement, Cases 1, 2 and 4 from Category 1, Cases 7, 9, and 11 from Category 2 and Cases 12, 14 and 17 from Category 3 have been selected. The steel stress in these selected cases lies within 293 MPa to 333 MPa. The experimental crack widths of these selected cases have been compared with the allowable crack width limits of the aforementioned codes, as shown in Figure 6. The selected allowable limits in Figure 6 are for the adverse/corrosive environmental conditions. Considering the limitation according to the ACI 224 code, only the case with 15 mm concrete cover thickness satisfies the criterion. The EC2, MC2010 and BS codes have a similar limit for the allowable crack width (0.3 mm) for specimens in adverse environmental conditions. Except for the two cases with 50 mm and 90 mm concrete cover thickness, other cases satisfy this guideline. When considering the ACI 318 limit, which is 0.33 mm, only one case, with a 50 mm cover, shown in Table 4 does not satisfy the criteria. When considering the JSCE guideline, which is shown in Table 4, all the cases in Category 3 satisfy this criterion, but the cases in Category 1 and 2 do not satisfy it.

Therefore, in order to identify the most suitable allowable crack width limit, it is important to investigate the reasons for the aforementioned differences in each code. Further, to discover the effect of concrete cover thickness on the allowable crack width, an extensive literature survey has been carried out. The focus is to identify how the existing limits are placed and to check whether the increased crack width of specimens with an increase in concrete cover has an effect on the durability and the aesthetic aspect of an RC structure.

Table 4 - The limit value of crack width as per JSCE standards (Table 8.3.2 in JSCE standard)

	Environmental condition		
	Normal	Corrosive	Severely corrosive
Deformed bars and plain bars	0.005c	0.004c	0.0035c
Note – 'c' is concrete cover thickness			

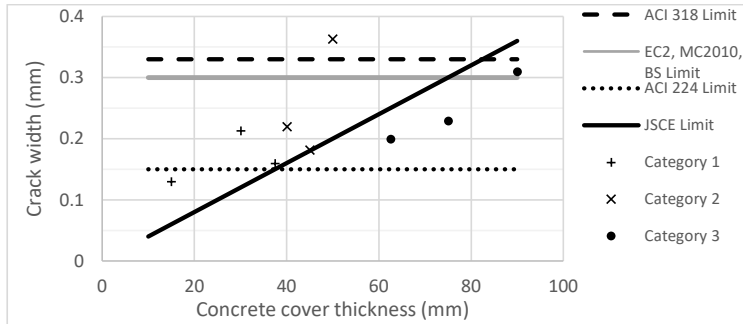


Figure 6 - Experimental crack widths of the selected specimens from Categories 1, 2 and 3 (Table 3) and the allowable crack width limits of different codes in adverse environmental conditions

6. CRACK WIDTH LIMITATION CONSIDERING THE DURABILITY

There is consensus that cracks appearing in reinforced concrete structures lead to the penetration of CO₂, chloride, corrosive agents and water to the reinforcement and can initiate reinforcement corrosion [3, 98]. Reinforcement corrosion could lead to a reduction in the amount of steel in the reinforcement and the corrosive products expanding in volume. To reduce the adverse effect of cracking, the current practice is to limit the width of the crack. Further, increasing the concrete cover is one of the main measures that has been identified to enhance the durability of an RC structure. However, as per the previous discussion, the crack width also increases with the simultaneous increase in concrete cover. This reveals that the discussed actions considered to increase durability contradict one another. Therefore, in order to identify how the existing allowable crack width limits are decided, based on durability, a literature survey has been carried out.

6.1 Previous studies on crack width and reinforcement corrosion

In the available literature, various types of experiments that have studied the effect of crack width on reinforcement corrosion can be identified. However, when considering the results of some of these experiments, the effect of crack width on reinforcement corrosion is quite complicated. Depending on the experimental duration and the outcome of the results of the available experiments, the authors have divided them into four categories: 1. the 'crack width' does not have a 'relatively short-term' effect on corrosion; 2. the 'crack width' has a 'relatively short-term' effect on corrosion; 3. the 'crack width' does not have a 'long-term' effect on corrosion; and 4. the 'crack width' has a 'long-term' effect on corrosion, as given in Table 5. Experiments conducted for up to 10 years are categorized as 'relatively short-term' experiments; those which have continued for longer, or experiments conducted for more than 10 years, are considered 'long-term experiments'.

When considering the experiments of Category 1, the conclusion is that the cracks cause the initiation of corrosion, regardless of crack width. The studies in this category have observed a similar amount of corrosion in locations with different crack widths. However, it is important to identify that most of the experiments categorized in Category 1 had released the load during exposure. Therefore, even where the surface crack width remains open, there is a possibility of closing the internal crack. This could be a reason why a similar amount of corrosion is observed at cracks with different surface crack widths. The experiment in Category 4 concludes that the crack width has an effect on long-term corrosion. However, the specimens tested in the experiment used air-entrained concrete, and only 11 specimens out of 82 were able to be tested, due to excessive damage. It is quite impossible to explain the damage to this number of mentioned specimens within 25 years (service life), with the conventional method of corrosion.

Table 5 - The details and the outcome of previous experiments on crack width and corrosion

Category ¹	Study	Experiment Details					Results	Remarks
		Specimen size ^{a, b}	Cover ^b	Crack width ^b	Exposure	Period (years)		
1	Makita et al. [99]	Length 750		0.05-0.3	Seawater	2.7	Corrosion does not relate to crack width	Specimens were unloaded during exposure.
	Berke et al. [100]	762×152×152	38	0.2 (mean)	NaCl solution	1.3		
	Lin [101]	914×76×152		0.1 0.15 0.18	Seawater	2 - 10	Corrosion does not relate to crack width	Specimens were loaded during exposure.
	Tremper [102]	200×200×63	28	0.127-0.508	Coastal exposure	10	Corrosion only in cracked locations.	Specimens were unloaded.
	Francois et al. [103]	3000×150×280		< 0.5	NaCl & CO ₂ prone	10	No relationship to crack width.	
	Kahhaleh [104]		50	Around 0.33	NaCl solution	1.1	Corrosion does not relate to crack width	Both loaded and unloaded.
	Chen et al. [105]	1100×180×100	30	0.1-0.4	NaCl solution	3	Corrosion does not relate to crack width	Cracks induce corrosion
2	Ohta (i) [106]	1000×150×150	20 40	0-0.1 0.1-0.2 0.2-0.3	Coastal	10	20 mm cover, every cracked location is similarly corroded.	40 mm cover, corrosion relates to crack width.
	Schiessl (i) [25, 107]	1950×250×150	25 35	0.075-0.55	Mixed	4	Corrosion and crack width are related.	
	Carevic and Ignjatovic [108]	500×100×100	25	0.05 - 0.3	2% CO ₂ with 65% humidity	0.1	Corrosion is 3 times higher in 0.3 mm cracked locations.	
	Schiessl and Raupach [109]	700×97×150	15	0.1 - 0.5	Saltwater	2	Corrosion increases with increasing crack width.	
	Swamy [110]	Length 760	50 70	0.11-0.25	Marine		Corrosion above 0.15 mm cracks.	
	Misra et al. [111]	2100×100×200	10		Marine	1	Crack width above 0.5 mm shows severe corrosion.	
	Vennesland et al. [112]	500×100×100		0.1-2.0	Seawater	0.3		
	Miyagawa [113]	1000×50×50	20	< 0.3	NaCl solution		Corrosion above 0.2 mm cracks.	
	Li et al. [114]	400×100×100	40	0-0.5	NaCl solution	1.8	Corrosion and crack width are related	Plain bars were used.
	Houston et al. [115]		25 50 75		NaCl solution	2.8	50 / 75 mm covers, corrosion above 0.13 mm cracks	25 mm cover, corrosion in every location.
3	Ohta et al. [106]	1000×150×150	20 40	0-0.1 0.1-0.2 0.2-0.3	Coastal	20	Corrosion and crack width are not related.	Every cracked location is similarly corroded.
	Schiessl (ii) [25, 107]	1950×250×150	25 35	0.075-0.55	Mixed	10		
4	O'Neil [116]		19	0-0.4 Above 0.4	Tidal wave with freeze and thaw	25	Corrosion above 0.4 mm cracks. 11/82 specimens tested.	air-entrained concrete.

Notes ^a Length × width × height of test specimens ^b units is 'mm'

Category¹

1. Crack width has no effect on corrosion (relatively short-term), 2. Crack width has an effect on corrosion (relatively short-term), 3. Crack width has no effect on corrosion (long-term), 4. Crack width has an effect on corrosion (long-term)

By observing Categories 2 and 3, it can be concluded that the corrosion initiation takes place at cracks and, at this stage, the 'crack width' plays a vital role. However, when the testing time increases, the crack width does not influence corrosion. This could be the main reason why MC 1978 prescribes limiting the crack width in severe conditions to 0.1 mm and releases it in MC 90 and MC2010 to 0.3 mm. It can be assumed that MC 1978 had considered the short-term tests, and this limitation was changed after considering the results of long-term experiments. The two main causes for reinforcement corrosion are chloride-induced damage and carbonation [117]. When the Chloride ions in the surrounding environment reach to the reinforcement, that cause to damage the protective layer around the reinforcement. The carbonation means the change in the alkaline pH of concrete to neutral pH [118]. This mainly happens when the atmospheric Carbon Dioxide penetrate into concrete and react with the Calcium Hydrate in concrete. This reaction cause to increase the Calcium Carbonate fraction in concrete which cause to neutralize the pH value. The protective layer around the reinforcement gets damaged within the neutralized pH environment and this cause to initiate corrosion. When there are cracks in concrete, the time required to penetrate the carbonation or chloride layer to the rebar is drastically reduced, and corrosion can be initiated in the early stages [3]. At this stage, as per the findings in Category 2, corrosion can be proportional to the crack width. However, in long-term, the penetration depth will reach to the reinforcement. Then, as per the findings in Category 3, after the penetration depth reach to the reinforcement, there is no difference in the amount of corrosion in locations with small crack widths and large crack widths or in uncracked locations.

6.2 Deciding the allowable crack width limits on durability for structures with different concrete covers

Schiessl's experiment mentioned in the report in [107] has been considered by many researchers in the field; it tried to elaborate criteria for limiting the value of crack width. In the mentioned study, the level of corrosion in the reinforcement is categorized, based on the measured corrosion height (' t_m ' - based on the prepared 'rust calibration scale' by the author in [107]), as 'passive corrosion' ($t_m < 0.01$ mm) or 'active corrosion' ($t_m > 0.01$ mm). For specimens exposed for four years, active corrosion could be observed from crack widths of 0.125 mm onwards. Further, this study tried to emphasize the possibility of increasing the limit of allowable crack width, with the increase in concrete cover. For specimens exposed for 10 years, active corrosion could be observed, even at uncracked locations. However, Schiessl identified that, when the concrete cover is 25 mm, 66% of cracks are active in corrosion when the crack width is 0.3 mm. When the concrete cover is increased to 35 mm, only 50% of cracks are shown to be active in corrosion for a 0.3 mm crack width. Based on the results of this long-term experiment, it can be stated that increasing the concrete cover has the potential to increase the limit of allowable crack width. Therefore, this study can be further improved for RC specimens with increased concrete cover thickness and develop an allowable crack width limit which is dependent on concrete cover thickness.

7. CRACK WIDTH LIMITS CONSIDERING THE AESTHETIC ASPECT

Each code of practice has specified the allowable crack width limits, based on the structure's exposure class. When deciding this allowable limit for the structure's built-in environmental conditions, where there is no risk of corrosion, the limits are given in consideration of the aesthetic acceptance of the structure. Although, RC structures are designed and constructed by experts in the field, they are used by ordinary citizens, who do not have any expertise or knowledge in the field. Therefore, users should always feel that it is safe to use them. It is obvious that unsatisfactory appearance, due to cracks, causes safety alarms and lowers the acceptance of a structure [119]. However, the aesthetic acceptance of cracks in RC structures is one of the research areas which has attracted the least attention [120]. Leonhardt [1] stated that, if the structure has a reasonable cover thickness with good quality concrete, a crack width of 0.4 mm is not

harmful to its durability (corresponding with the outcome of O’Neil [116]), but in order to avoid unnecessary concern among casual observers, the crack width should be limited to 0.2 mm. However, it is not possible to state a fixed value for all types of RC structures and for every type of user, as the viewer’s attitude can have a greater influence than what is actually observed [121]. On the other hand, it is not possible to limit the widths of controllable cracks to a fine level, as this would increase the cost of the structure. In order to justify the statement that the user’s attitude is of greater influence than the actual effect of the cracks, the study performed by Padilla and Robles [122] gives good agreement. The study was based on cracks in a low-cost housing scheme and clearly emphasized how the different sizes of crack widths affected tenants, landlords or engineers. Figure 7 illustrates different observers’ attitudes towards a crack and the actual effect of a crack on a structure. According to this figure, when the time has come for actual concern about the cracks, the users of the structure have already abandoned it.

7.1 The allowable crack width limits on the aesthetic acceptance of structures with different concrete covers

The concrete cover thickness is decided on to protect the reinforcement against corrosion, for the safe transmission of bond forces and for adequate fire resistance [7]. Therefore, even for structures that are not threatened by corrosion, large covers can be decided on, due to the safe transmission of bond forces and for adequate fire resistance. As mentioned in the introduction, according to EC2, for the safe transmission of bond forces, concrete covers can be large as 56 mm for cases with bundled bars. The surface crack width increases with the increase in concrete cover thickness. The limit of visibility of cracks is expressed by ‘crack width’ [1, 119], and a proper guide should be available to the client to decide the allowable crack widths. The study conducted by Campbell-Allen, mentioned in the report in [119], identified that the minimum crack width of a structure is a function of viewing distance, a structure’s prestige and the nature of the surface (the visibility of cracks changes when they are wet or filled with impurities). The authors proposed several categories of structures, depending on their prestige, and graphically interpreted the acceptable crack widths, depending on the distance of the viewer. Figure 8 shows the proposed criterion and, as it shows for the high-prestige structures, even for longer viewing distances, the allowable crack width limits have to be limited to a relatively low level.

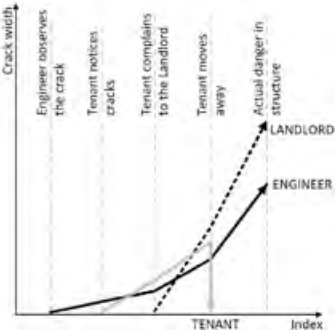


Figure 7 - Different observers’ attitudes to a crack (adapted from Padilla and Robles 1971)

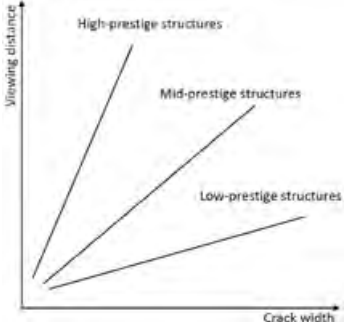


Figure 8 - Aesthetically acceptable crack width (adapted from Campbell-Allen 1979)

The outcomes of the aforementioned study by Campbell-Allen [119] can be extended for every type of structure and used to estimate the allowable maximum crack width in respect of the aesthetic aspect. Every structure (or part of the structure) can be categorized into different prestige levels, depending on its usage (purpose of the structure and number of users). For example, monumental structures, pedestrian bridges, etc. can be categorized as ‘higher prestige level’ and structures like dams, highway bridges and storage buildings can be categorized as structures with a ‘lower prestige level’. Then, the client can identify the

category of the structure and the average viewing distance, to measure the allowable crack width limit as per aesthetic satisfaction. It can be concluded that, for structures categorized at the higher prestige level, the increasing concrete cover thickness causes a comparatively higher amount of tensile reinforcement to be required, to limit the crack width. Therefore, for such cases, the use of bundled bars, etc. have to be reconsidered at the structural design stage.

8. SUMMARY AND CONCLUSIONS

The background of the widely used crack width calculation models has been discussed, starting with the complex cracking phenomenon. Empirically based crack width calculation models in ACI and BS codes and the semi-analytical models in EC2, MC2010 and JSCE codes have been examined. The crack width governing parameters in the aforementioned models have been categorized, and the extensive background study of each model led to deciding on suitable models for cases with large concrete cover thickness. Then, the necessity of considering the shear-lag effect (which is reported in several studies), identifying the proper bond-slip behaviour, has been highlighted in this paper. Based on a study comparing the experimental results with the model predictions in Section 4, it has been identified that the EC2 model predictions are more conservative, and both ACI and BS code model predictions gave a good agreement with the experimental crack widths of the specimens with concrete cover thickness above 60 mm.

It can be seen that the allowable crack width limits in the aforementioned codes of practice have changed from time to time and differ from each other. Therefore, an extensive literature survey has been conducted to investigate the background of the allowable crack width limits. According to the durability aspect, the allowable crack width limits can be identified as increasing with the concrete cover thickness, as in the JSCE code. This is based on the long-term study conducted by Schiessl (1975). However, this study was conducted for specimens with 25 mm and 35 mm cover thicknesses. The same study can be extended for specimens with different cover thicknesses, to identify the allowable crack width limits for cases with different concrete cover thicknesses.

Concrete cover thickness is decided based on durability, safe transmission of bond forces and for fire resistance. According to the EC2 model, to provide the safe transmission of bond forces, the cover thickness can be up to 55 mm. Therefore, even for structures which are not built-in severe exposure classes, the cover thickness can be large. The allowable crack width limits of such structures are mainly based on the aesthetic appearance. In order to control the crack widths of such structures effectively, the authors suggest using the study conducted by Campbell-Allen (1979) and deciding the allowable limit based on the structure's prestige level (the purpose and number of users of the structure). Finally, this study has identified and highlighted the necessary improvements in the existing crack controlling methods, to effectively control the cracks of structures with large concrete covers.

REFERENCES

1. Leonhardt F: "Cracks and crack control in concrete structures". *PCI Journal*, Vol. 33, No. 4, 1988, pp. 124-145.
2. Makhlof H M & Malhas F A: "The effect of thick concrete cover on the maximum flexural crack width under service load". *Structural Journal*, Vol. 93, No. 3, 1996, pp. 257-265.
3. Beeby A: "Concrete in the oceans technical report no. 1". *Cement and Concrete Association, Slough, UK*, No., 1978.
4. JSCE: "Standard specifications for concrete structures-2007 "design"". JSCE Guidelines for Concrete", 2007.
5. CEB-FIP: "90. Design of concrete structures. Ceb-fip-model-code 1990". *British Standard Institution, London*, 1993.

6. fib: "Fib model code for concrete structures", *Structural Concrete*, 2010.
7. CEN: "EN 1992-1-1 Eurocode 2: Design of concrete structures - part 1-1: General rules and rules for buildings", 2004.
8. ACI: "Building code requirements for structural concrete:(ACI 318-95); and commentary (aci 318r-95)", 1995.
9. Model Code: "Ceb-fip model code for concrete structures", Comité Euro-International du Béton, Paris, France; 1978.
10. BS Institute: "EN 1991-1-1 eurocode 2: Design of concrete structures, general rules and rules for buildings." UK, 1992.
11. BS: "8110: Part 1, structural use of concrete—code of practice for design and construction", 1985.
12. Gergely P & Lutz L A: "Maximum crack width in reinforced concrete flexural members". *ACI Special Publication*, Vol. 20, No., 1968, pp. 87-117.
13. Kaar P H & Hognestad E: "High strength bars as concrete reinforcement, part 7: Control of cracking in t-beam flanges"; Portland Cement Association, Research and Development Laboratories; 1965.
14. Sygula S: "Vergleichende untersuchungen über biege-rißformeln für stahlbeton". *Beton-und Stahlbetonbau*, Vol. 76, No. 5, 1981, pp. 114-117.
15. AIJ: "Aij: Standard for structural calculation of rc structures", Tokyo, 1986.
16. Balazs G L: "Cracking analysis based on slip and bond stresses". *Materials Journal*, Vol. 90, No. 4, 1993, pp. 340-348.
17. Tan R, Hendriks M A, Geiker M & Kanstad T: "Modified cracked membrane model for consistent crack width predictions of reinforced concrete structures subjected to in-plane loading". *Engineering Structures*, Vol. 196, No., 2019, pp. 109362.
18. Oh B H & Kang Y J: "New formulas for maximum crack width and crack spacing in reinforced concrete flexural members". *Structural Journal*, Vol. 84, No. 2, 1987, pp. 103-112.
19. Marakeset G & Kioumars M: "Need for further development in service life modelling of concrete structures in chloride environment". *Procedia Engineering*, Vol. 171, No., 2017, pp. 549-556.
20. Connal J & Berndt M: "Sustainable bridges: 300 year design life for second gateway bridge". *Proceedings: 7th Austroads Bridge Conference, Auckland, New Zealand 2009*.
21. Vegvesen S: "Håndbok n400 bruprosjektering". Oslo: Vegdirektoratet, 2009.
22. Danner T & Geiker M R: "Long-term influence of concrete surface and crack orientation on self-healing and ingress in cracks—field observations". *Nordic Concrete Research*, Vol. 58, No. 1, 2018, pp. 1-16.
23. Basteskår M, Engen M, Kanstad T & Fosså K T: "A review of literature and code requirements for the crack width limitations for design of concrete structures in serviceability limit states". *Structural Concrete*, Vol. 20, No. 2, 2019, pp. 678-688.
24. ACI 224: "Control of cracking in concrete structures-ACI 224r-01", *American Concrete Institute*, 2001.
25. Schießl P: "Zur frage der zulässigen rissbreite und der erforderlichen betondeckung im stahlbetonbau unter besonderer berücksichtigung der karbonatisierung des betons". Technische Universität München; 1976.
26. Debernardi P G, Guiglia M & Taliano M: "Effect of secondary cracks for cracking analysis of reinforced concrete tie". *ACI Materials Journal*, Vol. 110, No. 2, 2013, pp. 207.
27. Tan R, Eileraas K, Opkvitne O, Žirgulis G, Hendriks M A, Geiker M, Brekke D E & Kanstad T: "Experimental and theoretical investigation of crack width calculation methods for rc ties". *Structural Concrete*, No., 2018.
28. Broms B B & Lutz L A: "Effects of arrangement of reinforcement on crack width and spacing of reinforced concrete members". *Proceedings: ACI Journal Proceedings, 1965*, 1395-1410.
29. Illston J & Stevens R: "Internal cracking". *Concrete (London)*, Vol. 6, No. 7, 1972.
30. Leonhardt F: "Crack control in concrete structures, iabse surveys, no. S4/77". *International Association for Bridges and Structural Engineering*, No., 1977, pp. 26.
31. Nielsen M: "Beton 1—del 3, 2. Udgave (concrete structures 1—part 3)". Department of Civil Engineering, Technical University of Denmark, Lyngby; 2005.
32. Goto Y: "Cracks formed in concrete around deformed tension bars". *Proceedings: ACI Journal Proceedings, 1971*, 244-251.

33. Beeby A: "Crack control provisions in the new eurocode for the design of concrete structures". *ACI Special Publication*, Vol. 204, No., 2001, pp. 57-84.
34. Park R & Paulay T: "Reinforced concrete structures": John Wiley & Sons; 1975.
35. Tan R, Hendriks M A & Kanstad T: "Evaluation of current crack width calculation methods according to eurocode 2 and fib model code 2010". In: *High tech concrete: Where technology and engineering meet*. edn.: Springer; 2018: 1610-1618.
36. Base G D, Read J B, Beeby A & Taylor H: "An investigation of the crack control characteristics of various types of bar in reinforced concrete beams". In: *Research Report No 18*. Cement and Concrete Association, London: Cement and Concrete Association Wexham Springs, Slough England; 1966.
37. Borges J F: "Cracking and deformability of reinforced concrete beams": Laboratório Nacional de Engenharia Civil; 1965.
38. Base G D, Read J B, Beeby A & Taylor H: "An investigation of the crack control characteristics of various types of bar in reinforced concrete beams": Cement and Concrete Association, Wexham Springs, Slough, England; 1966.
39. de Saint-Venant M: "Mémoire sur la torsion des prismes: Avec des considérations sur leur flexion ainsi que sur l'équilibre intérieur des solides élastiques en général: Et des formules pratiques pour le calcul de leur résistance à divers efforts s' exerçant simultanément": Imprimerie nationale; 1856.
40. Beeby A W: "The influence of the parameter ϕ/ρ eff on crack widths". *Structural Concrete*, Vol. 5, No. 2, 2004, pp. 71-83.
41. Saliger R: "High grade steel in reinforced concrete". *Proceedings: Second Congress of IABSE, Berlin-Munich 1936*.
42. Watstein D & Parsons D: "Width and spacing of tensile cracks in axially reinforced concrete cylinders". *Journal of Research, National Bureau of Standards*, Vol. 31, No. 1, 1943, pp. 1-24.
43. Naotunna C N, Samarakoon S M S M K & Fosså K T: "Experimental and theoretical behavior of crack spacing of specimens subjected to axial tension and bending.". *Structural Concrete*, Vol. 1-18, No., 2020.
44. Beeby A & Scott R: "Cracking and deformation of axially reinforced members subjected to pure tension". *Magazine of Concrete Research*, Vol. 57, No. 10, 2005, pp. 611-621.
45. Taliano M: "Cracking analysis of concrete tie reinforced with two diameter bars accounting for the effect of secondary cracks". *Engineering Structures*, Vol. 144, No., 2017, pp. 107-119.
46. Rots J G & Blaauwendraad J: "Crack models for concrete, discrete or smeared? Fixed, multi-directional or rotating?". In: *Heron*. Edited by Seven-Laboratory, vol. 34. Netherlands: Delft University of Technology; 1989.
47. Unanwa C & Mahan M: "Statistical analysis of concrete compressive strengths for california highway bridges". *Journal of Performance of Constructed Facilities*, Vol. 28, No. 1, 2012, pp. 157-167.
48. Naotunna C N, Samarakoon S M S M K & Fosså K T: "Comparison of the experimental crack spacing behaviour with the theoretical predictions". In: *The Nordic Concrete Federation*. Oslo, Norway; 2019.
49. Gergely P & Lutz L A: "Maximum crack width in reinforced concrete flexural members". *Material Science Special Publication*, Vol. 20, No., 1968, pp. 87-117.
50. Beeby A W: "An investigation of cracking in slabs spanning one way". In: *Cement and Concrete Association*. 1970.
51. Borosnyói A & Snóbli I: "Crack width variation within the concrete cover of reinforced concrete members". *Építőanyag*, Vol. 62, No. 3, 2010, pp. 70-74.
52. Husain S I & Ferguson P M: "Flexural crack width at the bars in reinforced concrete beams". In. Center for Highway Research: The University of Texas at Austin; 1968.
53. Tammo K & Thelander S: "Crack opening near reinforcement bars in concrete structures". *Structural Concrete*, Vol. 7, No. 4, 2006, pp. 137-143.
54. Naotunna C N, Samarakoon S M S M K & Fosså K T: "Experimental investigation of crack width variation along the concrete cover depth in reinforced concrete specimens with ribbed bars and smooth bars". *Case Studies in Construction Materials*, No., 2021.
55. Pérez Caldentey A, Corres Peiretti H, Peset Iribarren J & Giraldo Soto A: "Cracking of rc members revisited: Influence of cover, ϕ/ρ , e_f and stirrup spacing—an experimental and theoretical study". *Structural Concrete*, Vol. 14, No. 1, 2013, pp. 69-78.

56. Debernardi P G & Taliano M: "An improvement to eurocode 2 and fib model code 2010 methods for calculating crack width in rc structures". *Structural Concrete*, Vol. 17, No. 3, 2016, pp. 365-376.
57. Tammo K & Thelandersson S: "Crack behavior near reinforcing bars in concrete structures". *ACI Structural Journal*, Vol. 106, No. 3, 2009, pp. 259.
58. Wang J J, Tao M X & Nie X: "Fracture energy-based model for average crack spacing of reinforced concrete considering size effect and concrete strength variation". *Construction and Building Materials*, Vol. 148, No., 2017, pp. 398-410.
59. Oh H J, Cho Y K & Kim S-M: "Experimental evaluation of crack width movement of continuously reinforced concrete pavement under environmental load". *Construction and Building Materials*, Vol. 137, No., 2017, pp. 85-95.
60. DIN: "En-1992-1-1/NA. 2011–01, National Annex – Nationally determined parameters – Eurocode 2: Design of concrete structures–part 1-1: General rules and rules for buildings. DIN construction standards committee ", Beuth Verlag GmbH, Berlin; 2011.
61. Broms B B: "Crack width and crack spacing in reinforced concrete members". *Proceedings: ACI Journal Proceedings*, 1965, 1237-1256.
62. Naotunna C N, Samarakoon S M S M K & Fosså K T: "Comparison of the behavior of crack width-governing parameters with existing models". In: *Proceedings of the International Conference on Sustainable Materials, Systems and Structures (SMSS2019)* vol. Rilem Publications.Vol. 4; 2019: 124-131.
63. Rimkus A & Gribniak V: "Experimental investigation of cracking and deformations of concrete ties reinforced with multiple bars". *Construction and Building Materials*, Vol. 148, No., 2017, pp. 49-61.
64. Rospars C & Chauvel D: "Ceos. Fr experimental programme and reference specimen tests results". *European Journal of Environmental and Civil Engineering*, Vol. 18, No. 7, 2014, pp. 738-753.
65. Bisch P: "The ceos. Fr research project-behaviour and assessment of massive structures: Cracking and shrinkage". *Proceedings: Crack width calculation methods for large concrete structures, Oslo, Norway 2017*, 11.
66. Lee G Y & Kim W: "Cracking and tension stiffening behavior of high-strength concrete tension members subjected to axial load". *Advances in Structural Engineering*, Vol. 12, No. 2, 2009, pp. 127-137.
67. Deluce J R: "Cracking behaviour of steel fibre reinforced concrete containing conventional steel reinforcement". University of Toronto; 2011.
68. Tan R, Hendriks M A, Geiker M & Kanstad T: "Analytical calculation model for predicting cracking behavior of reinforced concrete ties". *Journal of Structural Engineering*, Vol. 146, No. 2, 2020, pp. 04019206.
69. Bado M F, Casas J R & Kaklauskas G: "Distributed sensing in reinforced concrete members for reinforcement strain monitoring, crack detection and bond-slip calculation". *Engineering Structures*, Vol. 226, No., 2021, pp. 111385.
70. Doerr K: "Bond behavior of ribbed reinforcement under transversal pressure". *Proceedings: Nonlinear behavior of reinforced concrete structures; contributions to IASS symposium, 1978*, 3-7.
71. Beconcini M L, Croce P & Formichi P: "Influence of bond-slip on the behaviour of reinforced concrete beam to column joints". *Proceedings: Proceedings of International fib Symposium "Taylor Made Concrete Structures: New Solutions for our Society"*, Amsterdam, 2008, 19-21.
72. Ciampi V, Eligehausen R, Bertero V V & Popov E P: "Analytical model for deformed bar bond under generalized excitations". *ACI*, No., 1981.
73. Ciampi V, Eligehausen R, Bertero V V & Popov E P: "Analytical model for concrete anchorages of reinforcing bars under generalized excitations": College of Engineering, University of California Berkeley, CA, USA; 1982.
74. Rilem: "RC 6 bond test for reinforcement steel. 2. Pull-out test, 1983", *RILEM recommendations for the testing and use of constructions materials*, 1994, pp. 218-220.
75. Cervenka V, Cervenka J & Pukl R: "Atena—a tool for engineering analysis of fracture in concrete". *Sadhana*, Vol. 27, No. 4, 2002, pp. 485-492.
76. Kim J K & Park Y D: "Shear strength of reinforced high strength concrete beams without web reinforcement". *Magazine of Concrete Research*, Vol. 46, No. 166, 1994, pp. 7-16.

77. Naotunna C N, Samarakoon S M S M K & Fosså K T: "Identification of the influence of concrete cover thickness and ϕ/ρ parameter on crack spacing (forthcoming)". In: *XV International Conference on Durability of Building Materials and Components*. Barcelona; 2020.
78. Kaklauskas G, Ramanauskas R & Jakubovskis R: "Mean crack spacing modelling for rc tension elements". *Engineering Structures*, Vol. 150, No., 2017, pp. 843-851.
79. Olsen D H & Nielsen M P: "Ny teori til bestemmelse af revneafstande og revnevidder i betonkonstruktioner": Afdelingen for bærende konstruktioner, Danmarks tekniske højskole; 1990.
80. Marti P, Alvarez M, Kaufmann W & Sigrist V: "Tension chord model for structural concrete". *Structural Engineering International*, Vol. 8, No. 4, 1998, pp. 287-298.
81. McLeod C H & Viljoen C: "Quantification of crack prediction models in reinforced concrete under flexural loading". *Structural Concrete*, Vol. 20, No. 6, 2019, pp. 2096-2108.
82. Caldentey A P: "Proposal of new crack width formulas in the eurocode 2, background, experiments, etc.". *Proceedings: Crack width calculation methods for large concrete structures, Oslo 2017*, 17.
83. Bažant Z P & Oh B H: "Spacing of cracks in reinforced concrete". *Journal of Structural Engineering*, Vol. 109, No. 9, 1983, pp. 2066-2085.
84. Radnić J & Markota L: "Experimental verification of engineering procedures for calculation of crack width in concrete elements". *International Journal for Engineering Modelling*, Vol. 16, No., 2003, pp. 63-69.
85. Ouyang C & Shah S P: "Fracture energy approach for predicting cracking of reinforced concrete tensile members". *Structural Journal*, Vol. 91, No. 1, 1994, pp. 69-78.
86. Shah S P, Swartz S E & Ouyang C: "Fracture mechanics of concrete: Applications of fracture mechanics to concrete, rock and other quasi-brittle materials": John Wiley & Sons; 1995, pp.
87. Beeby A: "The prediction and control of flexural cracking in reinforced concrete members". *ACI Special Publication*, Vol. 30, No., 1971, pp. 55-76.
88. Caldentey A P & García R: "Cracking of rc structures: Differences between tension and flexure". *Proceedings: Design and construction of sustainable concrete structures: causes, calculation and consequences of cracks, Oslo Norway 2019*, 3.
89. García R & Caldentey A P: "Cracking of rc: Tension vs. Flexure", Madrid: Technical University of Madrid (UPM); 2018.
90. García R & Caldentey A P: "Influence of type of loading (tension or bending) on cracking behaviour of reinforced concrete elements. Experimental study". *Engineering Structures*, Vol. 222, No., 2020, pp. 111134.
91. Beeby A, Alander C, Giuriani E, Plizzari G & Pantazopoulou S: "The influence of the parameter ϕ/ρ_{eff} on crack widths. Author's reply and discussion". *Structural Concrete (London, 1999)*, Vol. 6, No. 4, 2005, pp. 155-165.
92. Walraven J: "Model code 2010-first complete draft-volume 2: Model code", vol. 56: fib Fédération internationale du béton; 2010.
93. Gribniak V, Rimkus A, Caldentey A P & Sokolov A: "Cracking of concrete prisms reinforced with multiple bars in tension—the cover effect". *Engineering Structures*, Vol. 220, No., 2020, pp. 110979.
94. Dawood N & Marzouk H: "Crack width model for thick reinforced concrete plates subjected to in-plane forces". *Canadian Journal of Civil Engineering*, Vol. 38, No. 11, 2011, pp. 1262-1273.
95. Dawood N & Marzouk H: "Experimental evaluation of the tension stiffening behavior of hsc thick panels". *Engineering Structures*, Vol. 33, No. 5, 2011, pp. 1687-1697.
96. Barre F, Bisch P, Chauvel D, Cortade J, Coste J F, Dubois J P, Erlicher S, Gallitre E, Labbé P & Mazars J: "Control of cracking in reinforced concrete structures: Research project ceos. Fr": John Wiley & Sons; 2016.
97. Norge S: "NS-EN 1992-1-1: 2004 and NA: 2008". "Eurocode 2", 2008.
98. Hornbostel K & Geiker M: "Influence of cracking on reinforcement corrosion". *Proceedings: Crack width calculation methods for large concrete structures, Oslo 2017*, 53.
99. Makita M, Mori Y & Katawaki K: "Marine corrosion behavior of reinforced concrete exposed at tokyo bay". *ACI Special Publication*, Vol. 65, No., 1980, pp. 271-290.
100. Berke N S, Dallaire M, Hicks M & Hoopes R: "Corrosion of steel in cracked concrete". *Corrosion*, Vol. 49, No. 11, 1993, pp. 934-943.

101. Lin C: "Bond deterioration due to corrosion of reinforcing steel". *ACI Special Publication*, Vol. 65, No., 1980, pp. 255-270.
102. Tremper B: "The corrosion of reinforcing steel in cracked concrete". *Proceedings: ACI Journal* *Proceedings*, 1947, 18 (10): 1137-1144.
103. Francois R & Arliguie G: "Reinforced concrete: Correlation between cracking and corrosion". *ACI Special Publication*, Vol. 126, No., 1991, pp. 1221-1238.
104. Kahhaleh K Z: "Corrosion performance of epoxy-coated reinforcement". The University of Texas at Austin 1995.
105. Chen E, Berrocal C G, Löfgren I & Lundgren K: "Correlation between concrete cracks and corrosion characteristics of steel reinforcement in pre-cracked plain and fibre-reinforced concrete beams". *Materials and Structures*, Vol. 53, No. 2, 2020, pp. 1-22.
106. Ohta T: "Corrosion of reinforcing steel in concrete exposed to sea air". *ACI Special Publication*, Vol. 126, No., 1991, pp. 459-478.
107. Schiessl P: "Admissible crack width in reinforced concrete structures. Contribution ii, 3-17". *Proceedings: Preliminary reports Vol II, Inter-association Colloquium on the Behaviour of in Service of Concrete Structures, 1975*.
108. Carević V & Ignjatović I: "Influence of loading cracks on the carbonation resistance of rc elements". *Construction and Building Materials*, Vol. 227, No., 2019, pp. 116583.
109. Schiebl P & Raupach M: "Laboratory studies and calculations on the influence of crack width on chloride-induced corrosion of steel in concrete". *Materials Journal*, Vol. 94, No. 1, 1997, pp. 56-61.
110. Swamy R: "Durability of rebars in concrete.". *Proceedings: The GM Idorn International Symposium on Durability of Concrete*, sponsored by Committee 201 on Durability, held at the 1990 Annual ACI Convention in Toronto, Ontario, Canada, 1992.
111. Misra S & Uomoto T: "Reinforcement corrosion under simultaneous diverse exposure conditions". *ACI Special Publication*, Vol. 126, No., 1991, pp. 423-442.
112. Vennesland O & Gjoro O: "Effect of cracks in submerged concrete sea structures on steel corrosion". *Materials Performance*, Vol. 20, No. 8, 1981, pp. 49-51.
113. Miyagawa K O T: "Chloride corrosion of reinforcing steel in cracked concrete". *ACI Special Publication*, Vol. 65, No., 1980, pp. 237-254.
114. Liu W & Wang S: "The effect of crack width on chloride-induced corrosion of steel in concrete". *Advances in Materials Science and Engineering*, Vol. 2017, No., 2017.
115. Houston J T, Atimtay E & Ferguson P M: "Corrosion of reinforcing steel embedded in structural concrete": Center for Highway Research, University of Texas at Austin; 1972, pp.
116. O'Neil E F: "Study of reinforced concrete beams exposed to marine environment". *ACI Special Publication*, Vol. 65, No., 1980, pp. 113-132.
117. Eto S, Matsuo T, Matsumura T, Fujii T & Tanaka M Y: "Quantitative estimation of carbonation and chloride penetration in reinforced concrete by laser-induced breakdown spectroscopy". *Spectrochimica Acta Part B: Atomic Spectroscopy*, Vol. 101, No., 2014, pp. 245-253.
118. Marcus P: "Corrosion mechanisms in theory and practice": CRC Press; 2011.
119. Campbell-Allen D: "The reduction of cracking in concrete". Sydney: School of Civil Engineering, University of Sydney; 1979.
120. EICC & Favre R: "Ceb design manual on cracking and deformations": École Polytechnique Fédérale de Lausanne; 1985.
121. Johnston J: "Mechanism of vision—a review". In: *Sensory evaluation of appearance of materials*. edn.: ASTM International; 1973.
122. Padilla J D & Robles F: "Human response to cracking in concrete slabs". *ACI Special Publication*, Vol. 30, No., 1971, pp. 43-54.

Paper 3: Experimental and theoretical behavior of crack spacing of specimens subjected to axial tension and bending.

Naotunna, C.N., Samarakoon, S.M.S.M.K., and Fosså, K.T. (2020)

In: *The Journal of Structural Concrete*, pp. 775-791, DOI: [10.1002/suco.201900587](https://doi.org/10.1002/suco.201900587).

Experimental and theoretical behavior of crack spacing of specimens subjected to axial tension and bending

Chavin N. Naotunna  | Samindi M. K. Samarakoon | Kjell T. Fosså

Department of Mechanical and Structural Engineering and Material Science, University of Stavanger, Stavanger, Norway

Correspondence

Chavin N. Naotunna, Kjell Arholmgate 41, 4036 Stavanger, Norway.
Email: chavin.guruge@uis.no

Abstract

Crack spacing has been identified as an important parameter in predicting the crack widths in reinforced concrete (RC) structures. An experimental program has been conducted to investigate the crack spacings when reinforced concrete beams are subjected to both axial tension and flexure. The stochastic nature of cracking behavior makes the experimental program complicated. A large sample size of the crack spacing data was recorded, in order to give a statistical overview. Recent studies in the literature were used to verify the experimental results. The existing crack spacing prediction models have been developed based on different theoretical approaches, namely bond-slip, no-slip, and combined approaches. In this study, Eurocode 2, Model Code 2010, Japanese Code, Eurocode 2 with German Annex and Beeby's crack spacing models were selected, as they represent each theoretical approach. Experimental results of this study and from selected literature were compared with the aforementioned prediction models. Japanese Code gave better predictions for axial tensile tests. For the four-point bending test, all the calculation models gave good agreement with the results, except for Eurocode 2 with German Annex.

KEYWORDS

axial tension, bar diameter, bending, concrete cover thickness, crack spacing, crack spacing models, experiments, RC specimens

1 | INTRODUCTION

Cracks occur due to the service load in reinforced concrete (RC) structures being controlled at the design stage. Widely used crack controlling methods limit the “calculated crack width” to a prescribed “allowable crack width”. There are various types of crack width calculation models, based on different approaches. For example, the American Concrete Institute (ACI)¹ and the British

Standards Institute (BS)² models are based on an empirical approach. The governing standards in Europe, which are Eurocode 2 (EC2)³ and Model Code 2010 (MC 2010),⁴ are based on a semi-analytical approach. Similarly, the Japanese Society of Civil Engineers' code (JSCE)⁵ is based on a semi-analytical approach. The mentioned semi-analytical models predict the crack width by integrating the differences in strain between reinforcement and concrete between two cracks.⁶ Therefore, these models identify the crack width by multiplying the crack spacing with the mean strain difference between reinforcement and concrete. Many researchers have identified that the crack width is governed by the crack spacing parameter rather than by the mean strain difference between concrete and

Discussion on this paper must be submitted within two months of the print publication. The discussion will then be published in print, along with the authors' closure, if any, approximately nine months after the print publication.

reinforcement.⁷ The concrete strength has been identified as a parameter which affects the crack width.^{8,9} However, Tammo and Thelandersson¹⁰ have identified that, when the crack spacing and reinforcement type are constant while the concrete strength differs, the crack width is the same. These facts reveal the importance of the crack spacing parameter.

As mentioned previously, the current method of controlling the adverse effects from cracks is only to limit the width of the crack. However, many researchers are focusing on whether the distribution of cracks (densely or sparsely spaced cracks) has an influence on durability. Recent studies have proved that crack spacing (distribution of cracks) also has an influence on the corrosion rate of the reinforcement. Therefore, identifying a good crack spacing prediction model can be advantageous in other ways than just estimating the crack width. When predicting the distribution of cracks with crack spacing models, it is important to keep in mind that many previous studies have proved that the cracks coincide with the stirrup locations. For example, the results of the experiments conducted in Makhlof and Malhas,¹² for concrete covers of 30, 50, and 60 mm, and those conducted by Caldentey et al.,¹³ for 20-mm covers prove the aforementioned statement. Therefore, the crack spacing models might not predict the distribution of cracks accurately. However, the same study¹³ proved that this effect is removed when the concrete cover becomes large (i.e., 70 mm). Therefore, a good crack spacing prediction model can be used to estimate the distribution of cracks for structures with larger concrete covers. When building structures in adverse environmental conditions, large concrete cover thicknesses are required. Concrete cover thickness can be as large as 120 mm, according to the Norwegian Public Road Administration guidelines.¹⁴ For example, the Hafsrfsjord Bridge in Norway is constructed with a concrete cover thickness of 90 mm.¹⁵ Therefore, as the cracks do not coincide with the stirrup positions in large covers, a good crack spacing prediction model can be used to predict the distribution of cracks.

Cracking in RC structures is an ongoing topic, which started many decades ago. There is already a considerable body of previous literature, which can be found on the effects of crack spacing governing parameters. For example, recent studies^{13,16} have identified that crack spacing increases with the concrete cover, both in flexure and axial tension, respectively. Recent studies^{17,18} have been conducted to identify the effect of the reinforcement layout, in both flexure and axial tension, respectively. Likewise, the effect of the reinforcement surface,¹⁹ concrete strength,^{8,10} spacing of tensile reinforcement²⁰ and so on have been studied previously. It is important to note that

there are many more relevant studies in the literature, other than those mentioned.

As there are numerous studies which have focused on parametric behaviors, this study does not focus on such effects. However, cracking behavior in RC structures has a stochastic behavior, because of the anisotropic nature of concrete. For this reason, researchers sometimes have disagreements on the effects of certain parameters. The discussion paper by Beeby et al.²¹ is a good example of such a situation. The answer to such issues could be the usage of a large data sample for one specific condition. When the amount of data increases in such experiments of a stochastic nature, the sample can be considered as reaching close to its population. When considering the statistical parameters (mean, SD, so on.) from such a sample, these can be considered as representing the population.

One of the main objectives of this study is to identify the crack spacing, while emphasizing the importance of the “sample size” of the data. Therefore, practical size beams were tested in axial tension and bending. In order to increase the amount of data for better representation, several identical specimens were tested. Then, after statistically proving that the data distribution was normal, the mean and maximum crack spacing values were obtained. The next objective was to evaluate the existing crack spacing prediction model. From a theoretical investigation, several existing crack spacing models had been identified, which are based on different theoretical approaches. The results of the conducted experiment and the results of similar studies in recent literature were used to examine the predictions of different crack spacing models.

2 | THE THEORETICAL APPROACH TO CRACK SPACING CALCULATION MODELS

As mentioned earlier, the semi-analytical crack width calculation models predict the crack width, by multiplying the crack spacing with the mean strain difference. The theoretical approach to crack spacing estimation has mainly been based on two approaches: namely, bond-slip approach, and no-slip approach. Both approaches are based on the two assumptions that a crack is formed when the stress in concrete reaches its tensile strength and at the crack total force is carried only by the reinforcement. The bond-slip approach was first introduced in 1936 by Saliger.²² The main idea of this approach is that the slip occurs between reinforcement and concrete. It has been considered that the slip is largest at the crack and decreases when moving away from the crack. Due to this slip, the concrete strain is not similar to the reinforcement strain at the crack. When the slip is zero between two cracks (at the transfer length away

from the crack), the concrete strain can be considered similar to the reinforcement strain (Figure 1a). According to this approach, the theoretical crack width is considered similar along the concrete cover thickness. By considering these facts and assuming the bond between reinforcement and concrete within the transfer length as a constant (τ_m), Equation (1) can be derived for the transfer length (S_a).

$$S_a = \frac{f_{ct}\varphi}{4\tau_m\rho_{eff}} \quad (1)$$

where “ τ_m ” is the mean bond stress, “ f_{ct} ” is the tensile strength of concrete, “ φ ” is the tensile reinforcement diameter and “ ρ_{eff} ” is the effective reinforcement ratio ($\rho_{eff} = A_s / A_{c,eff}$, where A_s and “ $A_{c,eff}$ ” are the tensile reinforcement area and effective tensile area of concrete, respectively).

The no-slip approach was first defined by Broms in 1965.²⁵ In this approach, a perfect bond is assumed between reinforcement and surrounding concrete. Therefore, it does not allow slip to occur, and, theoretically, the crack width at the reinforcement is zero. At the crack where the reinforcement stress is the largest, the stress is considered as spreading, similar to the St. Venant’s principle,²⁶ therefore, the distance from the crack to where the uniform stress distribution of the concrete specimen becomes proportional to the concrete cover thickness (Figure 1b). Equation (2) represents the transfer length according to this no-slip approach (S_b). Later, Borges²⁷ further developed a model, by combining these bond-slip and no-slip approaches. Figure 1c represents this behavior graphically, and Equation (3) illustrates the basic model of the transfer length from this combined model (S_c).

$$S_b = KC \quad (2)$$

where, “K” is a constant, and “C” is the concrete cover thickness.

$$S_c = S_a + S_b \quad (3)$$

When the spacing between two cracks is greater than two times the transfer length, there is a possibility of

generating another crack in between. Therefore, the theoretical crack spacing values in the stabilized cracking stage can vary between one to two transfer lengths.²⁴ When focusing on calculating the “maximum crack width”, the “maximum crack spacing” becomes the governing parameter. Various “maximum crack spacing” models can be found, based on the aforementioned three approaches. Details of such models can be found in Borosnyói and Balázs.²⁸ To compare the experimental results of this study, the following existing crack spacing models were selected, as they represent each of the aforementioned approaches. The German National Annex of EC2 (DIN)²⁹ proposes a model based on the bond-slip approach. The JSCE model and Beeby’s model in Beeby and Scott³⁰ are based on the no-slip approach. Finally, the EC2 and MC 2010 crack spacing models were selected, as they were developed based on the combined approach. The details of these selected models are shown in Table 1.

3 | MATERIAL AND METHODS

The focus of this study is to examine the crack spacings of specimens subjected to service load. The experimental program consisted of four-point bending load tests and axial tensile tests. The axial tensile test was conducted, as it represents the tensile region of a bending member.³⁴ Furthermore, relevant mechanical properties of concrete, such as compressive strength and tensile strength, were measured, in order to minimize the assumptions in calculations. Ready-mix concrete was used in the experiments, and Table 2 shows the composition of the concrete mixture. The grade of the reinforcement used was B500NC. The reinforcement properties were selected according to the standard, NS 3576-3.³⁵ Yield strength and Young’s modulus of the selected reinforcement are 500 MPa and 200 GPa, respectively. The specimens were cast at a room temperature of 20°C. As per the studies by Hansen and Pedersen,³⁶ it was identified that, for good strength development, the specimens should be stored at 20°C.

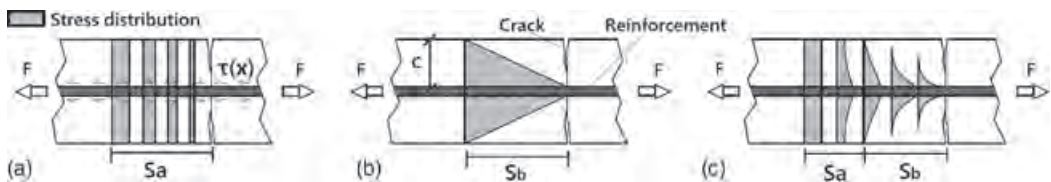


FIGURE 1 Estimation of crack spacing (a) bond-slip approach;²³ (b) no-slip approach; (c) combined approach²⁴

TABLE 1 Selected crack spacing models in the study

Model	Equations	Remarks	
EC2 and MC 2010	<p>EC2 crack spacing model</p> $s_{r,max} = k_3 c + k_1 k_2 k_4 \varphi / \rho_{p,eff}$ <p>$\rho_{s,ef}$ effective steel ratio c cover k_1 factor for bond properties k_2 factor for distribution of strain k_3 recommended 3.4 k_4 recommended 0.425 φ Bar diameter $\rho_{s,ef}$ effective steel ratio</p>	<p>MC 2010 crack spacing model</p> $l_{s,max} = k c + (1/4) (f_{ctm} / \tau_{bms})$ $s_{s,max} = 2. [k c + (1/4) (f_{ctm} / \tau_{bms})]$ <p>k empirical parameter on cover c cover τ_{bms} mean bond strength φ_s Bar diameter f_{ctm} tensile strength of concrete</p>	<p>Based on combined approach (combination of the bond-slip and the no-slip approaches)</p> <p>The ratio of maximum crack spacing to mean crack spacing, considered in both EC2 and MC 2010, is 1.7. This ratio was introduced to the EC2 from Braam³¹ and to MC 2010 model from CEB.³² "f_{ctm} / τ_{bms}" term in Equation (1) is replaced by k_1 in EC2, while MC 2010 uses $\tau_{bms} = 1.8. f_{ctm}$ for the stabilized cracking stage. EC2 uses a "k_2" factor to take into account the variation in strain distributions in flexure or axial tension and MC 2010 considers that only the "effective concrete area" can represent the effect.³³ MC 2010 limits the concrete cover thickness to 75 mm.</p>
DIN	$s_{r,max} = \frac{\varphi}{3.6 \rho_{p,eff}} \leq \frac{\sigma_s \varphi}{3.6 f_{ct,eff}}$ <p>σ_s steel stress $f_{ct,eff}$ tensile strength of concrete</p>	<p>Based on the bond-slip approach. Therefore, the cover term is excluded.</p> <p>The DIN model proposes using the parameters in the EC2 model as k_1. $k_2 = 0$, $k_3 = 0$ and $k_4 = 1/3.6$.</p>	
Beeby's model in Beeby and Scott ³⁰	$s_{r,max} = 2 (3.05 c)$ <p>c concrete cover thickness</p>	<p>Based on the no-slip approach. The expression is developed based on experimental results of axially reinforced members subjected to pure tension. The ratio of maximum crack spacing to mean crack spacing considered to develop this model is 1.5.</p>	
JSCE model	$s_{r,max} = 1.1 k_1 k_2 k_3 \{4c + 0.7(c_s - \emptyset)\}$ <p>where $k_2 = \frac{15}{(f_c + 20)} + 0.7 k_3 = \frac{5(n+2)}{7n+8}$ $s_{r,max}$ maximum crack spacing c concrete cover thickness k_1 constant on the surface of rebar (1.0 for deformed and 1.3 for plain bars) k_2 constant on the concrete quality f_c design compressive strength of concrete n number of layers of tensile rebar k_3 constant to take account of the multiple layers of tensile bars c_s distance of the tensile rebar (from center to center) \emptyset diameter of the tensile rebar</p>	<p>Based on the no-slip approach. The crack spacing model is based on the concrete cover and the distance between tensile bars. While both EC2 and MC 2010 predict increasing crack width with concrete strength, JSCE code predicts the opposite. However, this behavior matches with the findings in Ouyang and Shah⁸ and Shah et al.⁹ Further, this code considers the effects of tensile bar layers and spacing between tensile bars as factors for crack spacing.</p>	

The specimens that were cast for the bending and axial tensile tests were covered with polythene and stored in a 20°C controlled room. The concrete specimens that

were cast to investigate the compressive strength and tensile strength of concrete were stored in a water tank at 20°C.

3.1 | Axial tensile test

The most commonly used method of axial tensile testing of RC specimens is with a single reinforcement bar and for limited length specimens. The issue with such an experiment is the generation of a very limited number of cracks. The identified difference between the external block of the cracked specimens (the segment between the loading ends and the first crack from each end) and the internal blocks makes this issue worse.¹⁷ Therefore, 2-m-length specimens were selected, with the purpose of excluding the results from both external blocks of cracked specimens. The specimens were designed to generate a large number of cracks and therefore to obtain a large number of crack spacing data. To generate a large number of cracks, the specimens were designed to have a higher effective steel area and a lower concrete cover thickness. The reinforcement ratio of the selected specimens is about 8%, which quite deviates from the widely used members in practice. However, as mentioned earlier, the axial tensile specimens are assumed to represent only the tensile region of a bending member. Therefore, the reinforcement ratio of axial tensile specimens cannot be compared in the same way with that of ordinary structural members.

As mentioned in the introduction part, the focus of this experimental program is not to analyze the effect of any parameters on crack spacing. The focus is to observe the crack spacing behavior, by emphasizing the importance of the sample size of data. Therefore, three similar specimens with $0.2 \text{ m} \times 0.2 \text{ m} \times 2 \text{ m}$ (width \times height \times length) were

cast with four 32-mm-diameter reinforcement bars. The concrete cover thickness of the specimens was selected as 35 mm. The details of the axial tensile RC specimens are given in Figure 2. No spacers were used along the whole length of the specimens, as they have been identified as crack inducers.³⁷ The concrete cover along the specimen was maintained by holding the four reinforcements from the binding wires to a fixed position on top. As the length of the specimen is relatively large, it could not use a conventional displacement-controlled testing machine to load the specimen. The tensile load was applied with “force-controlled” test bench apparatus located in the I.K.M. Laboratory facility in Tananger, Norway. It was possible to apply the load in steps, and it was decided to increase the load in 100-kN steps.

Special attention was paid to the loading method, and the load was applied to the reinforcement, through the nut and bolt mechanism, as shown in Figure 3. Both edges of each reinforcement were screwed to fit with M24 bolts. In order to connect the specimens with the loading apparatus, a standard HEB S355 600 section (H-section) was selected. The connection of the HEB section with the specimens was assured for the failure modes of a T-stub section,³⁸ as per the guidelines in Eurocode 3.³⁹ The web and flange sections of the HEB section were checked for the tensile, shear, and tear-out failure modes separately. Furthermore, the HEB section was verified for the residual stresses that can occur at the web-flange connection. The nut-bolt connection was assured for the tensile and thread-stripping failure modes. Afterwards, the system was assured to resist a load of 900 kN, where the stress in reinforcement can reach up to 280 N/mm^2 .

TABLE 2 Composition of the concrete mixture in one cubic meter

Material	Quantity per cubic meter (kg m^{-3})
Standard cement FA	309
Sand (0/8 mm)	1,063
Gravel (8/16 mm)	829
Water	152
Admixtures Dynamon SX-23	1.59
Mapepair 25 1:19	0.74

3.2 | The four-point bending test

The available four-point bending test apparatus had the maximum constant moment span of 800 mm. Two similar beams were cast with $0.25 \text{ m} \times 0.3 \text{ m} \times 2.2 \text{ m}$ (width \times height \times length) dimensions. The bending specimens were designed with two 32-mm-diameter tensile reinforcements and a cover of 35 mm, as in Figure 4. Furthermore, the beam was designed to avoid shear failure by using shear links, apart from in the constant bending zone.

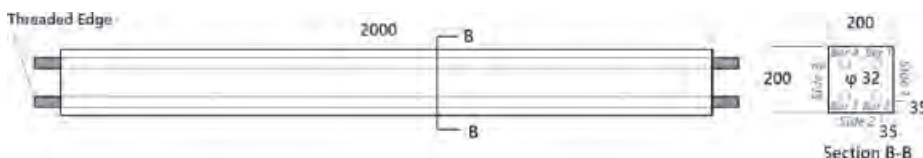


FIGURE 2 Details of the axial tensile specimen (all dimensions are in mm)

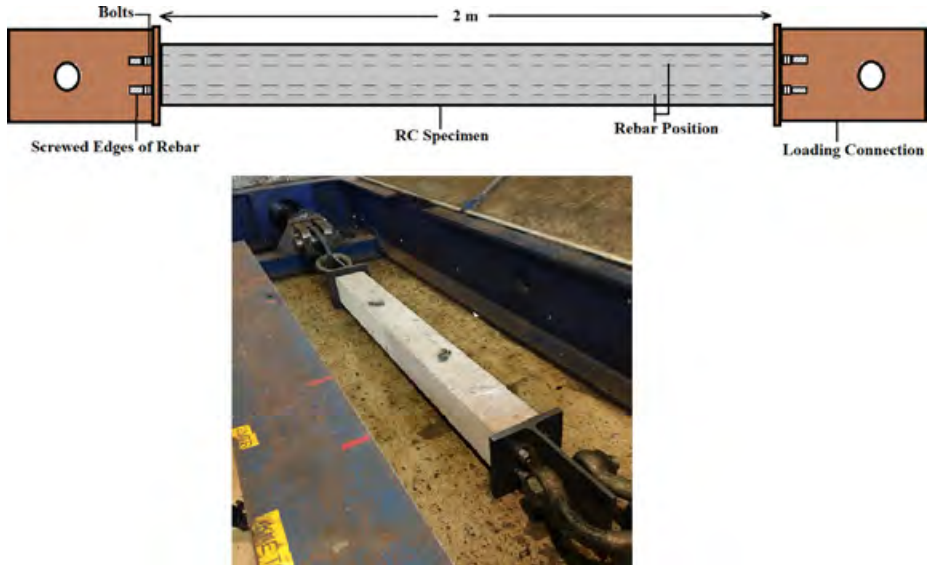


FIGURE 3 Axial tensile specimen with the loading connections

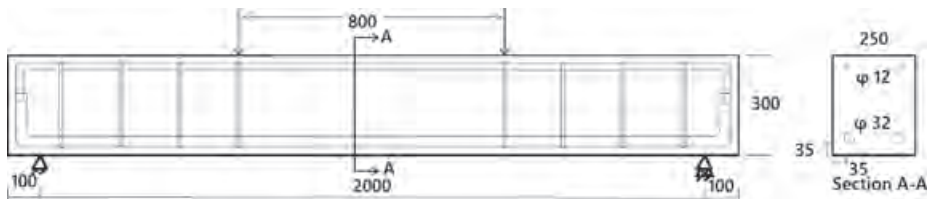


FIGURE 4 Details of bending specimens (all dimensions are in mm)

No stirrups were used at the constant bending zone, as previous studies have proved that stirrups can induce cracks. For example, Makhoul and Malhas's¹² experiments for 30-, 50-, and 60-mm concrete cover specimens and Caldentey et al.'s¹³ experiments for 20-mm concrete cover specimens proved the discussed scenario. Similar to the axial tensile specimens, no spacers were used within the constant bending zone, as they have been identified as crack inducers. The four-point bending load was applied with "Toni Technik" apparatus with a loading rate of 5 kN/min. Specimens were loaded, exceeding the stabilized cracking stage, up to 290 kN of final load.

3.3 | Testing of mechanical properties of concrete

For the better comparison of the obtained crack spacing data during the experiments with the model predictions,

the mechanical properties of concrete were investigated. A compressive strength test of concrete was carried out by using six 100-mm cubes, according to the standard, NS-EN 12390-3. As per the theoretical approach used to calculate the crack spacing values according to the codes, the "highest stress reached under concentric tensile load" is to be measured, and a direct tension test is preferred. However, a "splitting tensile test" was conducted, according to the standard, NS-EN 12390-6. Afterwards, the obtained splitting tensile results were multiplied by a factor of 0.9, which is proposed by EC2 to convert the measurements to direct tensile strengths of concrete.³ It was required that the experimental values be adapted before being used in the prediction models. Furthermore, the "axial tensile experiment" was delayed due to practical issues. The adjustments performed for the experimental values are listed in Table 3. The compressive and tensile strengths of concrete are factors of age.⁴¹ Therefore, the prescribed corrections mentioned in EC2 were

TABLE 3 Tested parameters and standard code requirements

Parameter	Calculation model requirements	Standard	Conducted experiment	Remarks
Compressive strength	150 mm *300 mm cylindrical strength	NS-EN 12390-3	100-mm cube compressive test	Results from 100-mm cube test have been converted to 150-mm cube strength. ⁴⁰ Then converted to cylindrical strengths as per EC2.
Tensile strength	Direct tensile strength	NS-EN 12390-6	Splitting tensile test	Used the EC2 specified factor (0.9) to convert the results to direct tensile values.

TABLE 4 Experimental mean values and code required values

Parameter	Experimental mean value (N/mm ²)	Values used in models (N/mm ²)	
		Four-point bending test (adjusted to test date)	Axial tensile test (adjusted to test date)
Compressive strength	41.5	31.5	35
Tensile strength	3.2	2.9	3.2

carried out, to obtain the parameter values respective to the bending and axial tensile test dates. The obtained results from the experiments, converted values to match the prediction models, and corrections made to match the testing age are listed in Table 4.

3.4 | Crack spacing measurements

The focus is to measure the crack spacing, propagated along the tensile reinforcement. Therefore, each face of the specimen has two sets of readings of crack spacing, corresponding with the two tensile reinforcements, close to each face. However, in the bending case, the “crack spacing” measurements are considered only on the bottom face (when the load is applied from the top). In the axial tensile case, all four faces of each specimen can be considered for obtaining crack spacing measurements. Figures 5 and 6 explain the method of crack spacing measurements, in both loading cases.

4 | RESULTS OF THE EXPERIMENTS

4.1 | Statistical analysis of data

It is necessary to represent a logical estimation for the “mean or maximum crack spacing” values, rather than mentioning the value of one piece of data out of many readings. In order to do that first, it was necessary to

check whether the obtained data can fit with a normal distribution. There are many tests (goodness-of-fit) for doing that, and some such methods are described in Sheskin.⁴² It is recommended that tests for skewness and for kurtosis, as well as the Kolomogorov–Smirnov test and so on, are carried out. The skewness test predicts the asymmetry of the sample data. A perfectly symmetric distribution has two identical mirror images when it is split in the middle. In such cases, the result from the skewness test is zero. The test for kurtosis checks the heights of the tails of a given distribution relative to its normal distribution. When the sample distribution behaves perfectly to a normal distribution, the result of the excess kurtosis test is zero. In order to assume the histogram fits a standard normal distribution, the skewness (lopsided), and the excess kurtosis (thickness of the tails) values have to lie closer to zero.⁴³ The Kolomogorov–Smirnov test, known as the “KS test,” is based on the cumulative distribution function (cdf) of the sample data. The test statistic is the maximum absolute vertical difference between the sample “cdf” and the “cdf” from the hypothesized normal distribution. In order to accept the sample distribution as normal, the maximum difference must be less than the critical values of different significance levels. When considering the two-tailed case, the significance level varies from 0.001 to 0.2.⁴² When the aforementioned maximum difference is less than the critical value of 0.2 significance, the “*p*” value of the sample being a normal distribution is “1.” Similarly, when the maximum difference is greater than the critical value of 0.001 significance, the “*p*” value of the sample being a normal distribution is “0”.⁴² These tests were carried out to

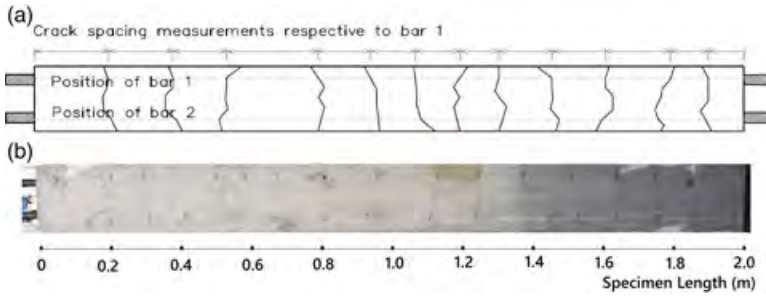


FIGURE 5 (a) Method of measuring crack spacing; (b) Crack spacing measurements of an axial tensile specimen

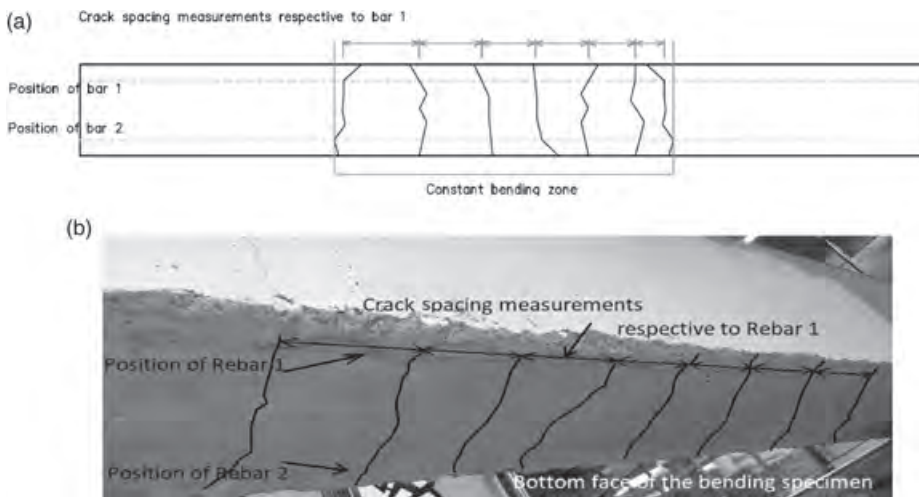


FIGURE 6 (a) Method of measuring crack spacing; (b) Crack spacing measurements at the soffit of a bending specimen

check the normality of the sample crack spacing data obtained from both the axial tensile test and the four-point bending test. As the normality is proved for both data sets, the mean and maximum crack spacing values have been determined as per the methods applied in Gribniak et al.⁴⁴ The 95% upper prediction bound has been considered as the maximum crack spacing and it was obtained from Equation (4).

$$95\% \text{ upper bound} = m_r + 1.96s_r \sqrt{1 + \frac{1}{n}} \quad (4)$$

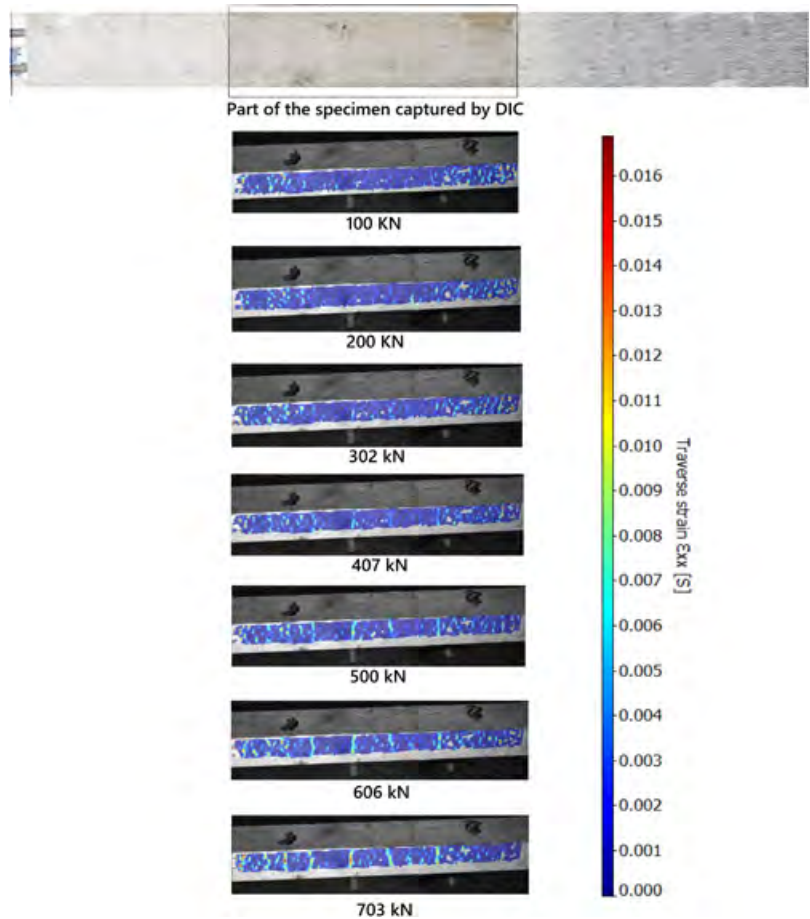
where “ m_r ” is the mean of the sample, “ s_r ” is the SD of the sample, and “ n ” represents the size of the data sample.

4.2 | Results of axial tension experiment

As previously mentioned, three similar specimens were tested by applying an axial tensile load beyond the stabilized cracking stage. For safety reasons, no one was

allowed to be near the specimens while they were loaded. Therefore, the cracking behavior was observed with a digital image correlation (DIC) system, to make sure that the specimen reached the stabilized cracking stage. Figure 7 shows the captured cracking behavior from the DIC system at different loading stages. As shown in Figure 7, the DIC could not capture the whole specimen, due to practical difficulties. It can be seen that the cracks are quite visible to the DIC system at 500 kN and, at both 600 and 700 kN, the width of the same crack is increasing while the load is increasing. This confirms that the beam has reached the stabilized cracking stage. Moreover, the cracks could be observed by a “crack detection microscope” after the specimens had been unloaded. Therefore, the crack positions could be marked on the specimens, by thorough observation with the crack detection microscope. However, only three faces of each specimen could be observed with the microscope, as the top surface of the cast beams does not have a smooth surface on which to place the microscope flat. Therefore,

FIGURE 7 Cracking behavior of “axial tensile specimen 1” captured by the digital image correlation system



altogether nine faces could be observed, and the number of tensile cracks in a face varied from 13 to 15. As each specimen face consists of two sets of crack spacing data (relative to the two tensile reinforcements corresponding to each face), 18 sets of crack spacing data could be obtained from the three specimens (3 elements \times 3 surfaces \times 2 bars = 18 sets). Altogether, the total number of items of crack spacing data was 266.

Then, 36 number (two end observations of 18 sets of data) of end block data were discarded for the following reasons. From their study, Gribniak et al.⁴⁵ identified that the end sections of the specimens (at the loading ends) do not satisfy the Navier–Bernoulli plane section hypothesis (reinforcement strain is larger than concrete strain). Furthermore, this literature reveals that the assumption that all the cracked sections transfer to reinforcement is a simplified approach. The experimentally identified crack width variation along the concrete cover in references,^{46–}

⁴⁸ proves that the crack width near the reinforcement is almost negligible. Therefore, a total discontinuation of concrete is hard to assume. For these reasons, assuming that the cracking behavior of end blocks is similar to that of internal blocks becomes doubtful. Therefore, the experimental data were selected without considering the data of the external blocks. This made the sample size of data reduce from 266 to 230. The histogram of the 230 data is shown in Figure 8. It can be observed as a bell-shaped one-peak curve. However, the mean and the maximum crack spacing values were obtained after going through the statistical analysis steps mentioned in Section 4.1. The skewness and excess kurtosis values of the new sample are 0.38 and -0.57 , respectively. Furthermore, the maximum difference obtained from the KS test is still less than the 0.02 significance level. Therefore, a normal distribution can be assumed, with a mean value of 133 mm. The maximum crack spacing

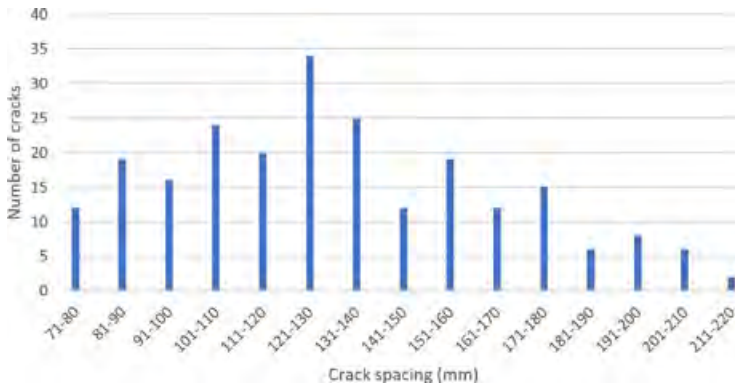


FIGURE 8 Histogram of measured crack spacing values in axial tensile experiment excluding the external stress blocks

value is obtained from Equation (4), and the value is 202 mm.

In order to compare the effect of the external blocks with the obtained results, the statistical analysis given in Section 4.1 was conducted for the 266 pieces of data (with the external blocks). The calculated skewness and excess kurtosis values of the data set were 0.29 and -0.62 , respectively. The aforementioned values lie close to zero and are similar to the behavior of normal distribution. Furthermore, the maximum difference obtained from the “KS” test is less than the 0.02 significance level. Considering these “goodness-of-fit” test results, it can be considered that the crack spacing sample is normally distributed. Then, the obtained mean and maximum crack spacing values are 135 and 203 mm, respectively. However, as can be seen, no significant difference could be observed between the two methods.

4.3 | Results of the four-point bending test

Two similar specimens (as in Figure 4) were tested using the four-point bending test. Eight cracks could be observed in each specimen in the constant bending zone. The crack spacing measurements were obtained at the bottom of the beam. Two data sets were obtained from each specimen, corresponding with the two tensile reinforcements. Therefore, four data sets of crack spacings were observed. Altogether, there were 28 items of crack spacing data. Since the focus was the bottom face of the specimen, there was not enough space to capture the crack zone with the DIC system. Therefore, the cracks were marked by inspecting with the crack detection microscope, when the specimen was loaded.

The histogram of the crack spacing data is represented in Figure 9. It can also be observed as a bell-shaped

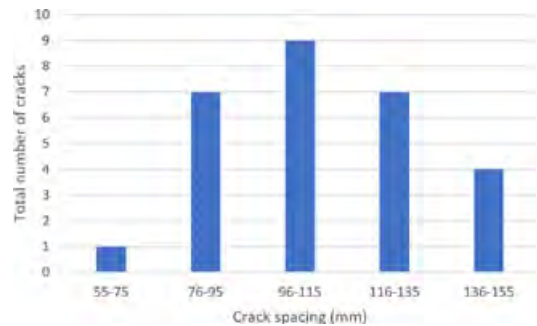


FIGURE 9 Histogram of measured crack spacing values in four-point bending test

one-peak curve. Similar to the axial tensile test, the data sample has proved normal, following the tests mentioned in Section 4.1. The calculated skewness and excess kurtosis values of the sample are 0.09 and -0.14 , respectively. The aforementioned values lie close to zero. The maximum difference obtained from the “KS” test is less than the 0.2 significance level. Considering these test results, it can be assumed that the sample is normally distributed. Then, the mean crack spacing value was obtained as 112 mm, and, from Equation (4), a maximum crack spacing of 160 mm was obtained.

5 | DISCUSSION

5.1 | Discussion of the axial tension experiment results

Table 5 shows the details of 18 samples of crack spacing data sets obtained from the axial tensile tests, without considering the external block. As can be seen, the mean

TABLE 5 Details of the crack spacings obtained from axial tensile test excluding the external block

Parameter	Measured crack spacing (mm)																		
	Beam 1						Beam 2						Beam 3						
	Side ^a 1		Side 2		Side 3		Side 1		Side 2		Side 3		Side 1		Side 2		Side 3		
	Bar 1	Bar 2	Bar 2	Bar 3	Bar 3	Bar 4	Bar 1	Bar 2	Bar 2	Bar 3	Bar 3	Bar 4	Bar 1	Bar 2	Bar 2	Bar 3	Bar 3	Bar 4	
No. of crack spacings	12	12	12	12	12	12	12	12	13	13	14	14	14	14	14	14	14	12	12
Maximum spacing	200	205	205	200	190	180	200	210	195	215	180	190	175	160	210	210	215	210	
Mean spacing	145	146	143	143	143	144	142	141	132	130	120	123	116	122	125	121	140	139	
Standard deviation	34	34	32	38	31	27	34	43	36	39	29	31	31	26	36	34	41	43	
Variance	1,164	1,146	1,043	1,430	931	751	1,179	1,860	1,294	1,488	848	941	976	664	1,265	1,174	1,720	1,882	

^aRefer to Figure 2 to identify the “side” and “bar” numbers.

values of each sample vary from 116 to 146 mm. Similarly, the maximum crack spacing values (i.e., the directly observed maximum value without using Equation (4)) change from 160 to 215 mm in each sample. Base et al.⁴⁹ conducted a statistical approach, named “Student’s *t* test”, to confirm that the data sets belong to the same population. The same test was conducted to further confirm that the obtained 18 data sets belonged to the same population. This method uses the mean, variance, and number of observations of two data sets, to make sure that they belong to a similar population. After confirming that the 18 sets belonged to the same population, it was possible to consider all 230 items of crack spacing data in one sample and perform further analysis. When considering the sample size combining all the data, the mean, and maximum crack spacing values are 133 and 202 mm (Section 4.2). This highlights that, when the sample size of data is small, the results can be completely different with large sample sizes. This study shows the importance of increasing the sample size of data, especially for such studies with a stochastic nature.

The ratio of the maximum crack spacing to the mean crack spacing of the 230 data sets is 1.5. As mentioned in Table 1, both the EC2 and MC 2010 models have considered this ratio as 1.7.^{31,32} Experimental “maximum crack spacing” values are compared with the prediction models, as that is the parameter influencing the “maximum crack width”. It was considered a “short-term loading condition” in the “stabilized cracking stage”, for the assumptions required in the calculations. For the parameter, “effective tensile area of concrete”, the whole cross section area of the specimen was assumed. This assumption is justified by the fact that most cracks propagate from the bars to the surface of the specimen, in such involving the whole section. When compared with the

predictions in Table 6, the conducted experimental result “error” is relatively small compared with the other mentioned specimens (except for DIN predictions). One reason for that could be the use of a relatively large sample size of data.

To further verify the experimental findings, the data from similar types of tests are considered from Tan et al.,¹⁶ Barre et al.⁵⁰ and Rimkus and Gribniak.¹⁸ Table 6 shows the specimen details, experimental crack spacing values, and predicted crack spacing values of the selected cases. Figure 10 shows the range of parameter variations of these selected cases in Table 6. However, it is important to note that the sample size of these data is not as large as that of the conducted experiment. Furthermore, the method for identifying the maximum crack spacing is also dissimilar to that of the conducted experiment. The experiment in Tan et al.¹⁶ has been applied to the load, not directly to the reinforcement. Therefore, even where the specimen length is 3 m, the cracking data is obtained in the middle 2 m. The load applications in References Barre et al.⁵⁰ and Rimkus and Gribniak¹⁸ are similar to those of the conducted experiment, where the load is applied to the reinforcement. However, the results of those experiments are included with the readings of external blocks. Therefore, before analyzing the results of the aforementioned studies, it is important to keep in mind the discussed differences.

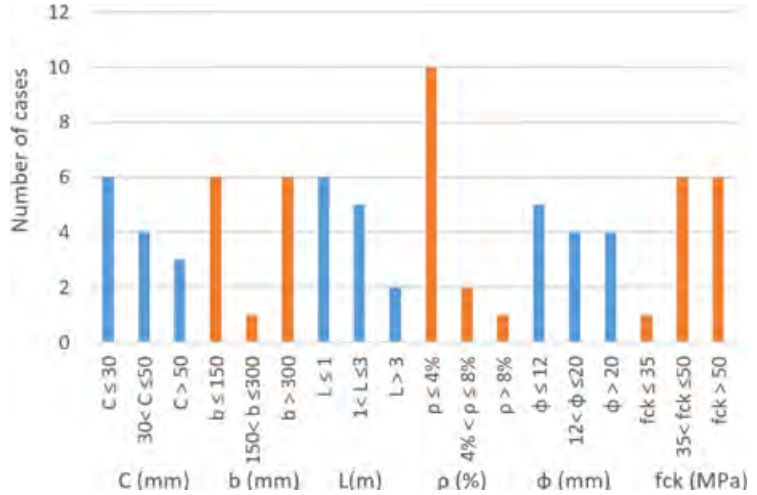
As per Table 6, the maximum to mean crack spacings values vary from 1.2 to 1.7 in all selected cases. The crack spacing model is a mathematical model that can predict the crack spacing values conservatively, for different possible arrangements of effecting parameters. EC2 predictions are on the conservative side for all the cases, and MC 2010 predictions are conservative, except for cases 1 and 8. However, EC2 predictions are more than two

TABLE 6 Experimental and predicted crack spacing values of selected axial tensile experiments

Study	Case no.	Width × height × length (m × m × m)	Concrete cover (mm)	Bar profile (no × diameter)	Experimental crack spacing (mm)			Predicted max crack spacing (mm)				Error ^a %					
					Mean	Max	Max/mean	EC2	MC 2010	JSCE	Beebly	DIN	EC2	MC 2010	JSCE	Beebly	DIN
Conducted test	1	0.2 × 0.2 × 2	35	4 × 32	133	202	1.5	254	181	199	214	111	-26	10	1	-6	45
Tan et al. ¹⁶	2	0.4 × 0.4 × 3	40	8 × 20	163	250	1.5	569	434	209	244	354	-128	-74	16	2	-42
	3		40	8 × 32	178	240	1.3	407	301	201	244	221	-70	-25	16	-2	8
	4		90	8 × 20	217	290	1.3	739	534	375	549	354	-155	-84	-29	-89	-22
	5		90	8 × 32	266	320	1.2	577	401	367	549	221	-80	-25	-15	-72	31
Barre et al. ⁵⁰	6	0.355 × 0.355 × 3.2	65	4 × 25	200 ^b	330 ^b	1.7	664	590	390	397	446	-98	-79	-18	-20	-35
	7		45	8 × 16	174 ^b	288 ^b	1.7	534	437	268	275	348	-85	-51	7	5	-21
Rimkus and Gribniak ¹⁸	8	0.15 × 0.15 × 0.5 ^c	30	12 × 8	100 ^b	146 ^b	1.5	203	143	127	183	82	-39	2	13	-25	44
	9		30	16 × 6	92 ^b	133 ^b	1.4	203	143	122	183	83	-53	-8	8	-38	37
	10		30	16 × 5	73 ^b	103 ^b	1.4	224	159	131	183	99	-117	-54	-27	-78	4
	11		30	4 × 14	100 ^b	127 ^b	1.3	276	202	168	183	144	-117	-59	-32	-44	-13
	12		30	4 × 12	86 ^b	148 ^b	1.7	305	226	165	183	167	-106	-53	-11	-24	-13
	13		30	4 × 10	113 ^b	143 ^b	1.3	346	259	173	183	198	-142	-81	-21	-28	-39

^aError = (Experimental Value - Predicted Value)/Experimental Value.^bAverage value of several similar test specimens.^cSpecimen lengths of Rimkus & Gribniak¹⁸ vary between 379 mm and 505 mm.^dExperimental crack spacing values and material properties of specimens 8 to 13 are considered as mean values of specimens with similar bar profiles.

FIGURE 10 Number of cases to the range of parameter variations of the selected axial tensile experiments mentioned in Table 6; where “C” is the concrete cover, “b” is the specimen width or height, “L” is the specimen length, “ρ” is the reinforcement ratio, “φ” is the bar diameter and “fck” is the compressive strength of concrete



times larger than the experimental values in 6 out of 13 cases.^{16,18,51} Furthermore, Table 6 includes the data of specimens with relatively large concrete cover thicknesses, including 65 mm (case No. 6) and two specimens with 90 mm (case nos. 4 and 5). When considering the maximum crack spacing values of these cases with EC2 and MC 2010, the predicted error values are significantly large, compared with the other model predictions. For these three cases, the JSCE model gives better and conservative predictions, compared with the other mentioned predictions.

When considering the predictions from Beeby’s model, which is based on no-slip theory: except for two cases, all the other predictions are on the conservative side. Furthermore, the underestimated cases have a relatively small error, which lies below 5%. JSCE predictions have the least error, considering all cases; however, 6 out of 13 cases are underestimated. These underestimated error percentages are below 16%. When considering the “crack width calculation” model in JSCE code, the effect of concrete strain has been neglected. Therefore, the effect of underestimations of crack spacing values can be considered as adjusted when calculating the maximum crack width. As previously mentioned in Section 2, the JSCE model is developed based on no-slip theory. Therefore, these results may indicate the conclusion mentioned in Beeby⁵² and Beeby and Scott³⁰ that the bond-slip theory has a negligible influence on crack spacing and therefore on the crack width. Furthermore, case Nos. 8–13 have six different reinforcement arrangements, but with the same concrete cover thickness. However, the mean crack spacings of these cases are nearly the same, as in Table 6. These results contribute to the statement that

TABLE 7 Details of the crack spacings obtained from the four-point bending test

Parameter	Measured crack spacing (mm)			
	Beam 1		Beam 2	
	Bar 1	Bar 2	Bar 1	Bar 2
No. of spacings	7	7	7	7
Maximum spacing	150	150	155	135
Mean spacing	109	111	113	114
Standard deviation	19	24	38	15
Variance	371	594	1,465	229

Mean spacing, Standard deviation and Variance have been rounded to zero decimal places.

bond-slip theory has a negligible influence. However, this statement must be confirmed by further studies.

5.2 | Discussion of the four-point bending test

Table 7 shows the details of the four sets of data of crack spacings obtained from the four-point bending test. The mean crack spacing values of each data set vary from 109 to 114 mm. Similarly, the maximum crack spacing of each data set varies from 135 to 155 mm (i.e., direct measurements without using Equation (4)). Based on the Student’s *t*-value, it could be confirmed that the four data sets belong to a similar population (i.e., more than 95% probability of being in the same population). Therefore, it

TABLE 8 Experimental and predicted crack spacing values of selected bending experiments

Study	Case number	Width × height × length ^a (m × m × m)	Concrete cover ^b	Tensile bar profile	Experimental crack spacing (mm)			Predicted max crack spacing (mm)						Error ^c %			
					Mean	Max	Max/mean	EC2	MC 2010	JSCE	Beeby	DIN	EC2	MC 2010	JSCE	Beeby	DIN
Conducted experiment	1	0.25 × 0.3 × 0.8	35	2 × 32	112	160	1.4	172	157	241	214	87	-8	2	-51	-33	46
Caldentey et al. ¹³	2	0.35 × 0.45 × 3.42	32	4 × 25	131	234	1.8	193	196	199	195	138	18	16	15	17	41
	3		32	4 × 12	173	269	1.6	259	309	206	195	245	4	-15	23	27	9
	4		82	4 × 25	227	423	1.9	364	296	403	500	139	14	30	5	-18	67
	5		82	4 × 12	236	412	1.7	502	525	404	500	364	-22	-27	2	-21	12
Gribniak et al. ¹⁷	6 ^d	0.28 × 0.3 × 1.0	20	9 × 10	109	138	1.3	120	125	134	122	85	13	9	3	12	39
	7 ^d		20	12 × 8	94	125	1.3	117	120	117	122	80	6	4	6	2	36
	8 ^d		20	15 × 6	90	120	1.3	122	128	101	122	88	-2	-7	16	-2	26
	9		20	5 × 14	87	134	1.5	128	138	111	122	98	4	-3	17	9	27
	10		20	2 × 22	86	142	1.7	172	209	219	122	169	-21	-47	-54	14	-19
	11		20	3 × 14	74	131	1.8	168	204	152	122	164	-28	-56	-16	7	-25

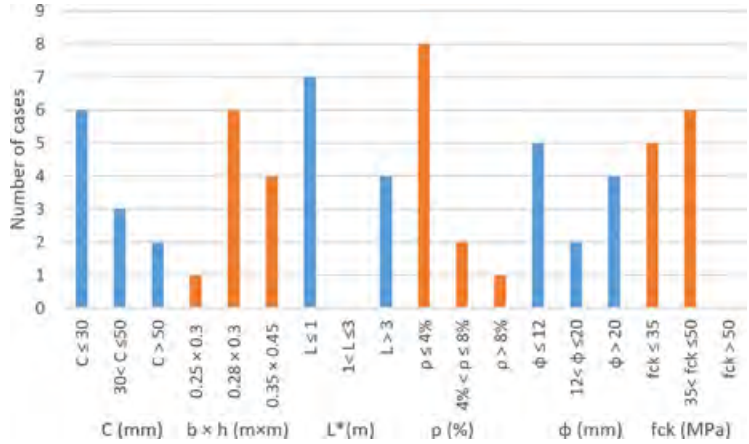
^alength^a is the length of the constant bending zone.

^bCover to the tensile reinforcement.

^cError = (experimental value - predicted value)/experimental value.

^dSpecimens 6,7,8 have three layers of tensile reinforcement.

FIGURE 11 Number of cases to the range of parameter variations of the selected bending experiments mentioned in Table 8; where “C” is the concrete cover, “b” is the specimen width, “h” is the specimen height, “L*” is the length of constant bending zone, “ρ” is the reinforcement ratio, “φ” is the bar diameter and “fck” is the compressive strength of concrete



is possible to consider all data sets of crack spacings in one sample. The mean and maximum crack spacing values of this sample are 112 and 160 mm, respectively (Section 4.3). Similar to the axial tensile case, this shows the importance of selecting a large sample size of data.

To verify the obtained data, the results have been compared with four-point bending tests conducted in Gribniak et al.¹⁷ and Caldentey et al.¹³ Table 8 shows the specimen details, experimental crack spacing values and, predicted crack spacing values of the selected cases. Figure 11 shows the range of parameters of the selected cases mentioned in Table 8. The sample sizes of these tests are not similar to the conducted experiment. Furthermore, both these tests measured the crack spacing at the side of the beam, where the conducted experiment measured at the beam soffit. For the use of calculation models, it was considered a “short-term loading condition” in the “stabilized cracking stage,” similar to the axial tensile case. For the effective height of concrete ($h_{c,eff}$), the values recommended by EC2 and MC 2010 are considered. It is recommended to use the minimum value of $2.5(h-d)$, $(h-x)/3$ or $h/2$. The “h” denotes the total depth of the cross section, “d” the effective depth, “x” the depth of the neutral axis and “φ” the diameter of tensile reinforcement. According to Table 8, the maximum crack spacing of the conducted experiment gives a good agreement with the EC2 and MC 2010 predictions. Both the JSCE and Beeby’s models are more on the conservative side, whereas DIN has considerably underestimated the predictions. The ratio between the maximum and mean crack spacing of the conducted experiment is 1.4. According to Table 8, this ratio gives a good agreement with the discussed cases, as they vary from 1.3 to 1.9.

The significance of the results is that, unlike in the axial tensile case, EC2 predictions have a relatively good estimation of maximum crack spacing in all the cases. This is due to the use of the “ k_2 ” coefficient, which is the factor for distribution of strain, as 0.5. Theoretical and analytical explanations of this coefficient are represented in Caldentey³³ and Mcleod et al.,⁵³ respectively. However, the predictions of 6 out of 11 cases are on the non-conservative side, where the maximum error value is 18%. Similar to the axial tensile case, two cases with relatively large concrete cover thickness of 82 mm (case nos. 4 and 5) have been selected. For these two cases, the JSCE and Beeby’s models predict relatively good results.

6 | CONCLUSIONS

A study has been carried out to investigate the crack spacings of the RC specimens subjected to axial tension and bending. There is a considerable body of literature available on the parametric analysis of crack spacing. Therefore, an experimental program was carried out, focusing on the effect of sample size of data. As the objective was to increase the number of items of data, several identical practical scale specimens were tested in both axial tension and bending. The obtained results were verified with similar types of experimental results available in the recent literature. The next aim was to study the applicability of existing crack spacing models. For that purpose, several crack spacing models were selected, as they cover the three main approaches: namely, bond-slip, no-slip, and combined approaches. The following conclusions were drawn based on the experimental program and a comparison of the results with the selected literature.

- It could be identified that the sample size of data has an effect of representing the mean or maximum crack spacing value. The results of axial tensile tests are included with 18 sets of data. When considering the mean and maximum of each data set, they are different from each other. Furthermore, when considering all the data of 18 sets in a single sample, the mean, and maximum values are significantly different from the aforementioned values. The behavior is similar to the test results of bending experiment. Therefore, it is important to increase the number of data, as it then become a more reasonable representation.
- The maximum to mean crack spacing ratio of the conducted axial tensile test is 1.5. This value matches to the similar tests mentioned in the literature. When considering the model predictions of maximum crack spacings, the EC2 predictions are conservative for all the selected cases. For some cases, the overestimation exceeds the value of 150% when concrete cover thickness is large (i.e., 65 and 90 mm). The JSCE model gives relatively good predictions among the other discussed models for axial tensile experiments.
- The ratio of the maximum to mean crack spacings of the conducted bending experiment is 1.4. This value gives good agreement with the results of the discussed similar experiments, as they vary from 1.3 to 1.9. When considering the model predictions, EC2 predictions are close to the experimental results with the use of the “ k_2 ” coefficient.
- When considering the maximum crack spacing predictions of EC2, it can be identified that the effect of curvature has a role in the cracking behavior of specimens subjected to flexure. However, this behavior must be clarified with further studies.

ACKNOWLEDGMENT

The authors would like to thank the Statens Vegvesen Ferry-free E39 project, for the financial support given to conduct the experiments, and Dr Reignard Tan, for sharing some of the important data of an experiment he conducted. The experiments were conducted at the Concrete Laboratory of the University of Stavanger and at the I.K. M. laboratory facility in Tananger, Norway. Special thanks go to the UiS laboratory manager, John C. Grønli, laboratory engineers Jarle Berge, Jørgen Grønsund, Emil Kristiansen, Caroline Einvik and research assistants, Børge Kallesten and Morten Bye, for the variety of support given during the experiments.

CONFLICT OF INTEREST

The authors declare no conflict of interest.

DATA AVAILABILITY STATEMENT

The data that support the findings of this study are available from the corresponding author upon reasonable request.

ORCID

Chavin N. Naotunna  <https://orcid.org/0000-0003-4994-2675>

REFERENCES

1. ACI. ACI Building Code Requirements for Structural Concrete (ACI 318–95) and Commentary (ACI 318R-95): American Concrete Institute; 1995.
2. BS. BS 8110: Part 1, Structural use of concrete—code of practice for design and construction. London, UK: British Standard Institute, 1985.
3. CEN. EN 1992-1-1, Eurocode 2: Design of concrete structures—part 1-1: General rules and rules for buildings. Brussels: European Committee for Standardization, 2004.
4. fib. fib Model Code for concrete structures 2010. International Federation for Structural Concrete. Berlin: Ernst & Sohn, 2013.
5. JSCE. JSCE standard specifications for concrete Structures-2007 “design”. Japan: *Concrete Committee of Japanese Society of Civil Engineers*, 2007.
6. Balazs GL. Cracking analysis based on slip and bond stresses. *Mater J*. 1993;90(4):340–348.
7. Wang JJ, Tao MX, Nie X. Fracture energy-based model for average crack spacing of reinforced concrete considering size effect and concrete strength variation. *Construct Build Mater*. 2017;148:398–410.
8. Ouyang C, Shah SP. Fracture energy approach for predicting cracking of reinforced concrete tensile members. *ACI Structur J*. 1994;91(1):69–78.
9. Shah SP, Swartz SE, Ouyang C. Fracture mechanics of concrete: Applications of fracture mechanics to concrete, rock and other quasi-brittle materials. New York: John Wiley & Sons, 1995.
10. Tammo K, Thelandersson S. Crack behavior near reinforcing bars in concrete structures. *ACI Structur J*. 2009;106(3):259.
11. Bezuidenhout SR, Van Zijl GPAG. Corrosion propagation in cracked reinforced concrete, toward determining residual service life. *Structur Concr*. 2019;20(6):2183–2193.
12. Makhlof HM, Malhas FA. The effect of thick concrete cover on the maximum flexural crack width under service load. *Structur J*. 1996;93(3):257–265.
13. Caldentey AP, Peiretti HC, Iribarren JP, Soto AG. Cracking of RC members revisited: Influence of cover, ϕ/ρ_s , e_f and stirrup spacing—an experimental and theoretical study. *Structur Concr*. 2013;14(1):69–78.
14. Vegvesen S. Håndbok N400 Bruprosjektering. Oslo: Vegdirektoratet, 2009.
15. Basteskår M, Engen M, Kanstad T, Fosså KT. A review of literature and code requirements for the crack width limitations for design of concrete structures in serviceability limit states. *Structur Concr*. 2019;20(2):678–688.
16. Tan R, Eileraas K, Opkvitne O, Žirgulis G, Hendriks MAN, Geiker M, Brekke DE, Kanstad T. Experimental and theoretical

- investigation of crack width calculation methods for RC ties. *Structur Concr.* 2018;19:1436–1447.
17. Gribniak V, Caldentey AP, Kaklauskas G, Rimkus A, Sokolov A. Effect of arrangement of tensile reinforcement on flexural stiffness and cracking. *Eng Struct.* 2016;124:418–428.
 18. Rimkus A, Gribniak V. Experimental investigation of cracking and deformations of concrete ties reinforced with multiple bars. *Construct Build Mater.* 2017;148:49–61.
 19. Radnić J, Markota L. Experimental verification of engineering procedures for calculation of crack width in concrete elements. *Int J Eng Model.* 2003;16:63–69.
 20. Bažant ZP, Oh BH. Spacing of cracks in reinforced concrete. *J Structur Eng.* 1983;109(9):2066–2085.
 21. Beeby AW, Ålander C, Cairns J, Eligehausen R, Mayer U, Lettow S. Discussion: The influence of the parameter ϕ/ρ_{eff} on crack widths. *Structur Concr.* 2005;6(4):155–165.
 22. Saliger R. High grade steel in reinforced concrete. Paper presented at the preliminary publication, 2nd congress of IABSE. Berlin-Munich: IABSE Publications, 1936.
 23. Rasmussen AB. Modelling of reinforced concrete in the serviceability limit state: A study of cracking, stiffness and deflection in flexural members. PhD Thesis, Aarhus University; 2019. <https://doi.org/10.7146/aul.329.223>
 24. Beeby AW. Crack control provisions in the new Eurocode for the design of concrete structures. *ACI Special Publication.* 2001;204:57–84.
 25. Broms BB. Crack width and crack spacing in reinforced concrete members. Paper presented at the *ACI Journal Proceedings.* 1965;62:1237–1256.
 26. de Saint-Venant M. *Mémoire sur la torsion des prismes: avec des considérations sur leur flexion ainsi que sur l'équilibre intérieur des solides élastiques en général: et des formules pratiques pour le calcul de leur résistance à divers efforts s' exerçant simultanément*: Imprimerie Nationale; 1856.
 27. Borges JF. *Cracking and deformability of reinforced concrete beams*: Laboratório Nacional de Engenharia civil; 1965.
 28. Borosnyói A, Balázs GL. Models for flexural cracking in concrete: The state of the art. *Structur Concr.* 2005;6(2):53–62.
 29. DIN: EN-1992-1-1/NA. 2011–01, National Annex-Nationally determined parameters-Eurocode 2: Design of concrete structures-Part 1-1: General rules and rules for buildings; 2011.
 30. Beeby AW, Scott RH. Cracking and deformation of axially reinforced members subjected to pure tension. *Mag Concr Res.* 2005;57(10):611–621.
 31. Braam CR. Control of crack width in deep reinforced concrete beams. Ph.D. Thesis, Delft University, the Netherlands; 1990.
 32. CEB. CEB design manual on cracking and deformations. Lausanne, Switzerland: École Polytechnique Fédérale de Lausanne, 1985.
 33. Caldentey AP. Proposal of new crack width formulas in the Eurocode 2, background, experiments, etc. Paper presented at the Crack width calculation methods for large concrete structures, Oslo; 2017.
 34. Debernardi PG, Guiglia M, Taliano M. Effect of secondary cracks for cracking analysis of reinforced concrete tie. *ACI Materials Journal.* 2013;110(2):207.
 35. NS 3576-3:2012 Steel for the reinforcement of concrete-Dimensions and properties-Part 3: Ribbed steel B500NC; 2012.
 36. Hansen PF, Pedersen E. Curing of concrete structures: Report. Lyngby: BKI; 1984.
 37. Beeby AW. An investigation of cracking in slabs spanning one way (technical report). London: Cement and Concrete Association, 1970.
 38. Brown D, Iles D, Brettle M, Malik A. Joints in steel construction: Moment-resisting joints to Eurocode 3. Vol BCSA/SCI Connections Group. London: The British Constructional Steelwork Association Limited; 2013.
 39. CEN. EN 1993-1-1, Eurocode 3: Design of Steel Structures: Part 1-1: General rules and rules for buildings. Brussels: European Committee for Standardization, 2005.
 40. Gul M. Effect of cube size on the compressive strength of concrete. *Int J Eng Dev Res.* 2016;4:956–959.
 41. Ahmed M, Mallick J, Hasan MA. A study of factors affecting the flexural tensile strength of concrete. *J King Saud Univ-Eng Sciences.* 2016;28(2):147–156.
 42. Sheskin DJ. Handbook of parametric and nonparametric statistical procedures. 2nd ed. USA: Chapman and Hall/CRC, 2000.
 43. Joanes D, Gill C. Comparing measures of sample skewness and kurtosis. *J Royal Stat Soc: Series D (The Statistician).* 1998;47(1):183–189.
 44. Gribniak V, Mang HA, Kupliauskas R, Kaklauskas G. Stochastic tension-stiffening approach for the solution of serviceability problems in reinforced concrete: Constitutive modeling. *Comput Aided Civ Inf Eng.* 2015;30(9):684–702.
 45. Gribniak V, Rimkus A, Torres L, Jakstaite R. Deformation analysis of reinforced concrete ties: Representative geometry. *Structur Concr.* 2017;18(4):634–647.
 46. Borosnyói A, Snóbli I. Crack width variation within the concrete cover of reinforced concrete members. *Építőanyag.* 2010;62(3):70–74.
 47. Carino NJ, Clifton JR. Prediction of cracking in reinforced concrete structures, US Department of Commerce, National Institute of Standards and Technology; 1995.
 48. Husain SI, Ferguson PM. Flexural crack width at the bars in reinforced concrete beams. Retrieved from Center for Highway Research. Texas: University of Texas at Austin, 1968.
 49. Base GD, Read JB, Beeby A, Taylor H. An investigation of the crack control characteristics of various types of bar in reinforced concrete beams. Slough, England: Wexham Springs, 1966.
 50. Barre F, Bisch P, Chauvel D, Cortade J, Coste JF, Dubois JP. Control of cracking in reinforced concrete structures. Hoboken, NJ: John Wiley & Sons Inc.; 2016.
 51. Tan R. Consistent crack width calculation methods for reinforced concrete elements subjected to 1D and 2D stress states: A mixed experimental, numerical and analytical approach. PhD Thesis, Trondheim, Norway: Norwegian University of Science and Technology, 2019.
 52. Beeby AW. The influence of the parameter ϕ/ρ eff on crack widths. *Structur Concr.* 2004;5(2):71–83.
 53. McLeod CH, Viljoen C. Quantification of crack prediction models in reinforced concrete under flexural loading. *Structur Concr.* 2019;20(6):2096–2108.

AUTHOR BIOGRAPHIES



Chavin N. Naotunna
Research Fellow
Department of Mechanical and
Structural Engineering and Material
Science
University of Stavanger
Stavanger, Kjell Arholmsgate 41, 4036
Stavanger, Norway.
Email: chavin.guruge@uis.no



Samindi M. K. Samarakoon
Associate Professor
Department of Mechanical and
Structural Engineering and Material
Science
University of Stavanger
Stavanger, Kjell Arholmsgate
41, 4036 Stavanger, Norway.
Email: samindi.samarakoon@uis.no



Kjell T. Fosså
Adjunct Professor
Department of IMBM
University of Stavanger
Manager Concrete Technology
Kværner AS, Concrete Solutions,
4020 Stavanger, Norway.
Email: kjell.tore.fossa@kvaerner.com

How to cite this article: Naotunna CN, Samarakoon SMK, Fosså KT. Experimental and theoretical behavior of crack spacing of specimens subjected to axial tension and bending. *Structural Concrete*. 2021;22:775–792. <https://doi.org/10.1002/suco.201900587>

Paper 4: Identification of the influence of concrete cover thickness and \emptyset/ρ parameter on crack spacing.

Naotunna, C.N., Samarakoon, S.M.S.M.K., and Fosså, K.T. (2020)

In: *Proceedings of the 15th International Conference on Durability of Building Materials and Components (DBMC 2020)*. Barcelona: pp.1797-1804, ISBN: 978-84-121101-8-0.

Identification of the Influence of Concrete Cover Thickness and \emptyset/ρ Parameter on Crack Spacing.

Chavin N. Naotunna, S.M Samindi M.K Samarakoon and Kjell T. Fosså

Department of Mechanical and Structural Engineering and Material science, Faculty of Science and Technology, University of Stavanger, Stavanger, Norway, chavin.guruge@uis.no

Abstract. Cracks due to the service load in the reinforced concrete structures are controlled at the design stage, by limiting the calculated crack width. Widely used crack width calculation models (Eurocode 2 and Model code 2010), estimates the crack width by multiplying the crack spacing with the mean strain difference of concrete and reinforcement. Concrete cover thickness and the ratio of diameter to reinforcement area to effective tensile area of concrete ($\emptyset/\rho_{p,ef}$) are the two main crack spacing governing parameters in the aforementioned models. The existing models are mostly applicable when concrete cover thickness is within the specified limit. For example, Model Code 2010 model limits the concrete cover thickness to 75 mm. In order to identify the influence of aforementioned two governing parameters on crack spacing, the results of recent experiments have been considered. According to some recent studies, it is found that the concrete cover thickness has a significant influence and the $\emptyset/\rho_{p,ef}$ parameter has a negligible effect on crack spacing. To investigate the reasons why the $\emptyset/\rho_{p,ef}$ parameter has a negligible effect on crack spacing, the involvement of bond properties is needed to study. Some authors have specified that the large diameter bars consist of higher bond force per unit surface area than the small diameter bars, due to the high rib area. Due to this reason, the similar bond behavior could be identified, from low number of large bar diameters and high number of small diameter bars. A literature review has been carried out to study the bond behavior on specimens subjected to pure tension. With the facts and available data, it is further verified that the $\emptyset/\rho_{p,ef}$ parameter has a negligible influence and concrete cover thickness has a significant effect on crack spacing.

Keywords: Crack Spacing, Concrete Cover, Bond Stress-Slip, Axial Tension.

1 Introduction

Cracks in the reinforced concrete (RC) structures create issues to the durability, aesthetic appearance and the liquid or gas tightness of the structure. Among the various types of cracks that can generate in a structure, the cracks due to service load is controlled at the design stage by limiting the calculated crack width. In the most widely used codes of practices (Ex. Eurocode 2, 2004; Model code 2010, 2013; etc.), the calculated crack width is governed by multiplying the crack spacing with the mean strain difference between reinforcement and concrete. Therefore, the crack spacing parameter can be identified as an important factor in crack controlling criteria. However, it has identified many limitations in the above-mentioned available crack controlling methods (Ex. limitation for the maximum value of concrete cover thickness). Further, there are many experimental evidences from previous literatures, that the experimental predictions do not match with the code prediction values.

In the aforementioned codes, the concrete cover thickness and $\emptyset/\rho_{p,ef}$ parameter (ratio of diameter to reinforcement area to effective tensile area of concrete) have identified as the two most governing factors of the crack spacing model. In order to improve the existing models, the authors have studied the behavior of aforementioned parameters with the help of available literatures. The crack width or crack spacing models developed in the mentioned codes are based on the axial tension experiments of an RC tie subjected to pure tension. Because a RC tie in pure tension can be represented the tensile region of a bending member with or without axial tension (Debernardi *et al.*, 2013). There are many previous experiments reported, which have

studied about the cracking behavior of RC members. Among them, it can be found various types of data to identify the crack width governing parameters. However, with the advancement of material and geometrical properties of concrete and reinforcement, the authors have selected two recent axial tensile experiments mentioned in (Tan *et al.*, 2018; Tan *et al.*, 2019) and (Rimkus and Gribniak, 2017), to identify the crack spacing governing parameters. The selected experiments consist of the RC ties with multiple reinforcement bars, which are more similar to the RC members in practice.

The concrete cover parameter and $\emptyset/\rho_{p,ef}$ parameter is available in the existing crack governing models are due to the ‘no-slip theory’ and ‘bond-slip theory’ respectively (Broms, 1965; Saliger, 1936). The ‘no-slip theory’ assumes a perfect bond between reinforcement and surrounding concrete. The ‘bond-slip theory’ considers that a slip occurs between the reinforcement-concrete interface. From the selected experimental data, it could identify that concrete cover thickness has a significant impact on crack spacing, and therefore to the crack width. When considering the effect of $\emptyset/\rho_{p,ef}$ parameter, it could identify that the parameter has a negligible effect on the crack spacing (Beeby, 2004; Rimkus and Gribniak, 2017). When trying to identify the reasons for this controversial conclusion, Ålander in (Beeby *et al.*, 2005) makes a statement, that when the bar diameter increases, the rib area also increases (even with similar rib pattern). This increased rib area in larger bar diameters cause to have a higher bond force per surface unit area, than the smaller bar diameters (Noghabai, 1995). This effect is not considered in the existing EC2 or MC 2010 models. The mentioned models assume the bond-stress is only a factor of tensile strength of concrete. For example, MC 2010 assumes that the mean bond stress between concrete and reinforcement is equal to 1.8 times the mean tensile strength of concrete in the stabilized cracking stage.

Balaz (1993), introduces a mathematical model to identify crack widths by using the well-known Ciampi-Eligehausen (Ciampi *et al.*, 1981; Eligehausen *et al.*, 1982) bond-slip model. Ciampi-Eligehausen, bond-slip model is based on Rilem-type pull-out test (RILEM, 1994) results. Therefore, at first this paper reviews literatures focusing on the effect of rebar size on bond properties in Rilem-type pull out tests. However, many existing literatures concluded that, bond strength and stiffness decrease with the increase of bar diameter (which is opposite to the expected results). Therefore, this paper investigates the actual bond-slip behavior of specimens subjected to ‘axial tension’.

2 The Behavior of Concrete Cover and $\emptyset/\rho_{p,ef}$ Parameter on Crack Spacing from the Recent Experiments

Table 1 shows the test results of axial tensile experiments of RC ties mentioned in Tan *et al.*, (2018) and Tan *et al.*, (2019). Table 1 confirms that the increase of concrete cover, cause to increase crack spacing. When comparing the specimen 1 and 3, with the increase of concrete cover, the maximum crack spacing (Table 1) increases. Likewise, the crack spacing values and specimen 2 and 4 behaves similarly.

Table 1. Crack spacing values measured in stabilized cracking stage (Tan *et al.*, 2019).

Specimen No.	Width \times height \times length (m \times m \times m)	No. of bars	Diameter (mm)	Cover (mm)	$\emptyset/\rho_{p,ef}$	$S_{r,mean}$ (mm)	$S_{r,max}$ (mm)
1	0.4 \times 0.4 \times 3	8	32	40	796	178	240
2	0.4 \times 0.4 \times 3	8	20	40	1274	163	250
3	0.4 \times 0.4 \times 3	8	32	90	796	266	320
4	0.4 \times 0.4 \times 3	8	20	90	1274	217	290

Considering specimen 1 and 2 (likewise, 3 and 4) with the same concrete cover thickness, specimen size and material properties, the effect of $\emptyset/\rho_{p,ef}$ parameter on crack spacing cannot be compared, due to difference in steel areas (Specimen 1 and 2 have $8 \times \pi \times 16^2 \text{ mm}^2$ and $8 \times \pi \times 10^2 \text{ mm}^2$ steel areas respectively). The same steel area can be represented with different sizes of reinforcement. If small diameter bars are used, the circumference area of the rebar are higher than when the same steel area is replaced by large diameter bars. For example, if one 16 mm bar is replaced with four 8 mm bars (similar steel area), the circumference area is doubled [$(4 \times \pi \times 8) / (1 \times \pi \times 16) = 2$]. Therefore, the higher number of smaller diameter bars consist of higher concrete-reinforcement interface area than the few number of large diameter bars arrangement. When bond area becomes large, transfer length will be low. In theory, the RC specimens with similar cross-sectional area and similar steel area, the larger bar diameter has the higher $\emptyset/\rho_{p,ef}$ value. According to the EC2 and MC 2010 crack spacing models, this cause to predict larger crack spacing values than the specimens with smaller bar diameter.

Rimkus and Gribniak (2017) have studied the effect of $\emptyset/\rho_{p,ef}$ on crack spacing, by keeping the steel area and other previously mentioned crack spacing governing parameters constant. In the study, the different values for $\emptyset/\rho_{p,ef}$ has been obtained by changing the rebar diameters. This experiment had tested 21 number of specimens with 150 mm x 150 mm (Height x width) cross section size and 30 mm concrete cover thickness. The study have tested three different steel areas of 315 mm², 450 mm² and 607.5 mm² (Steel ratio ($\rho_{p,ef}$) of 1.4 %, 2.0 % and 2.7 % respectively) and used different deformed bar sizes of 5 mm, 6 mm, 8 mm, 10 mm, 12 mm and 14 mm diameters to change the $\emptyset/\rho_{p,ef}$ ratio. However, the final conclusion of the experiment is that, the crack spacing has a negligible influence from the $\emptyset/\rho_{p,ef}$ parameter.

The conclusions of the aforementioned results in Rimkus and Gribniak (2017), gives a good agreement with the statement of Beeby (2004). Moreover, Beeby (2004) compares previous experiment results of (Farra and Jaccoud, 1994; Haqqi, 1983) and concluded that the $\emptyset/\rho_{p,ef}$ parameter does not influence on crack width or crack spacing. However, when the experiments in (Farra and Jaccoud, 1994; Haqqi, 1983) have altered the $\emptyset/\rho_{p,ef}$ parameter for the comparison, the reinforcement ratios also differed unlike in the experiments of (Rimkus and Gribniak, 2017). Therefore, the statement of Beeby (2004) is further confirmed from the experimental results of (Rimkus and Gribniak, 2017).

3 The Involvement of The Bond-Properties to the Crack Spacing Models.

It is vital to investigate reasons why the previous experimental findings shows that $\emptyset/\rho_{p,ef}$ parameter, (which appears from the 'bond-slip approach') does not influence on crack spacing. Alander, who had studied the reinforcement rib geometry on crack widths in Alander (2002), have made a good explanation for this reason in the discussion paper Beeby *et al.* (2005). According to their findings, the bond per surface area of every reinforcement is not similar, due to the different rib geometry. Moreover, when the diameter of a bar increases, the bond strength increases, due to the increase in rib area and height relative to the smaller bar diameters (nominal bar diameter to rib height is generally used as 22). Therefore, the assumption made on developing the existing crack spacing models that the bond stress is similar among every bar diameter have to be reconsidered.

The rib pattern or height are considered as the governing factors of the bond-strength and bond-stiffness of a reinforcement. The ratio of the nominal bar diameter to rib height is generally used as 22 in reinforcement (Metelli and Plizzari, 2014). Bond-index parameter quantitatively represent the effect of rib-pattern and rib-height of a specific reinforcement. The

bond-index is identified as the most governing rib parameter that influences bond-strength and bond-stiffness and EC2 specifies to have a minimum bond index of 0.056 for a bar exceeding the diameter of 12 mm. To investigate the statement made by Alander in Beeby *et al.* (2005) discussion paper, a literature review has been studied on the size effect of the bars on the bond between concrete and reinforcement. The details and the conclusions of some existing literatures are listed in the Table 2.

Table 2. Summary of the previous studies on the bond behavior for size effect.

Publication	Experiment	Diameter (mm) - [Bond Index]	Results
Bažant <i>et al.</i> (1995)	Unconfined Pull-out test	3.175, 6.35, 12.7, 25.4 [smooth bars]	Size effect presents. Bond strength is low in large bars.
Noghabai (1995)	Confined (steel casing) Pull-out test.	8, 16, 32 [Deformed bars]	Bond strength increases with the diameter. The embedded length is short (2.5*diameter).
Bamonte and Gambarova (2007)	Confined (steel casing) Pull-out and push-in tests.	Machine Ribbed 5, 12, 16, 28 – [0.086]	Bond strength decreases with the increase of bar diameter
Metelli and Plizzari (2014)	Unconfined Pull-out test	Machine Ribbed 12, 16, 20 – [0.04-0.105] Commercial (hot-rolled) 12 - [0.095,0.105] 20 - [0.079, 0.089] 40 - [0.054, 0.072] 50 - [0.04, 0.063]	Bond strength increases with the increase of bond index (rib area). Bond strength and stiffness decreases with the increase of bar diameter.
Shima <i>et al.</i> (1987)	Confined Pull-out test for long embedded length (40 times diameter).	Ribbed Bars 19.1 25.4 31.8	Bar Diameter has a small effect and bond strength is proportional to 2/3 power of concrete compressive strength.
Morita (1994)	Confined (large covers (5.5*dia.)) Axial tensile test.	3, 7, 13, 19, 25, 51 [Deformed bars]	Size effect does not present in specimens subjected to axial tension with large covers.

According to the Table 2, except in Noghabai (1995), other experiments have concluded that the bond strength decreases with the increase of bar diameter. These results does not agree with the previously mentioned statement by Alander in Beeby *et al.* (2005) discussion paper. This can lead to another direction, whether the pull-out or push-in tests represents the bond-behavior of an RC tie subjected to axial tension or flexure. The authors in (Alander, 2002; Beconcini *et al.*, 2008; Mazzarolo *et al.*, 2012) explains that the traditional Rilem-type tests (RILEM, 1994) does not represent the bond condition of a member subjected to bending or axial tension. The main reasons for the discrepancy are identified as the short anchorage length (embedded length is five times the bar diameter), one-way loading method (the concrete parallel to the reinforcement is in compression), failure mode (splitting failure that occurs in unconfined tests) in the standard pull-out tests. The short embedded length is decided in the Rilem-type test is to ensure the uniform distribution of the bond stress along the bar (Mazzarolo *et al.*, 2012) and to reach the bond-failure before rebar yields (Bamonte and Gambarova, 2007; Mazzarolo *et al.*,

2012). In order to make the experimental conditions closer to the practical situation, Shima *et al.*, (1987) have used longer embedded lengths (40 times diameter) and studied the size effect on bond stress (Table 2).

It has observed that the reinforcement-concrete interface in axial tensile members does not subject to the range of slip value as observed in the Rilem-type tests. The experimental investigation of the crack widths at the level of reinforcement in (Borosnyói and Snóbli, 2010; Husain and Ferguson, 1968; Tammo and Thelandersson, 2009) have proved that the slip is in the range of hundredth of a millimeter (ex. 0.01 mm to 0.06 mm). These studies have observed the crack width propagation along the concrete cover thickness by sealing the crack, with a hardened epoxy and examining by cutting the specimen. (Borosnyói and Snóbli, 2010; Caldentey *et al.*, 2013) have explained the reason for the relatively small crack widths at the reinforcement face. They have considered that it is due to the accumulation of strains in secondary cracks, which are identified as Goto cracks in Goto (1971). These secondary cracks are developed around the primary cracks (Debernardi *et al.*, 2013; Debernardi and Taliano, 2016) and therefore the ‘slip’ is considered as spread at the vicinity of primary crack. However, Yannopoulos (1989) has conducted experiments to study the variation of crack widths along the concrete cover thickness. During, the experiment, the increase length of specimens was measured using gauges that were fixed at the both end-faces perpendicular to the reinforcement of the axial tensile tie. One measurement was obtained 2.2 mm away from the reinforcement and the other measurement was obtained at the edge (i.e. at a distance of concrete cover) of the specimen. The obtained average change in length were 0.06 mm and 0.13 mm respectively. The conclusion is that, even the internal cracks do exist, their accumulation does not equal with the crack widths at the concrete surface. Therefore, the internal cracks (spread around primary cracks) cannot be considered as a contributor to the slip.

The experiment mentioned in Beeby (2004), contributes to the fact that, slip does not occur between reinforcement and concrete interface in axial tensile members. A layer of grout is applied at the end faces of RC tie (faces perpendicular to reinforcement) and observed no cracks in the reinforcement-concrete interface after the tensile load is applied. Due to these facts, the slip between reinforcement and concrete can be expressed as negligible and the cracking is according to the ‘no-slip theory’. However, to ensure this fact, the authors have studied through the aforementioned bond-slip experiments conducted for axial tensile experiments. The method of slip and bond-stress measurements in conducted axial tensile experiments are listed in Table 3. Except for the experiment mentioned in Doerr (1978), other listed experiments have not measured the concrete strain separately to obtain the slip. Either the researcher has neglected the concrete strain or calculated it from the force equilibrium using only the reinforcement strain. There is a possibility that these calculated concrete strain can be due to ‘no-slip’ conditions. The experiment mentioned in Doerr (1978), which had separately measured the ‘concrete strain’ with strain gauges, 16 mm away (one diameter length) from the reinforcement face. This measurement does not represent the slip at the reinforcement – concrete interface. Based on above reasons it is not clear whether the experiments given in Table 3 have measured the actual value of slip.

Table 3. Details of the axial tensile experiments focused on bond-slip.

Experiment	Details	Bond stress	Slip
Doerr (1978) Cylindrical specimen dia.= 150 mm. Length = 600 mm. Bar dia. = 16 mm Strain gauge on rebar and concrete. Spacing = 28 mm	Concrete strain gauges were placed 16 mm away from concrete, while casting. Electrical resistance wire strains were used. Specimen were sectioned to 28 mm size parts along the length.	Bond stress ($\tau(x)$) along the bar $\tau(x) = -\frac{1}{\pi\phi} \frac{dP(x)}{dx}$ $P(x)$ - Force in reinforcement. Where $P(x)$ can be identified by interpolating the steel strain at each segment.	Slip of the element 'a+1' ($s_{(a+1)}(x)$), $s_{(a+1)}(x) = \epsilon_{s,a} \cdot dx - \epsilon_{c,a} \cdot dx$ $\epsilon_{s,a}$ - Strain in reinforcement $\epsilon_{c,a}$ - Strain in concrete dx - spacing of strain gauges
Morita (1994) Rectangle specimens Square c/s = $12 \cdot \phi$ Length = $60 \cdot \phi$ Strain gauge only on rebar. Spacing = $5 \cdot \phi$	Concrete strain is neglected when calculating the slip, assuming the domination contributor to the slip is the internal cracks.	Bond-slip model identified by (Muguruma, Morita, and Yoshida, 1967) $\frac{d^2y s(x)}{dx^2} = \frac{4(1+np)}{Es} \cdot \tau(x)$ $s(x)$ - Slip n - Modulus ratio p - Steel Ratio	Slip is identified from the steel strain, neglecting concrete strain. Slip of the element 'a+1', $s_{(a+1)}(x) = \epsilon_{s,a} \cdot dx$
Beconcini <i>et al.</i> (2008) Cylindrical specimen dia.= 132 mm. Length = 1000mm. Bar dia. = 16 mm Strain gauge only on rebar. Spacing = 25mm	Specimen were sectioned to 25 mm size parts along the length. Concrete and steel stresses and strains of each section were identified with a constitutive model based on Ramberg Osgood formation and with the force equilibrium $F = F_s + F_c$.	Equilibrium of a rebar portion $d\sigma_s \cdot \frac{\pi\phi^2}{4} = \pi\phi\tau(x)$ σ_s - Steel stress calculated from steel strain	From the definition of slip $\frac{ds}{dx} = \epsilon_s - \epsilon_c$

When considering the bond-slip behavior of the specimens subjected to axial tension, it can be concluded that the 'bond-slip' theory can cause a negligible influence on crack spacing. Therefore the involvement of $\phi/\rho_{p,ef}$ parameter on crack spacing behavior have to be reconsidered. Further This description ends with agreeing the conclusion of Beeby (2004), that the $\phi/\rho_{p,ef}$ parameters has a negligible effect, while concrete cover thickness has a significant effect on crack spacing and therefore to the crack width.

4 Summary and Conclusions

Concrete cover thickness and $\phi/\rho_{p,ef}$ parameter have identified as governing parameters of crack spacing models in Eurocode 2 and Model code 2010. From the recent experimental results, it

could be identified that the concrete cover thickness has a significant effect on crack spacing. However, the $\phi/\rho_{p,ef}$ parameter, which present in the crack spacing model due to the ‘bond-slip theory’ has a negligible influence to the crack spacing. A possible reason for that can be the effect of different rib indexes of different bar sizes, which is not taken into account in the above-mentioned crack spacing models. Experimental results showed similar crack spacing values using low number of large bar diameters and high number of small bar diameters. Therefore, the bond per unit surface area have to be higher in large diameter bars than small diameter bars. A literature survey is carried out to identify the aforementioned effect and it is found that, the bond per unit surface area is getting lower with the increase of bar diameter. Moreover, it is vital to investigate the applicability of Rilem-type pull-out test results to study the bond behavior in a RC tie. The main contradiction is the, obtained slip value in axial tension is significantly smaller than Rilem-type pull-out tests. Further, there is an argument that the internal cracks contribute to the slip. However, the results of Yannopoulos (1989) have proved that the internal cracks do not have a significant contribution to the slip. Further, Beeby (2004) have experimentally proved that there is no slip occurred at the reinforcement-concrete interface of an RC tie in pure tension. Moreover, as mentioned in the available studies on bond-slip behavior subjected to axial tension, have not measured the concrete strain separately, to measure the slip value. Therefore, it can be concluded that the mentioned crack spacing models have overestimated the effect of bond-slip behavior.

ORCID

Chavin N. Naotunna: <https://orcid.org/0000-0003-4994-2675>

S.M Samindi M.K Samarakoon: <https://orcid.org/0000-0002-6847-972X>

References

- Alander, C. (2002). *The effect of rib geometry on crack widths and the service life of structures*. Paper presented at the 3rd International Symposium on Bond in Concrete.
- Balazs, G. L. (1993). Cracking analysis based on slip and bond stresses. *Materials Journal*, 90(4), 340-348.
- Bamonte, P. and Gambarova, P. G. (2007). High-bond bars in NSC and HPC: Study on size effect and on the local bond stress-slip law. *Journal of Structural Engineering*, 133(2), 225-234.
- Bažant, Z. P., Li, Z. and Thoma, M. (1995). Identification of stress-slip law for bar or fiber pullout by size effect tests. *Journal of engineering mechanics*, 121(5), 620-625.
- Beconcini, M. L., Croce, P. and Formichi, P. (2008). *Influence of bond-slip on the behaviour of reinforced concrete beam to column joints*. Paper presented at the Proceedings of International fib Symposium “Taylor Made Concrete Structures: New Solutions for our Society.
- Beeby, A. W. (2004). The influence of the parameter ϕ/ρ eff on crack widths. *Structural Concrete*, 5(2), 71-83.
- Beeby, A.W.,C. Å., J. Cairns, R. Eligehausen, U. Mayer, S. Lettow, Daniele Ferretti, I. Iori, Pietro G. Gambarova, Patrick Bamonte, Ezio Giuriani, Giovanni A. Plizzari, Stavroula Pantazopoulou and Souzana Tastani. (2005). Discussion : The influence of the parameter ϕ/ρ_{eff} on crack widths. *Structural Concrete*, 6(4):155-165. doi:10.1680/stco.2005.6.4.155
- Borosnyói, A. and Snóbli, I. (2010). Crack width variation within the concrete cover of reinforced concrete members. *Építőanyag*, 62(3), 70-74.
- Broms, B. B. (1965). Crack width and crack spacing in reinforced concrete members. *Paper presented at the ACI Journal Proceedings*.
- CEN. (2004). EN: EN 1992-1-1, Eurocode 2: Design of concrete structures - Part 1–1: General rules and rules for buildings In. Brussels: European Committee for Standardization.
- Ciampi, V., Eligehausen, R., Bertero, V. V. and Popov, E. P. (1981). Analytical model for deformed bar bond under generalized excitations.
- Ciampi, V., Eligehausen, R., Bertero, V. V. and Popov, E. P. (1982). *Analytical model for concrete anchorages of reinforcing bars under generalized excitations*: College of Engineering, University of California Berkeley, CA, USA.
- Debernardi, P. G., Guiglia, M. and Taliano, M. (2013). Effect of secondary cracks for cracking analysis of reinforced concrete tie. *ACI Materials Journal*, 110(2), 207.

- Debernardi, P. G. and Taliano, M. (2016). An improvement to Eurocode 2 and fib Model Code 2010 methods for calculating crack width in RC structures. *Structural Concrete*, 17(3), 365-376.
- Doerr, K. (1978). *Bond behavior of ribbed reinforcement under transversal pressure*. Paper presented at the Nonlinear behavior of reinforced concrete structures; contributions to IASS symposium.
- Farra, B. and Jaccoud, J.-P. (1994). *Influence du béton et de l'armature sur la fissuration des structures en béton: rapport des essais de tirants sous déformation imposée de courte durée*. Retrieved from fib. (2013). fib Model Code for concrete structures 2010. In *Structural Concrete*. Berlin: Ernst and Sohn.
- Goto, Y. (1971). *Cracks formed in concrete around deformed tension bars*. Paper presented at the Journal Proceedings.
- Haqqi, S. (1983). *Serviceability of reinforced concrete subjected to tension*. Polytechnic of Central London.
- Husain, S. I. and Ferguson, P. M. (1968). Flexural crack width at the bars in reinforced concrete beams.
- Mazzarolo, E., Scotta, R., Berto, L. and Saetta, A. (2012). Long anchorage bond-slip formulation for modeling of rc elements and joints. *Engineering Structures*, 34, 330-341.
- Metelli, G. and Plizzari, G. A. (2014). Influence of the relative rib area on bond behaviour. *Magazine of Concrete Research*, 66(6), 277-294.
- Morita, S. (1994). Experimental study on size effect in concrete structures. *Size effect in concrete structures*, 27-46.
- Muguruma, H., Morita, S. and Yoshida, H. (1967). Fundamental study on bond between steel and concrete. *Transaction of Architectural Institute of Japan*, 131, 1-6.
- Noghabai, K. (1995). *Splitting of concrete in the anchoring zone of deformed bars: a fracture mechanics approach to bond*. Luleå tekniska universitet.
- Pérez Caldentey, A., Corres Peiretti, H., Peset Iribarren, J. and Giraldo Soto, A. (2013). Cracking of RC members revisited: influence of cover, ϕ/ρ_s , e_f and stirrup spacing—an experimental and theoretical study. *Structural Concrete*, 14(1), 69-78.
- RILEM, T. (1994). RC 6 Bond test for reinforcement steel. 2. Pull-out test, 1983. *RILEM recommendations for the testing and use of constructions materials*, 218-220.
- Rimkus, A. and Gribniak, V. (2017). Experimental investigation of cracking and deformations of concrete ties reinforced with multiple bars. *Construction and Building Materials*, 148, 49-61.
- Saliger, R. (1936). High grade steel in reinforced concrete. *Paper presented at the Preliminary Publication, 2nd Congress of IABSE*. Berlin-Munich: IABSE Publications.
- Shima, H., Chou, L.-L. and Okamura, H. (1987). Micro and macro models for bond in reinforced concrete. *Journal of the Faculty of Engineering*, 39(2), 133-194.
- Tammo, K. and Thelandersson, S. (2009). Crack widths near reinforcement bars for beams in bending. *Structural Concrete*, 10(1), 27-34.
- Tan, R., Eileraas, K., Opkvitne, O., Žirgulis, G., Hendriks, M. A., Geiker, M., Brekke, D. and Kanstad, T. (2018). Experimental and theoretical investigation of crack width calculation methods for RC ties. *Structural Concrete*, 19(5), 1436 - 1447.
- Tan, R., Max, A. N., Hendriks, Mette, G. and Terje, K. (2019). Analytical calculation model for predicting the cracking behavior of reinforced concrete ties. *Structural Engineering*.
- Yannopoulos, P. (1989). Variation of concrete crack widths through the concrete cover to reinforcement. *Magazine of Concrete Research*, 41(147), 63-68.

Paper 5: Influence of concrete cover thickness and clear distance between tensile bars on crack spacing behavior: Experimental and numerical investigation.

Naotunna, C.N., Samarakoon, S.M.S.M.K., and Fosså, K.T. (2021)

(Submitted to journal).

Influence of concrete cover thickness and clear distance between tensile bars on crack spacing behavior of large-scale RC members: Experimental and numerical investigation

Chavin N. Naotunna¹, S.M. Samindi M.K. Samarakoon¹ and Kjell T. Fosså¹

¹ Department of Mechanical and Structural Engineering and Material Science, Faculty of Science and Technology, University of Stavanger, Stavanger, Norway

Abstract

Crack spacing is a governing parameter in predicting the crack width of reinforced concrete (RC) specimens. Recent studies have identified that the ‘no-slip’ theory is suitable for discussing the actual cracking behavior of RC specimens. Concrete cover (c) and the clear distance between tensile bars (s) are the governing crack spacing parameters, according to the ‘no-slip’ theory. The parameter ‘ s ’ has not been considered in widely used crack spacing models including Eurocode. An experimental program has been conducted, using large-scale RC specimens to investigate the behavior of ‘ c ’ and ‘ s ’ on crack spacings. These experiments have been numerically simulated with 3D non-linear finite element models for the verification of results. The experimental results showed that both ‘ c ’ and ‘ s ’ have an influence on the crack spacings. An equation has been developed with multiple linear regression analysis, and its predictions gave a good agreement with the experimental results in the literature.

Key words. Crack spacing, axial tension, concrete cover thickness, bar spacing, laboratory experiments, non-linear FEM, large-scale specimens.

1.0 Introduction

Crack controlling is a primary serviceability limit state requirement of reinforced concrete (RC) structures. At the design stage, cracks are controlled by limiting their calculated width to a maximum allowable crack width ^{1,2}. Crack spacing is a governing parameter in crack width calculation models ³. Widely used crack spacing prediction models have identified their influencing parameters by considering two main cracking theories, named bond-slip theory and no-slip theory. The governing parameter of the bond-slip theory is the ratio of the bar diameter to the effective steel area (σ/p) ⁴. According to the no-slip theory, the governing crack spacing parameter is the thickness of the concrete surrounding the tensile reinforcement ⁵. Concrete cover thickness and the tensile bar spacings can be identified as the governing crack spacing parameters, according to this

no-slip theory ⁵. Eurocode 2 and Model Code 2010 are the most widely used codes of practice in Europe for the design of RC structures. The crack spacing models in these two codes consider that the crack spacing is based on the combined theory ⁶. Combined theory assumes that the cracking behavior is similar to the combination of both bond-slip theory and no-slip theory. Therefore, in crack spacing models in both Eurocode 2 and Model Code 2010, the ' σ/ρ ' parameter and the concrete cover thickness parameter are included, to represent the bond-slip and no-slip theories, respectively.

Recent studies conducted by Rimkus and Gribniak ⁷, Beeby and Scott ⁸, etc. have identified that the ' σ/ρ ' parameter has a negligible influence on crack spacings. Further, the studies by Bado et al. ⁹, Beconcini et al. ¹⁰ and Doerr ¹¹ have identified a negligible amount of slip in the RC specimens subjected to axial tension. Additionally, by studying the crack width variation along the concrete cover thickness, Naotunna et al. ¹² have identified that the specimens with ribbed bars are subjected to a negligible amount of slip. These facts can conclude that the bond-slip theory has a relatively low influence on the cracking behavior of RC specimens with ribbed bars. On the other hand, it can be considered that the no-slip theory has a higher influence on the cracking behavior of RC specimens.

According to the no-slip theory, the two main parameters are concrete cover thickness and the spacing between the tensile bars. Tensile bar spacing has been considered as a parameter of crack spacing models in Japanese Code ¹³ and CEB-FIP Model Code 1978 ¹⁴ and so on. Further, the recent experimental program conducted in Gribniak et al. ¹⁵, which tested 150×150 -mm cross-sectional specimens reinforced with $\phi 10$ -mm bars, has identified that the bar spacing has an influence on the crack spacings.

RC members with limited cross-sectional width (i.e., beams), which require a relatively large steel area to withstand ultimate limit state load, commonly use reinforcement bars with a large bar diameter. In the construction industry, 32-mm bars are commonly used in bridges and offshore structures ¹⁶. However, studies which have performed experiments using large bar diameters are very limited in the literature. The main reason for this is that it is necessary to apply a relatively large load for the RC specimens to reach service load stress. When the RC structure is subjected to the service load, the steel stress can range from 200 N/mm^2 to 350 N/mm^2 ¹⁷. Recently, several studies have tested RC specimens with multiple bars, since the cracking behavior of such

specimens is more similar to that of RC members in practice^{3,7}. Therefore, an experimental program has been carried out with 2-m-long RC specimens with 200×200 -mm and 300×300 -mm cross sections reinforced with four ϕ 32-mm bars. The experimental program was designed to investigate the effect of concrete cover thickness and tensile bar spacing on crack spacings. The concrete cover thicknesses of the tested specimens were 35 mm, 60 mm, and 85 mm, and the clear distance between bars was 66 mm, 116 mm, and 166 mm. These experiments were simulated in 3D non-linear FEM models for the further verification of experimental results.

2.0 Materials and Methods

The focus of this experimental program is to investigate the effect of concrete cover thickness and tensile bar spacing on the crack spacings of RC members subjected to axial tension. In order to represent the tensile bar spacings, the 'clear distance between the tensile reinforcement' was considered as a parameter. An experimental program was conducted, to study the crack spacings in RC specimens at the concrete laboratory of the University of Stavanger and I.K.M. laboratory testing facility in Tananger, Norway. RC prisms of 2 m length were cast and reinforced with four ϕ 32-mm bars. Steel reinforcement quality was B500NC, according to the NS 3576-3 standard¹⁸, with a characteristic yield strength (f_{yk}) of 500 MPa and Young's modulus of 200 GPa. In the first series, three identical RC specimens were cast with a $200\text{-mm} \times 200\text{-mm}$ cross section. The conducted experimental program of the RC specimens in Series 1 has been reported in Naotunna et al.³. In the second series, three sets of RC specimens (two specimens per set) were cast with a $300\text{-mm} \times 300\text{-mm}$ cross section. The cracking behavior of RC specimens is quite complicated, due to the inhomogeneous behavior of concrete. Therefore, the experimental program was designed to have a large sample size of crack spacing data in each specimen set, to achieve a reasonable representation. All these RC specimens were cast at the concrete laboratory of the University of Stavanger, Norway. The specimens were cast at a room temperature of 20°C and also stored in a 20°C room after taking the necessary precautions for curing. Similar to Series 1, no spacers and stirrups were used to cast the RC specimens, as they can influence the cracks¹⁹. Details of the cast RC specimens are shown in Figure 1 and Table 1.

As mentioned in the Introduction, it is necessary to apply at least 650 kN of tensile load for the four 32 mm bars to reach the service load (for the reinforcement to have a stress of 200 N/mm^2). Axial tensile load was applied, as the four reinforcement bars in an RC specimen get a uniform

distribution of loads. For that, a nut and bolt mechanism was used, as shown in Figure 2. Also shown in Figure 2 (a), both ends of each reinforcement bar were threaded, to act as the nuts to fit M24 bolts. Then the fabricated load connection, using an HEB S355 1000 section, was attached to the RC specimen. In this method, the RC specimen was connected to the loading apparatus at the testing facility, as shown in Figure 2 (b). Since the bar positions differ in each specimen set, separate sets (couples) of load connections were fabricated per specimen set in Table 1. As per the Eurocode 3²⁰ guidelines, it could be assured to resist a load of 900 kN (where the stress in the reinforcement can reach 280 N/mm²). The specimens were loaded by means of the load-control method up to 900 kN, and the load was given in 100-kN steps, with almost 5-minute intervals.

For safety reasons, remaining close to the testing specimen while it was loaded, to measure crack width and the crack spacing, was not permitted. The primary objective of the experimental program was to observe the crack spacings. The cracks were marked in the tested specimen after the load was released, using crack detection microscopes. From the experience of Series 1 experiments reported in Naotunna et al.³, the cracks could be identified with a crack detection microscope even after the load was released. As shown in Figure 2 (b), at the loading machine, the testing RC specimen is covered on both sides by the protection walls. The RC specimens were loaded and unloaded from the top side of the loading machine. Therefore, it was difficult to focus the Digital Image Correlation (DIC) machine perpendicular to a face of an RC specimen, while the test was going on. Since the DIC readings have been obtained inclined towards a face of an RC specimen, they are not adequate to obtain crack widths. Figure 3 shows the propagations of cracks captured at different loading intervals by the DIC system of one of the specimens in set 3.

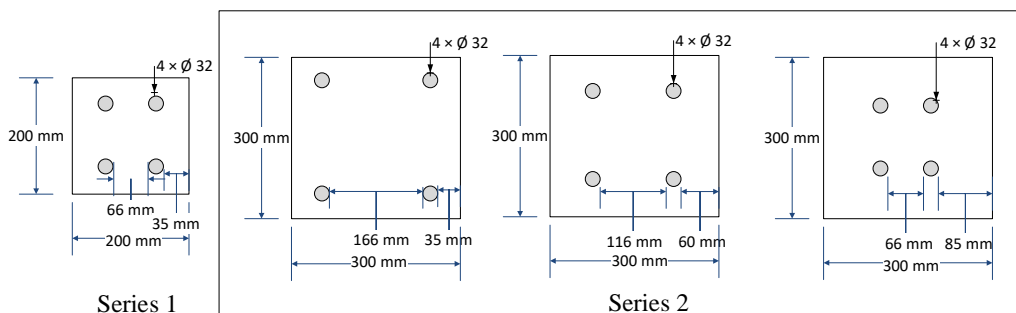


Figure 1. Cross-section details of the tested RC specimens (all specimens are 2 m in length).

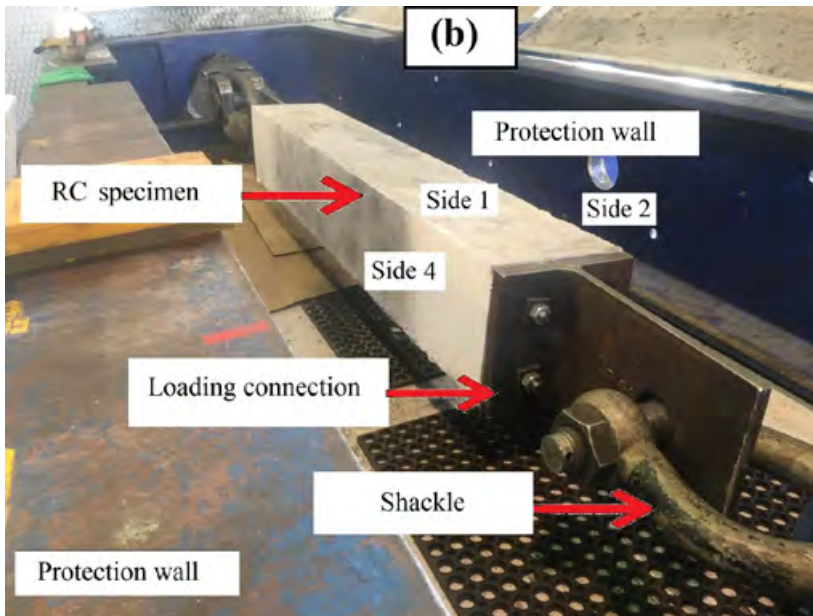
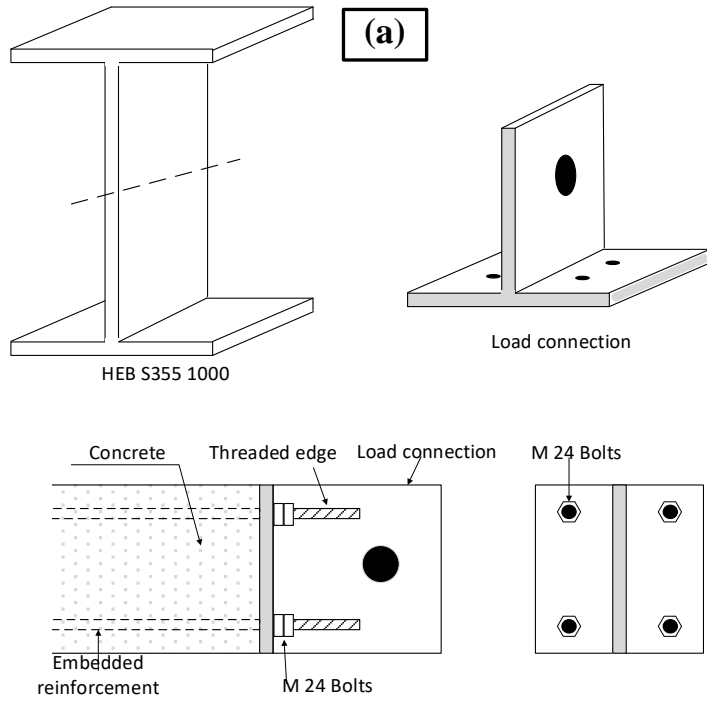


Figure 2. (a) Details of the loading connection, (b) testing of RC specimen.

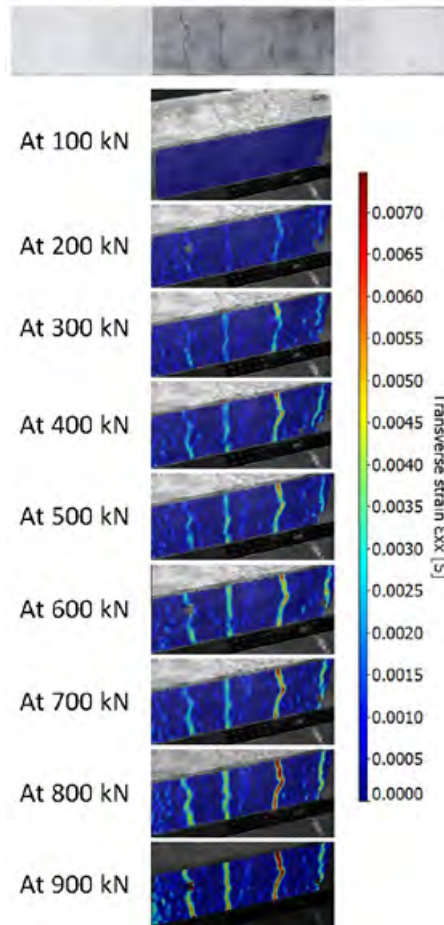


Figure 3. Propagation of cracks captured by the DIC system of one of the specimens in set 3.

Table 1. Details of the tested RC specimens.

Specimen Set	No. of identical specimens	Measured sides per specimen	Specimen width × height (mm × mm)	Cover depth (mm)	Clear distance between bars (mm)	Concrete compressive strength* (MPa)
1	3	3	200 × 200	35	66	35.00
2	2	4	300 × 300	35	166	40.95
3	2	4	300 × 300	60	116	40.95
4	2	4	300 × 300	85	66	40.95

Note

* Concrete compressive strength is the mean $\phi 150 \times 300$ mm cylindrical compressive strength in respect of the test date of the RC specimens.

3.0 Results of the experiment

After the cracks had been marked in the tested RC specimens, the crack spacing measurements were obtained. Since the crack width prediction models in Eurocode 2 and Model Code 2010 predict the crack widths at the concrete surface above the tensile reinforcement, the crack spacing measurements were obtained at the concrete surface, along the center lines of the tensile reinforcement. Figure 4 shows the method for measuring the crack spacing values. Therefore, for each side of an RC specimen, two sets of crack spacing measurements were obtained. In the RC specimen set 1, crack spacing measurements could only be obtained at three faces per specimen, due to irregular finishing of the top surface. However, in other RC specimen sets (specimen sets 2, 3 and 4), crack spacing measurements were obtained on all four sides. Figure 5 (a) to Figure 5 (c) shows the obtained crack spacing readings of specimen sets 2 to 4. Naotunna et al. ³ reported the crack spacing behavior of the tested specimen set 1.

The average and maximum crack spacing values were obtained by a method similar to that used in Naotunna et al. ³. Initially, the results were identified as following the normal distribution. In order to do that, several 'goodness-of-fit' tests were carried out, as specified in Sheskin ²¹. Skewness tests, excess kurtosis tests and KS tests (Kolmogorov–Smirnov test) were carried out, to observe whether the data follows the normal distribution. For a data set to follow the normal distribution, the values of skewness and excess kurtosis tests must lie closer to zero. According to the KS test, the absolute vertical difference between the cumulative distribution functions of the 'sample' and the 'hypothesized normal distribution' is less than the critical values of 0.2 significance; the 'p' value of the sample with a normal distribution is '1'. Similarly, if the aforementioned vertical difference is larger than the critical value of 0.001 significance, the 'p' value of the sample with a normal distribution is '0'. Table 2 shows the results of 'goodness-of-fit' tests conducted for the crack spacing values of each specimen. After normality had been proved for the data sets, the mean and maximum crack spacing values were obtained. The maximum crack spacing value has been considered as the 95% upper boundary of the data set, and Equation 1 was used to obtain those values. Table 3 shows the experimental crack spacing values of each specimen set. From Table 3, it can be seen that both mean and maximum crack spacing values increase from specimen sets 1 to 4. The ratio of the maximum to minimum crack spacing values of the four specimen sets are 1.5

and 1.6. Both Eurocode 2 and Model Code 2010 consider this ratio as 1.7^{22,23}, which gives a good match with the experimental results with more conservative predictions.

$$95\% \text{ upper bound} = m_r + 1.96s_r \sqrt{1 + \frac{1}{n}} \quad (1)$$

where 'm_r' is the mean of the sample, 's_r' is the standard deviation of the sample, and 'n' represents the size of the data sample.

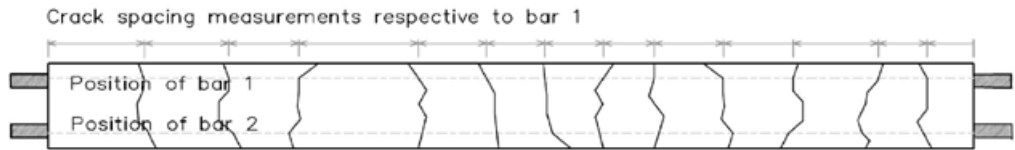


Figure 4. Method of measuring crack spacings.

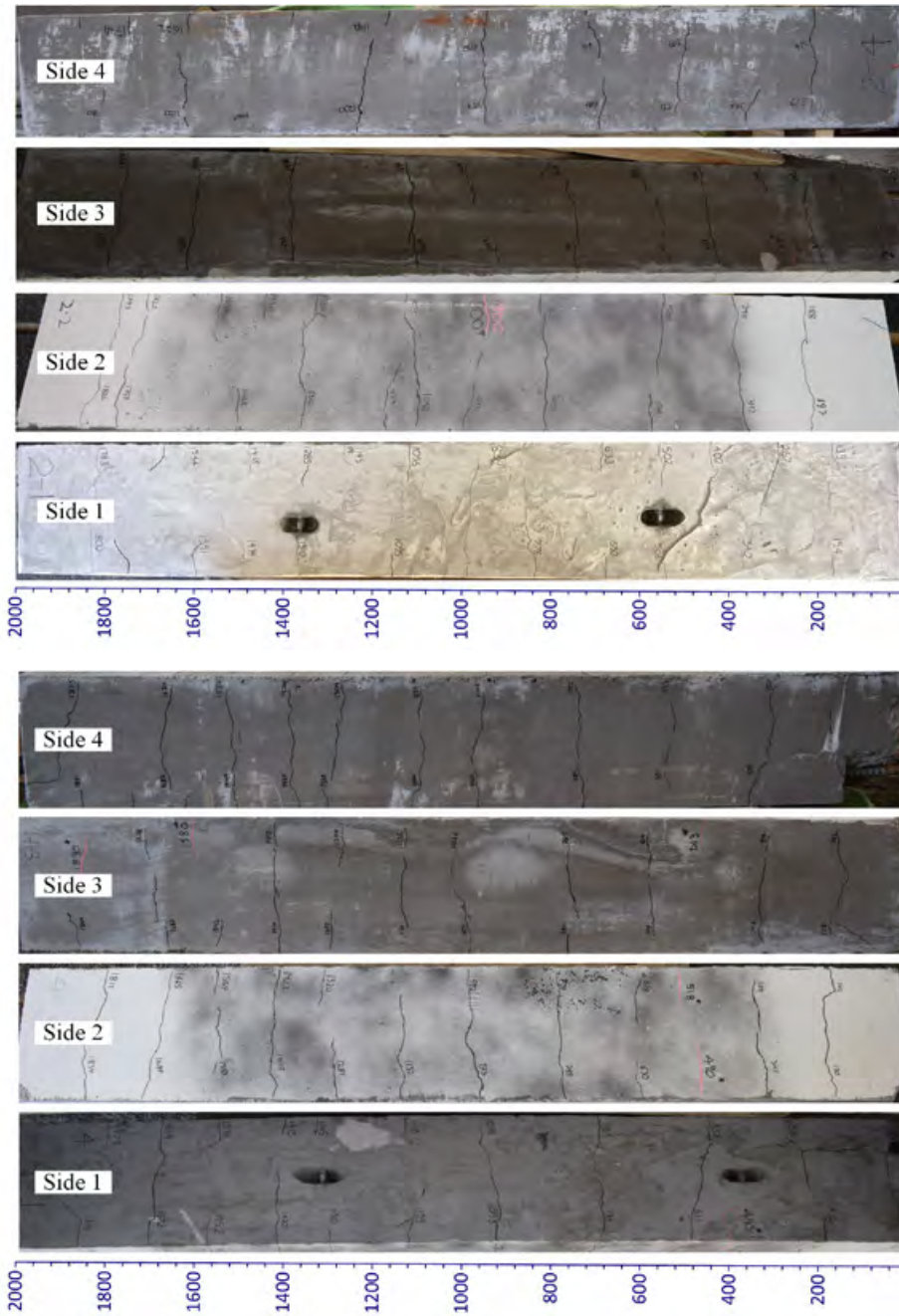


Figure 5 (a). Crack spacings of specimen set 2 (scale is in mm).

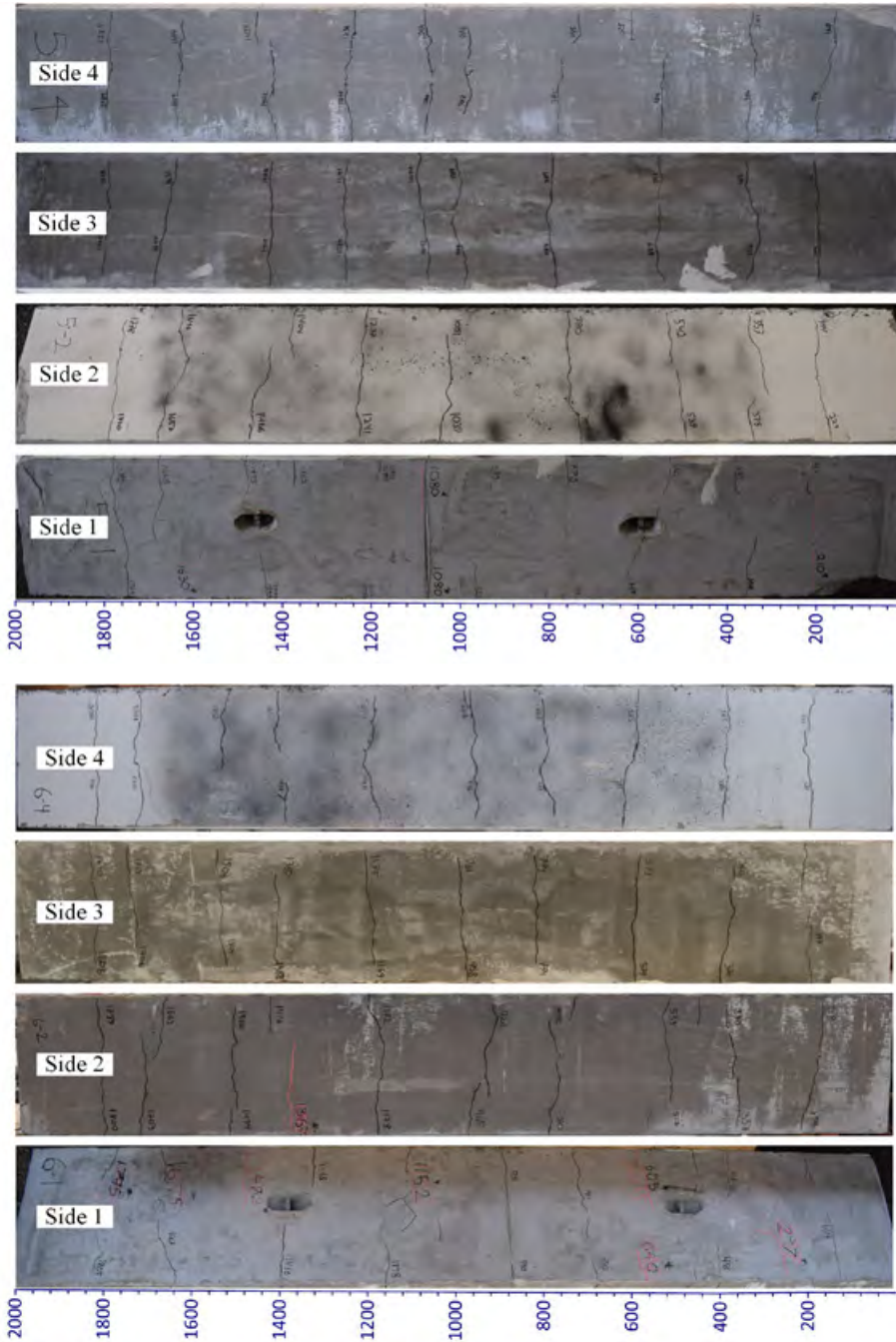


Figure 5 (b). Crack spacings of specimen set 3 (scale is in mm).

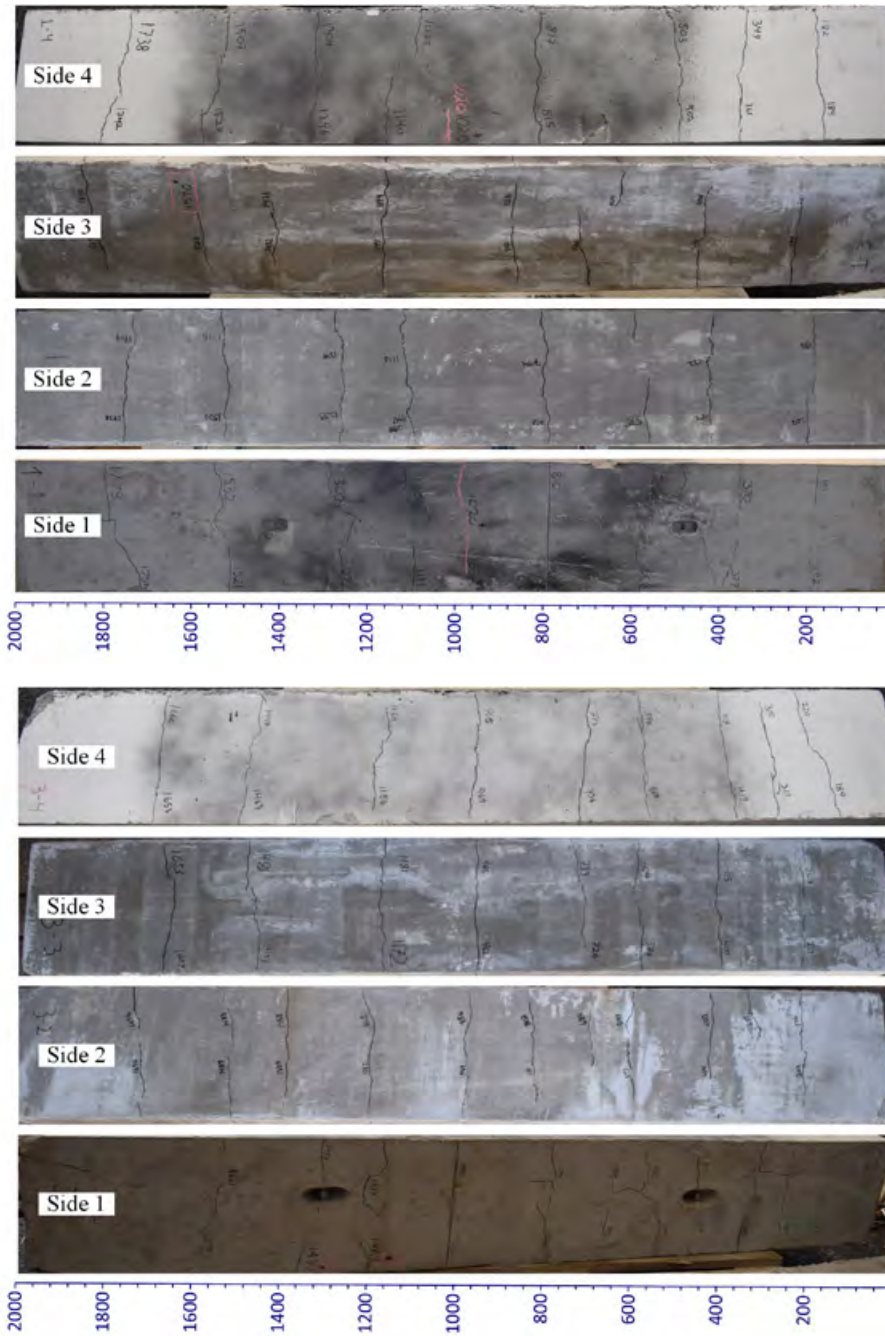


Figure 5 (c). Crack spacings of specimen set 4 (scale is in mm).

Table 2. Results of the ‘goodness-of-fit’ tests.

Specimen set	Skewness test	Excess kurtosis test	Significance of KS test
1	0.38	-0.57	0.02
2	0.37	0.8	0.2
3	-0.2	0.1	0.15
4	0.2	-0.1	0.2

Table 3. Experimental mean and maximum crack spacing values.

Specimen set	No. of crack spacing measurements	Experimental crack spacing (mm)		
		Mean	Max	Max/ Mean
1	266	133	202	1.5
2	191	168	264	1.6
3	174	184	273	1.5
4	157	204	327	1.6

4.0 Numerical simulation of the conducted experiments

For the better understanding and verification of the conducted experimental results, the tests were numerically simulated using 3D non-linear FEM simulation models. For this purpose, finite element software called ‘ATENA’ by ‘Cervenca Consulting’²⁴, Version 5.7.0 with ‘GiD 14.0.2’ interface, was used. For the numerical models, concrete was modeled using eight noded hexahedral elements, and the reinforcement was modeled as 1D elements. The cracks were modeled as smeared cracks (where the crack would occur inside the element), and therefore the reinforcement was also modeled as a smeared reinforcement^{25,26}. This method assumes a perfect bond between reinforcement and concrete, which does not allow a slip to occur in between. This method has recently proved to give the best fit for the experimental results in Rimkus et al.²⁷. The tensile failure (fracture) which occurs in concrete is modeled to follow Hordijk’s law²⁸, where the tensile stress of concrete perpendicular to the crack is a function of crack width. In the simulation model, the load was applied as a displacement-controlled method, by giving the displacement in 0.1-mm incremental steps to an end of four reinforcement bars. The solution of the numerical model is based on the Newton-Raphson method. The developed simulation models are shown in Figure 6.

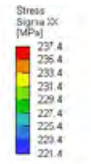
In the experiment, RC specimens were loaded horizontally. Similarly, the FEM simulation models were also loaded horizontally, and therefore vertical constraints, which are required at the initial

loading steps, were added at the bottom edges of the specimens. After several trials, the mesh size of the concrete elements was decided at 25 mm. The measured compressive strengths of concrete (see Table 2) were assigned to the concrete material model, and the other mechanical properties of concrete were selected to be generated according to Eurocode 2 provisions. When modeling the fracture part of concrete, there are several parameters in the material model which can influence cracking behavior. By conducting several trials, it could be seen that the ‘crack spacing min’ parameter, which is used to reduce the energy dissipation in fine meshes, has an influence on the cracking pattern. When modeling specimen sets 1, 2 and 3, a ‘crack spacing min’ parameter of 100 mm was used, and, for specimen set 4, 50 mm was used for this parameter. The obtained cracking behavior of the developed simulation models is shown in Figure 6. Table 4 shows a comparison of the mean crack spacing values in the experimental results and the FEM simulation models. As shown in Table 4, the FEM simulation models’ results give good agreement with the experimental mean crack spacing values. As in every other situation, there are several benefits in numerically simulating the physical experiments. Figure 6 shows the crack pattern and the stress distribution in the embedded reinforcement.

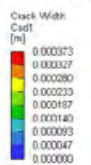
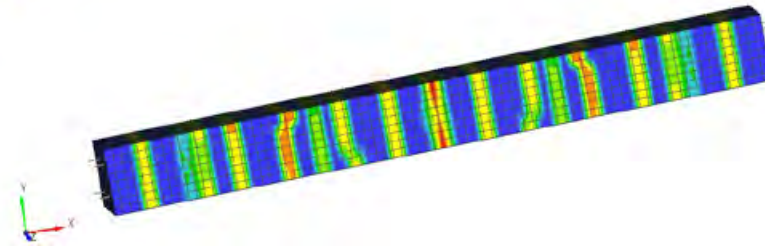
Table 4. Comparison of experimental and numerical mean crack spacing.

Specimen set	Mean crack spacing (mm)		Error %
	Experimental	Numerical	
1	133	125	6.0
2	168	167	0.6
3	184	182	1.1
4	204	200	2.0
$\text{Error} = \frac{(\text{Experimental value} - \text{Predicted value})}{\text{Experimental value}}$			

Specimen set 1

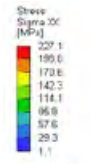


Time: 60.0000
 ATEENA
 x64 V. 5.7.0.183
 License 615
 University of Stav

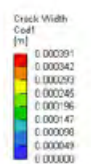
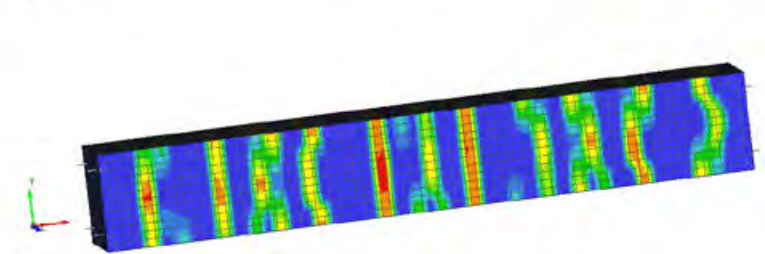


Time: 60.0000
 ATEENA
 x64 V. 5.7.0.18355
 License 615
 University of Stavanger

Specimen set 2



Time: 53.0000
 ATEENA
 x64 V. 5.7.0.183
 License 615
 University of Stav



Time: 53.0000
 ATEENA
 x64 V. 5.7.0.18056
 License 615
 University of Stavanger

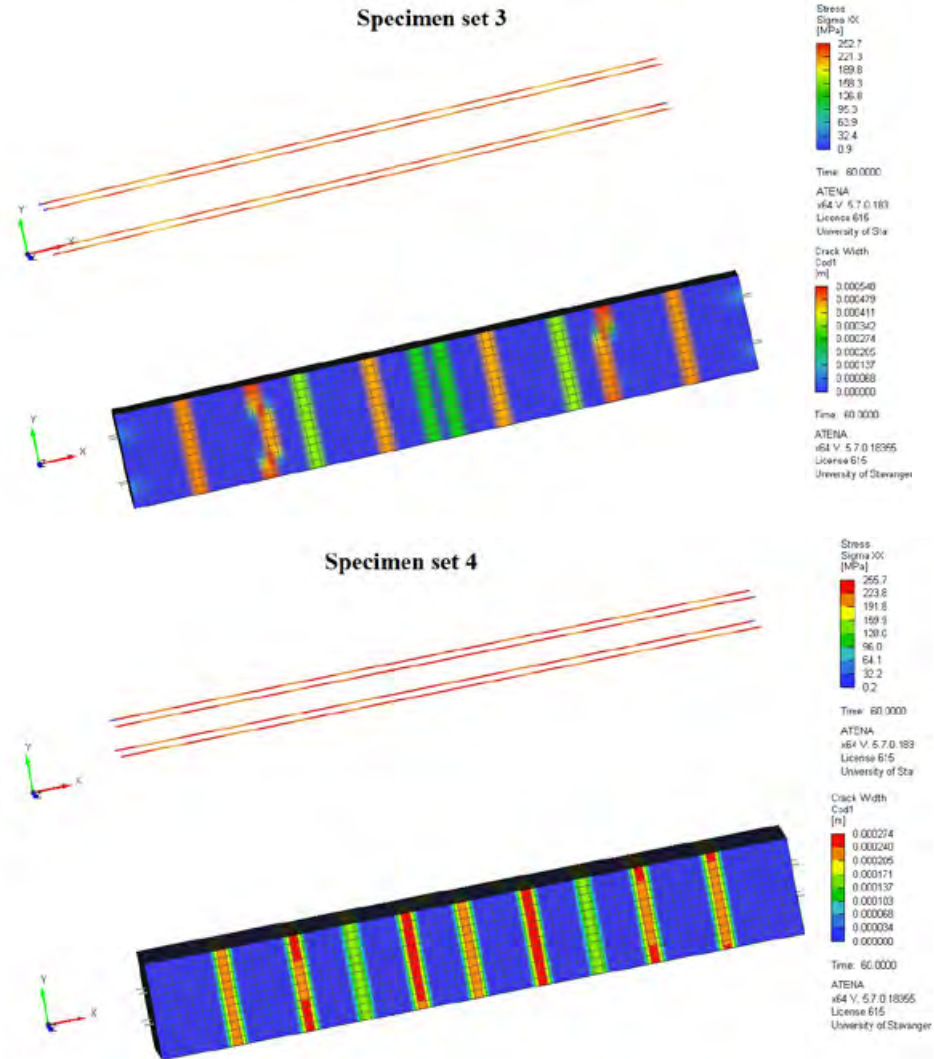


Figure 6. Cracking behavior of the 3D FEM simulation models (one side of each cracked specimen).

5.0 Discussion of the experimental results

As mentioned in Section 1, the governing parameter of the crack spacing models based only on the ‘bond-slip theory’ is the ratio of the bar diameter to the effective steel area (ϕ/p). The crack spacing models in the German National Annex of Eurocode 2²⁹, Deberandi and Taliano³⁰, and Taliano³¹

have considered the crack spacing to be solely based on the bond-slip theory. However, when considering specimen sets 2, 3 and 4, all these specimens have the same value for the bond parameter (σ/ρ). As can be seen in Tables 3 and 4, the crack spacing value changes, even with the same bond parameter, but with different bar spacings and concrete cover thicknesses. The average crack spacing values change from 168 mm to 204 mm, while the maximum crack spacing values change from 264 mm to 327 mm.

In order to observe the effect of a specific parameter on crack spacing, it is necessary to isolate the focused parameter (other influencing parameters must remain constant, while the parameter in focus changes). When changing the concrete cover thickness, it is not possible to keep the specimen's cross-section size constant, without changing the clear distance between bars. Specimen sets 1 and 2 have the same concrete cover thickness (35 mm) and different clear distances between bars. As shown in Figure 7, when the clear distance between bars increases, both mean and maximum crack spacings also increase. As shown in Figure 7, for the better comparison of the results, the mean crack spacing value of the RC specimen with a 30-mm concrete cover thickness and a 70-mm clear distance between tensile bars ¹⁵ has been included. from Gribniak et al. ¹⁵ When considering the results of experiment sets 1 and 3, the clear distance between bars increases from 66 mm to 166 mm, while the mean crack spacing increases from 133 mm to 168 mm. This means that, when the clear distance between bars increases 2.5 times, the mean crack spacing increases 1.3 times. Specimen sets 1 and 4 have the same clear distance between bars (66 mm) and different concrete cover thicknesses. Figure 8 shows that, when the cover thickness increases, both mean and maximum crack spacings also increase. Similar to Figure 7, for the better comparison of results, the mean crack spacing value of the RC specimen with 66 mm of clear distance between bars and with a concrete cover thickness of 30 mm has been included from Rimkus and Gribniak ⁷, for Figure 8. Considering the results of experimental sets 1 and 4, when the concrete cover thickness increases 2.4 times, the mean crack spacing increases nearly 1.5 times. Therefore, it can be identified that both concrete cover thickness and bar spacings are crack spacing governing parameters.

Figure 9 shows, in a three-dimensional graph, the behavior of mean crack spacing in the tested specimen sets. The mean crack spacing values of the nine tested specimens have been plotted against the concrete cover thickness and clear distance between bars. This graph clearly shows that

the effect of concrete cover thickness has a relatively larger influence on crack spacing than the clear distance between bars. A first-degree polynomial equation has been obtained by multiple linear regression analysis, as in Equation 2, which is the equation for the surface given in Figure 9. This surface, shown in Equation 2, gives a good fit with the experimental results, with an R-square value of 0.99. However, this equation was obtained only with results from the conducted experiments. This experimental program was conducted only for RC specimens with four reinforcement bars. Such types of specimens (RC specimens with four bars) were tested in Barre et al.³², Gribniak et al.¹⁵ and Rimkus and Gribniak⁷.

$$S_{r,\text{mean}} = 62 + 1.4 c + 0.3 s \quad (2)$$

where $S_{r,\text{mean}}$ is the mean crack spacing, 'c' is the concrete cover thickness, and 's' is the clear distance between tensile reinforcements.

The experimental mean crack spacing values of the conducted experiment and the aforementioned three studies have been compared with the predictions of Equation 2. Table 5 shows the comparison details of the experimental crack spacing values with the predictions from Equation 2. Since Equation 2 gave a good match with the conducted experimental results (R-square value of 0.94), as shown in Table 5, the error value is significantly small for cases 1 to 4. On the other hand, the predictions from Equation 2 gave a good match with other cases in Table 5, except for case nos. 10, 11 and 12. However, it is important to mention that cases 11 to 13 are from the test results of relatively short specimens, where the specimen length ranged from 379 mm to 505 mm.

Recently, Garcia and Caldentey³³ have identified that the influence of the casting position on the bond condition between reinforcement and concrete has an effect on the cracking behavior. According to the Eurocode 2 provisions, when specimen height is above 250 mm, reinforcements above 250 mm from the bottom of the specimen are considered poorly bonded reinforcements. However, when considering tested specimens whose height is 300 mm, the top reinforcement is still positioned within the good bond condition zone. Therefore, these test results cannot be used to check the effect of casting position on crack spacing. However, when observing the cracks in Figure 5, it can be seen that the cracking behavior in side 1 (top side in respect of concrete pouring direction) differs from the cracking behavior of the other sides. In side 1, the cracks are not properly generated as in the other sides. This can be considered an effect of the casting position, as mentioned in Garcia and Caldentey³³.

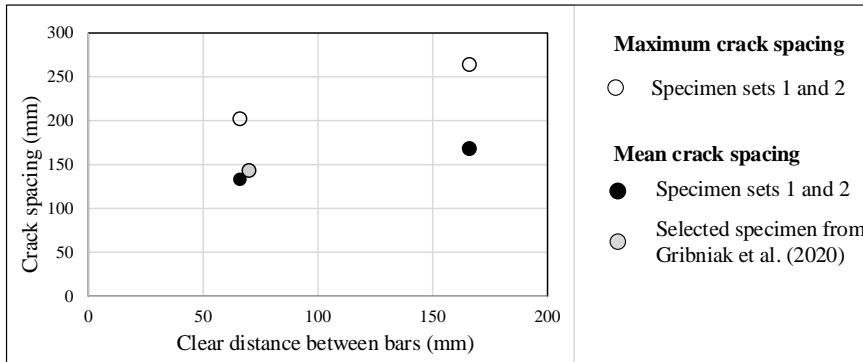


Figure 7. Clear distance between bars vs. crack spacings in specimen sets 1, 2 and selected specimen from Gribniak et al. (2020).

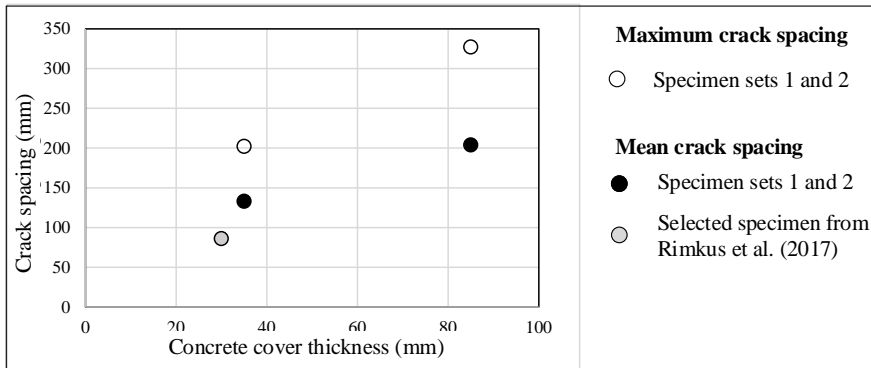


Figure 8. Concrete cover thickness vs. crack spacings in specimen sets 1 and 4 and selected specimen from Rimkus and Gribniak et al. (2017).

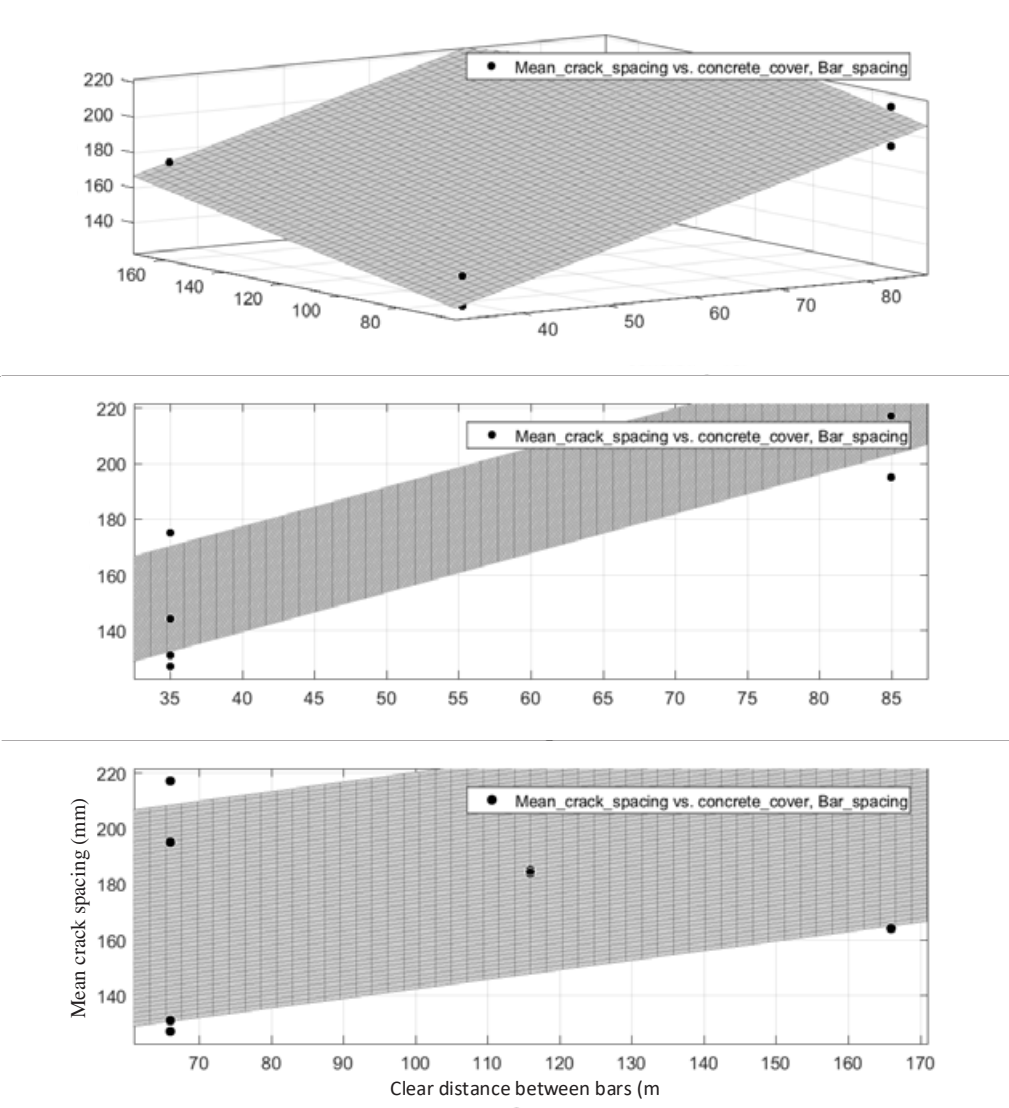


Figure 9. Mean cack spacing behavior in the nine tested specimens.

Table 5. Experimental and predicted mean crack spacing values.

Study	Case no	Width × Height × Length (m × m × m)	Reinforcement details	Concrete cover (mm)	Clear distance between bars (mm)	Mean crack spacing (mm)		Error ^c %
						Exp.	Predict.	
Naotunna et al. 2020	1	0.2 × 0.2 × 2	∅ 32 mm × 4	35	66	133	131	1.7
Conducted experiment	2	0.3 × 0.3 × 2	∅ 32 mm × 4	35	166	168	161	4.3
	3			60	116	184	181	1.7
	4			85	66	204	201	1.6
Barre et al. 2016	5	0.355 × 0.355 × 3.2	∅ 25 mm × 4	65	175	200	206	-2.8
	6		∅ 16 mm × 8	45	108.5	174	158	9.5
Gribniak et al. 2020 ^a	7	0.15 × 0.15 × 1.21	∅ 10 mm × 4	15	100	102	113	-10.8
	8			30	70	143	125	12.6
	9			40	50	144	133	7.6
	10			50	30	227	141	37.9
Rimkus and Gribniak 2017 ^b	11	0.15 × 0.15 × 0.5 ^b	∅ 14 mm × 4	30	62	100	123	-22.6
	12		∅ 12 mm × 4	30	66	86	124	-44.0
	13		∅ 10 mm × 4	30	70	113	125	-10.6
Note								
^a The results of the specimens with 1210 mm length have been considered								
^b Mean crack spacing value is the average of the results of several similar specimens (length 379 mm to 505 mm)								
^c Error = (Experimental value - Predicted value)/ Experimental value								

6.0 Conclusions

An experimental program was conducted to study the crack spacing behavior of RC specimens with multiple reinforcements subjected to axial tension. From the previous studies and a literature survey, it can be identified that the governing crack spacing parameters are concrete cover thickness and the clear distance between tensile bars. Several large-scale RC specimens with a cross section of 200 mm × 200 mm and 300 mm × 300 mm, and reinforced with four ∅ 32 mm bars, were tested. The following are the governing findings of this study.

- The mean and maximum crack spacing values depend on both parameters: concrete cover thickness and the clear distance between bars. The ratios of the maximum to the mean crack spacing values of the tested specimens are 1.5 and 1.6.
- The developed 3D non-linear FEM model can represent the crack pattern (mean crack spacing values) of the conducted experiments with good agreement. The numerical models were developed with a smeared crack model, to represent the perfect bond criteria. This

provide convincing evidence that the perfect bond criteria (or no-slip theory) can represent the cracking behavior of RC specimens subjected to axial tension.

- From the results of the tested specimens, it can be identified that concrete cover thickness parameter has a relatively larger influence on the crack spacing than the clear distance between bars. According to the experimental results, when the clear distance between bars increases 2.5 times, the mean crack spacing increases 1.3 times. When the concrete cover thickness increases 2.4 times, the mean crack spacing increases 1.5 times.
- For RC specimens with the same bond parameter (ϕ/ρ), but with different concrete cover thicknesses and different clear distances between bars, different mean and maximum crack spacing values were obtained.
- By using multiple linear regression analysis, an equation was developed that gives a good fit with the results of the conducted experimental program. This equation gave a good match with the experimental results of similar studies mentioned in the literature.

Acknowledgment

The authors would like to thank the Statens Vegvesen Ferry-free E39 project, for the financial support given to conduct the experiments.

The experiments were conducted at the Concrete Laboratory of the University of Stavanger and at the I.K.M. laboratory facility in Tananger, Norway. The authors would like to thank the UiS laboratory manager, John C. Grønli, laboratory engineers, Jarle Berge, Jørgen Grønsund, Emil Kristiansen, and Caroline Einvik. Special thanks go to Jarle Litlekalsøy and Alexander Runshaug, for the variety of support given during the whole experimental process.

References

1. Standardization ECf. Eurocode 2: Design of concrete structures - Part 1–1: General rules and rules for buildings In:2004.
2. Concrete IFFS. fib Model Code for concrete structures. In. *Structural Concrete*2010.
3. Naotunna CN, Samarakoon SMSMK, Fosså KT. Experimental and theoretical behavior of crack spacing of specimens subjected to axial tension and bending. *Structural Concrete*. 2020;18(1).
4. Saliger R. High grade steel in reinforced concrete. Paper presented at: Preliminary Publication, 2nd Congress of IABSE. Berlin-Munich: IABSE Publications1936.

5. Broms BB, Lutz LA. Effects of arrangement of reinforcement on crack width and spacing of reinforced concrete members. *ACI Journal Proceedings*. 1965;62(11):1395-1410.
6. Borges JF. *Cracking and deformability of reinforced concrete beams*. Laboratório Nacional de Engenharia Civil; 1965.
7. Rimkus A, Gribniak V. Experimental investigation of cracking and deformations of concrete ties reinforced with multiple bars. *Construction and Building Materials*. 2017;148:49-61.
8. Beeby AW, Scott RH. Cracking and deformation of axially reinforced members subjected to pure tension. *Magazine of concrete research*. 2005;57(10):611-621.
9. Bado MF, Casas JR, Kaklauskas G. Distributed Sensing (DOFS) in Reinforced Concrete members for reinforcement strain monitoring, crack detection and bond-slip calculation. *Engineering Structures*. 2021;226:111385.
10. Beconcini ML, Croce P, Formichi P. Influence of bond-slip on the behaviour of reinforced concrete beam to column joints. Paper presented at: Proceedings of International fib Symposium "Taylor Made Concrete Structures: New Solutions for our Society", Amsterdam2008.
11. Doerr K. Bond behavior of ribbed reinforcement under transversal pressure. Paper presented at: Nonlinear behavior of reinforced concrete structures; contributions to IASS symposium1978.
12. Naotunna CN, Samarakoon SSM, Fosså KT. Experimental investigation of crack width variation along the concrete cover depth in reinforced concrete specimens with ribbed bars and smooth bars. *Case Studies in Construction Materials*. 2021:e00593.
13. Engineering JCCJSoc. Standard Specifications for Concrete Structures-2007 "Design". In:2007.
14. CEB-FIP. Model Code 1978 -Design Code; Comité Euro-International du Béton. In. *CEB Bulletin d'Information*. London: Thomas Telford; 1978:124-125.
15. Gribniak V, Rimkus A, Caldentey AP, Sokolov A. Cracking of concrete prisms reinforced with multiple bars in tension—the cover effect. *Engineering Structures*. 2020;220:110979.
16. Mosley WH, Hulse R, Bungey JH. *Reinforced concrete design: to Eurocode 2*. UK: Macmillan International Higher Education; 2012.
17. ASBL ECP. *Commentary to Eurocode 2 - The Concrete Initiative (Rev A)*. 1050 Brussels, Belgium: European Concrete Platform ASBL; 2017.
18. Norge S. NS 3576-3:2012 Steel for the reinforcement of concrete - Dimensions and properties - Part 3: Ribbed steel B500NC. In:2012.
19. Beeby AW. *An investigation of cracking in slabs spanning one way*. April 1970.

20. Standardization Ecf. Eurocode 3: Design of Steel Structures: Part 1-1: General Rules and Rules for Buildings. In. *EN 1993-1-1:2005*.
21. Sheskin DJ. *Handbook of Parametric and Nonparametric Statistical Procedures. Second Edition*. . Chapman and Hall; 2000.
22. Braam C. *Control of crack width in deep reinforced concrete beams (Ph. D. Thesis)*. Netherlands, Delft University; 1990.
23. Concrete E-ICf. CEB design manual on cracking and deformations. In: Favre R, ed: Ecole Polytechnique Fédérale de Lausanne; 1985.
24. Cervenka V. Computer simulation of failure of concrete structures for practice. Paper presented at: 1st fib Congress 2002.
25. Cope R. Modeling of reinforced concrete behavior for finite element analysis of bridge slabs. *Numerical Method For Nonlinear Problems*. 1980;1:457-470.
26. Gupta AK, Akbar H. Cracking in reinforced concrete analysis. *Journal of Structural Engineering*. 1984;110(8):1735-1746.
27. Rimkus A, Cervenka V, Gribniak V, Cervenka J. Uncertainty of the smeared crack model applied to RC beams. *Engineering Fracture Mechanics*. 2020;233:107088.
28. Hordijk D. *Local approach to fatigue of concrete (Ph. D. Thesis)* 1991.
29. DIN. DIN: EN-1992-1-1/NA: 2011-01, National Annex-Nationally determined parameters- Eurocode 2: Design of concrete structures-Part 1-1: General rules and rules for buildings. 2011.
30. Debernardi PG, Taliano M. An improvement to Eurocode 2 and fib Model Code 2010 methods for calculating crack width in RC structures. *Structural Concrete*. 2016;17(3):365-376.
31. Taliano M. Cracking analysis of concrete tie reinforced with two diameter bars accounting for the effect of secondary cracks. *Engineering Structures*. 2017;144:107-119.
32. Barre F, Bisch P, Chauvel D, et al. *Control of cracking in reinforced concrete structures*. Wiley Online Library; 2016.
33. García R, Caldentey AP. Influence of type of loading (tension or bending) on cracking behaviour of reinforced concrete elements. Experimental study. *Engineering Structures*. 2020;222:111134.

Paper 6: A new crack spacing model for reinforced concrete specimens with multiple bars subjected to axial tension using 3D non-linear FEM simulations.

Naotunna, C.N., Samarakoon, S.M.S.M.K., and Fosså, K.T. (2021)

In: *The Journal of Structural Concrete* (accepted to publish).

A new crack spacing model for reinforced concrete specimens with multiple bars subjected to axial tension using 3D non-linear FEM simulations

Chavin Nilanga Naotunna – Corresponding Author.

Research Fellow.

University of Stavanger, Department of Mechanical and Structural Engineering and Material Science, Stavanger.

Address: Kjell Arholmsgate 41, 4036 Stavanger, Norway.

Telephone: +47 51832815

E-mail: chavin.guruge@uis.no

S.M Samindi M.K Samarakoon.

Associate Professor.

University of Stavanger, Department of Mechanical and Structural Engineering and Material Science, Stavanger.

Address: Kjell Arholmsgate 41, 4036 Stavanger, Norway.

Telephone: +47 51832387

E-mail: samindi.samarakoon@uis.no

Kjell Tore Fosså.

Adjunct Professor.

University of Stavanger, Department of IMBM.

Manager Concrete Technology.

Aker Solutions, Stavanger, Norway.

Telephone: +47 46402403

E-mail: kjell.tore.fossa@akersolutions.com

Abstract

Crack spacing is a governing parameter in widely used crack width calculation models. Axial tensile experiments are conducted to examine the crack spacing behavior of reinforced concrete specimens with multiple reinforcement bars. To reduce the time, cost and labor of the experiments, non-linear finite element simulations are widely used. In this study, 3D non-linear finite element simulation models have been developed with the smeared cracking approach to predict the average crack spacings. These models are calibrated and validated using both the experiment conducted by the authors and an experiment given in the literature. The governing crack spacing parameters have been identified as concrete cover thickness and clear distance between tensile bars. After conducting a series of 3D non-linear finite element method simulations with the calibrated model, an equation is developed to predict the average crack spacings using multiple linear regression analysis. The validity of the proposed crack spacing equation has been checked with 18 number of recent experimental results in the literature. The proposed crack spacing equation gives a good agreement with the results of these experiments.

Key words. Crack spacing, axial tension, concrete cover thickness, bar spacing, non-linear FEM.

1. Introduction

Crack spacing is an important parameter in predicting crack widths. Axial tensile tests are conducted to study the cracking behavior of reinforced concrete (RC) specimens with several reinforcement bars, because the behavior is much similar to actual RC members in practice (Rimkus & Gribniak, 2017). In

order to conduct such experiments, additional effort is required in designing the load application method (Gribniak & Rimkus, 2016). Conducting such experiments on relatively large RC specimens requires special type of test rigs (Naotunna, S.M. Samindi, & Fosså, 2020a), which are not commonly available. Due to several benefits, the finite element method (FEM) can be used to analyze the cracking behavior of RC structures. Reducing the time, cost and labor in laboratory experiments is one of the main benefits, while the ability to observe the internal behavior of an RC specimen is another benefit of FEM. Non-linear FEM has been used to study crack spacing behavior and has been reported in several pieces of research (Mang, Jason, & Davenne, 2016; Tan, Hendriks, Geiker, & Kanstad, 2020; Wang, Tao, & Nie, 2017; Wu & Gilbert, 2009). Crack analysis of reinforced concrete structures in FEM can mainly be carried out by using two crack models: namely, 'discrete crack' and 'smeared crack' models. The discrete crack model was developed, as a crack would create a complete discontinuity between element edges (Ngo & Scordelis, 1967; Nilson, 1968). In the discrete modeling, it is the necessity to pre-define the location and path of the crack along the finite element edges (Rots & Blaauwendraad, 1989). As the crack location is needed to pre-define, this method is not suitable for studying crack spacings. Ingraffea and Saouma (1985) proposed re-meshing the concrete element after the cracks appear. However, that would make the model much more complicated and require computational time and cost. In order to overcome these issues, the 'smeared crack model' can be used to study crack spacing behavior (Bernardi, Michelini, Minelli, & Tiberti, 2016). This model was first introduced by Rashid (1968). When a crack occurs in an element, this method proposes changing the constitutive properties (material stiffness, tensile strength perpendicular to crack direction, etc.) of the cracked concrete elements.

When considering existing crack spacing prediction models, they are mainly based on three theories, namely: 'bond-slip' (Saliger, 1936), 'no-slip' (Broms, 1965) and 'combined theories' (Borges, 1965). The 'bond-slip' theory considers that a slip occurs between the reinforcement and concrete. The 'no-slip' theory considers that there is a perfect bonding between reinforcement and concrete and therefore no slip would occur. According to this theory, within the concrete, the stress would transfer according to St. Venant's principle (de Saint-Venant, 1856), which means that the crack spacing is affected by the thickness of the surrounding concrete of the tensile reinforcement. The combined theory considers that crack spacing behavior is affected by the aforementioned two theories. However, the findings in Beeby (2004) and Mcleod (2013) emphasized that the no-slip theory has a dominant effect on the cracking behavior of RC specimens with deformed bars. Further, the axial tensile tests conducted on RC ties mentioned in Yannopoulos (1989) and Tammo et al. in (Tammo & Thelandersson, 2006, 2009) identified that a negligible amount of slip occurs at the end faces of RC ties (faces perpendicular to reinforcement).

The bond-slip behavior adapted to Model Code 2010 (MC 2010) is from the Ciampi–Eligehausen model (Ciampi, Eligehausen, Bertero, & Popov, 1981; Eligehausen, Popov, & Bertero, 1982), which is based on the Rilem-type pull-out tests (RILEM, 1983) (the same Ciampi–Eligehausen model is used to develop the crack width calculation model by Balazs (1993), which is also considered in *fib* bulletin 52 (CEB-FIP, 2010)). According to this MC 2010 bond-slip model the slip value can be up to 2 mm for the good-bond condition. On the other hand, the bond-slip behavior of RC specimens subjected to axial tension was identified in Beconcini et al. (2008) and Doerr (1978). The maximum slip values identified in these experiments are 0.055 mm and 0.1 mm, respectively. Therefore, when comparing the bond-slip behavior in MC 2010 and in axial tension, it could identify that the 'slip' in axial tension is almost negligible. These differences in the bond-slip behaviors between axial tension and pull-out tests have been thoroughly discussed in Naotunna et al. (2020b). For these reasons, for this study, the cracking behavior of an RC member is considered to be more related to the 'no-slip' theory.

From the existing literature, many crack spacing models based on the ‘no-slip’ theory can be identified. Such models are found in (A. Beeby & Scott, 2005; Broms, 1965; Broms & Lutz, 1965; Mesureur, Bernardi, & Rivillon, 1999). Further, several other crack spacing models can be identified without the ‘bond parameter (ϕ/ρ)’ (A. W. Beeby, 2004), which is the dominant parameter of crack spacing models developed from ‘bond-slip’ theory. The models mentioned in (Jaccoud, 1987; Janovic, 1986; JSCE, 2007; Oh & Kang, 1987) are such models; since the background of these models are not easy to find, it cannot be stated that these models are directly based on ‘no-slip’ theory. When considering the models in the aforementioned literature, the governing crack spacing parameters can be identified as concrete cover thickness (A. Beeby & Scott, 2005; Broms, 1965; Broms & Lutz, 1965; JSCE, 2007), spacing between tensile reinforcement (Broms & Lutz, 1965; Jaccoud, 1987; Janovic, 1986; JSCE, 2007), concrete quality (JSCE, 2007), reinforcement ratio (Oh & Kang, 1987) and number of tensile reinforcement layers in concrete (JSCE, 2007). Since 1965, concrete cover thickness has been identified as a dominant crack spacing governing parameter (Broms, 1965). Existing crack width calculation models in (FIB, 2013; ACI, 1995; BS, 1985; CEN, 2004; JSCE, 2007) have considered, and many recent experiments (Gribniak, Rimkus, Caldentey, & Sokolov, 2020; Pérez Caldentey, Corres Peiretti, Peset Iribarren, & Giraldo Soto, 2013; Rimkus & Gribniak, 2017; Tan et al., 2018) have proved, that concrete cover thickness is a crack-spacing parameter. Spacing between tensile bars has been considered a parameter of crack spacing in the past (Model Code 1978 (CEB-FIP, 1978), Bazant et al.’s model in (Bažant & Oh, 1983), etc.). Eurocode 2 (CEN, 2004) recommends a different calculation model for members with large tensile bar spacings. Further, the recent literature of Gribniak et al. (2020) and Hossin and Marzouk (2008) experimentally proved that spacing between tensile bars is a governing parameter of crack spacing. Many studies have identified that, although the cracking load is related to the strength of concrete, the cracking behavior (including the crack spacing) has a negligible effect from concrete strength (Al-Fayadh, 2001; Fields & Bischoff, 2004; Lorrain, Maurel, & Seffo, 1998; Theriault & Benmokrane, 1998). Other than that, Broms et al. (1965) and Theriault and Benmokrane (1998) identified that the reinforcement ratio is not a governing parameter of crack spacing. Therefore, in accordance with these facts, concrete cover thickness and tensile bar spacing have been considered governing crack spacing parameters for this study.

ATENA by Cervenka Consulting (Cervenka, Cervenka, & Pukl, 2002) is non-linear FEM analysis software that is widely used to simulate the cracking behavior of RC members. As mentioned, this study focuses on cracking behavior based on ‘no-slip’ theory (or perfect bond criteria). This condition can be represented by modeling with smeared reinforcement which leads to smeared cracking behavior (Cervenka, Jendele, & Cervenka, 2015). Recent studies mentioned in Mang et al. (2016) and Rimkus et al. (2020) have identified that the perfect bonding models give good agreement with the experimental cracking behavior.

The authors of this article have conducted an axial tensile experiment with 2 m x 0.2 m x 0.2 m (length, width, height) specimens and four 32-mm-diameter bars. The details of this experiment are mentioned in Naotunna et al. (2020a). As previously stated, such experiments consume a considerable amount of time, cost and labor. Therefore, a three-dimensional finite element simulation model has been developed to simulate this experiment. The crack spacing behavior has been calibrated with the results of this experiment. By using the same FEM parameters, the model has been verified to predict the mean crack spacing of a 3.2 m x 0.35 m x 0.35 m specimen with four 20-mm-diameter bars, mentioned in Barre et al. (2016). After the calibration and validation of the 3D FEM simulation model, several virtual experiments could be conducted to study the effect of ‘concrete cover thickness’ and ‘clear distance between tensile bars’ on crack spacing. The ‘mean crack spacing’ parameter is a good representative of the overall crack spacing behavior of an RC specimen. Therefore, widely used crack spacing models in Eurocode 2 (EC2) and MC 2010 first developed their model for mean crack spacing and multiplied it

by a factor (factor of 1.7) to predict the ‘maximum crack spacing’ (A. Beeby, 2001; Tan, 2019). Therefore, the obtained mean crack spacing values from the conducted virtual experiments have been used to develop a new crack spacing equation, which can be used in the axial tensile specimens with multiple reinforcement bars. The applicability of this developed equation has been checked with the results of recent experiments reported in the literature.

2. Use of axial tensile experiments to calibrate and validate 3D FEM simulation model

Axial tensile experiments can represent the tensile region of a bending member (Debernardi, Guiglia, & Taliano, 2013; Debernardi & Taliano, 2016), and several rebar layers can be placed in specimens, similar to in practice. In this study, the results of the experiment published by Naotunna et al. (2020a) have been used to calibrate the 3D FEM simulation model. In this experiment, three identical specimens with $2\text{ m} \times 0.2\text{ m} \times 0.2\text{ m}$ (length \times width \times height) were cast with four 32-mm-diameter reinforcement bars (Figure 1). The concrete cover thickness of the tested specimens was 35 mm. The mechanical properties of the concrete and the specimen details are shown in Table 1. The characteristic yield strength of the reinforcement was 500MPa, and Young’s modulus was 200GPa. After unloading the specimens, they were stored in a 20°C room temperature, with the necessities for concrete curing. During the test, the axial tensile load was applied to the reinforcement, and the test rig was connected to the specimen through a nut and bolt mechanism, as shown in Figures 1 and 2. Crack spacing measurements were taken, respective to the position of the reinforcement. Moreover, to validate the developed 3D FEM simulation model, the results of Barre et al. (2016) were considered; a detailed discussion is presented in Section 3.

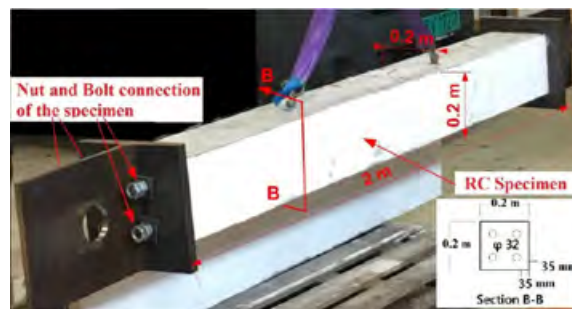


Figure 1. Details of the tested RC specimen in Naotunna et al. (2020).

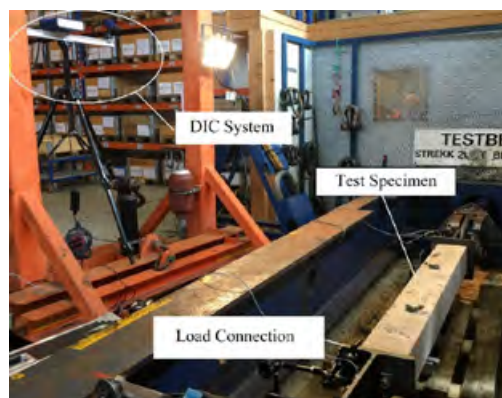


Figure 2. Tensile load application on the RC specimen mentioned in Naotunna et al. (2020).

Table 1. Parameters of the test specimens.

Specimen	Cross section (m × m)	Length (m)	Concrete strength (MPa)		Concrete cover (mm)	Bar profile no × diameter(mm)
			Compressive	Tensile		
Naotunna et al 2020.	0.2 × 0.2	2	35	3.2	35	4 × 32
Barre et al 2016.	0.355 × 0.355	3.2	43.6	3.7	65	4 × 25

3. 3D non-linear FEM simulation to study crack spacing

The crack simulation of the aforementioned experiment was carried out with the finite element software called ‘ATENA’ by ‘Cervenca Consulting’, Version 5.7.0 with ‘GiD 14.0.2’ interface. The modeling was conducted with the ‘GiD 14.0.2’ interface. When developing the 3D non-linear FEM simulation model, eight-noded hexahedral elements were used to model concrete. The reinforcement was modeled as smeared reinforcement, where reinforcement and concrete is discretized into element with the same geometrical boundaries (Dahmani, Khennane, & Kaci, 2010). Since the reinforcement is modelled as smeared reinforcement, material properties of reinforcement superimpose the concrete material properties within the defined space of reinforcement. The material stiffness matrix of smeared reinforcement is a function of direction of the reinforcement axis, elastic modulus of reinforcement and the reinforcement ratio. Since the reinforcement is modeled as smeared reinforcement, the cracks have idealized as smeared cracks (Cope, Rao, Clark, & Norris, 1980; Gupta & Akbar, 1984). This method does not allow ‘slip’ to occur between the reinforcement and concrete. The recent study by Rimkus et al. (2020), on the uncertainty of the smeared crack model, identified that the perfect bond model gives the best fit with the experimental results. When modeling the axial tensile experiment, the ‘fixed crack model’ was decided on, where the crack direction freezes to the principal stress direction of the crack occurrence (Hofstetter & Meschke, 2011). Since the axial tensile experiments were performed by keeping one end fixed and loading in the other end, a similar type of boundary conditions was applied in the FEM model. In this model, the external load is applied by a displacement-controlled method, with the displacement given as 0.1 mm incremental steps. Further, as the FEM is loaded in a horizontal direction, vertical constraints were added to the bottom edges of the specimen (required at the initial displacement steps). The solution of the numerical model is based on the Newton-Raphson method.

3.1 Material models

The constitutive model selected for concrete consists of a ‘fracture’ part to model the tensile failure, while the ‘plastic’ part is to model the compressive failure (Jan Červenka & Papanikolaou, 2008). The material model follows the De-Borst (1986) strain decomposition rule, where the strain in concrete decomposes into elastic, plastic and fracture. However, as the developed FEM simulation model is only subjected to tension, concrete strain will not decompose as plastic strain. When a crack occurs in concrete, to match the continuous algorithm of FE analysis, it is considered that an amount of tensile stress would transfer across the crack. This amount of stress is decided in accordance with Hordijk’s law (Hordijk, 1991). According to Hordijk’s law, the tensile stress of concrete perpendicular to the crack is a function of crack width. Detailed information about the fracture model, which is based on Rankine failure criterion, is mentioned in Cervenka and Papanikolaou (2008).

3.2 Calibration and validation of the 3D FEM simulation model

The axial tensile test published by Naotunna et al. (2020a), discussed in Section 2, is simulated by using non-linear FEM and the model is calibrated with the experimental mean crack spacing value. Hereafter, this 3D FEM simulation model is referred to as the ‘calibration model’. This is a symmetric model and,

therefore, in order to save computational time and cost, only a symmetric half of it can be modeled. However, since this is a crack spacing study, when a crack occurs near the edge of the symmetric half, obtaining the crack spacing value can be problematic. Therefore, the ‘complete specimen’ has been modeled in three dimensions, to obtain the crack spacings. The smeared crack model is sensitive to the size of the mesh (Cervenka et al., 2015). Mesh size must be larger than the maximum aggregate size (16 mm) to represent the inhomogeneous behavior of concrete (J Červenka, Červenka, & Laserna, 2018) and less than the reinforcement diameter (32 mm) to affect the bond conditions (Cervenka et al., 2015). In the aforementioned concrete model, there are several factors which can be used to influence the tensile behavior of concrete. Such parameters are ‘*crack spacing min*’, ‘*tension stiffening*’, ‘*shear factor*’ and so on. In heavily reinforced members, the cracks may not fully propagate and in such cases, it may need to adjust the ‘limiting value’ of tensile strength of concrete in the tension softening diagram. The ‘*tension stiffening*’ parameter is used to do these changes. In the software a value can be assigned to the ‘*tension stiffening factor*’ from 0 (the limiting tensile strength of concrete reaches to zero after cracking) to 1 (the limiting tensile strength of concrete does not drop after cracking). The ‘*shear factor*’ parameter is used to define a relationship between normal stiffness and shear stiffness of cracked concrete (shear stiffness is ‘*shear factor*’ \times normal stiffness obtained from the tension softening curve (Cervenka et al., 2016)). However, since the specimens are subjected to axial tension, this parameter is not dominant for the conducted experiment. Therefore, ‘*shear factor*’ has not been activated in this model. The ‘*crack spacing min*’ parameter is used to correct the fracture energy parameter based on the element size. Since the concrete softening curve is modeled with laboratory specimens of 100 to 150 mm size, the value of this parameter can be decided accordingly. According to the flow chart illustrated in Figure 3, after several trial-and-error iterations, the mesh size was decided as 25 mm, the value of ‘*tension stiffening*’ parameter was set at zero and the ‘*crack spacing min*’ parameter was set at 100 mm.

A 3D FEM calibration model is developed by using the mean concrete compressive and tensile strengths measured at the laboratory (refer Table 2). Young’s modulus and Poisson’s ratio are considered according to Eurocode 2 (CEN, 2004) provisions, the values being 34 GPa and 0.2, respectively. The fracture energy is automatically generated according to the equation proposed in Vos (Vos, 1983). Since the reinforcement is subjected only to axial tension, the smeared reinforcement is represented in a one-dimensional element. Characteristic yield strength and the Young’s modulus of the reinforcement are assigned as 500 MPa and 200 GPa, respectively. Figures 4 (a) and (d) show the cracking behavior of the calibrated FEM model at two loading steps: at 500 kN and 800 kN, respectively. Further, the steel stresses of the reinforcement can be observed, as given in Figure 4 (b) and (d). It is important to mention that, at the crack, the steel stress becomes higher than at the uncracked locations. The crack spacing of the numerical model is considered as the center to center distance between the cracked elements. As shown in the Table 2, the mean crack spacing values of the calibration model gives a good agreement with the experimental results, where the error value is less 6 %.

After calibration, the next task was to check whether the developed model can represent the crack spacing values for similar types of experiments (validate the model). For this task, the experimental results of a similar axial tensile experiment with four tensile reinforcement bars were required. An experimental program mentioned in Barre et al. (Barre et al., 2016) was considered for this case, and the FEM simulation model is named the ‘validation model’. The number of reinforcements and the tensile load application method are similar to the experiment considered in the calibration model. Details of the selected specimen are mentioned in Table 1, and the comparison of crack spacing values is shown in Table 2. The flow chart in Figure 3 clarifies the steps conducted to develop this validated model. The crack spacing values of the specimen are given in Figure 5. According to the comparison in Table 2, the developed 3D FEM simulation model shows the ability to predict the mean crack spacing behavior of specimens subjected to axial tension. Table 2 shows that the mean crack spacing values give very good

agreement with the experimental results. In both cases, experimental mean crack spacing value is 6% higher than in the FEM simulation models.

Table 2. Comparison of the experimental crack spacing values with the numerical model predictions.

Specimen	Mean crack spacing		
	FEM simulation models (mm)	Experimental (mm)	Error* %
Calibration (Naotunna et al., 2020)	125	133	6
Validation (Barre et al., 2016)	188	200	5.8

*Error = (Experimental Value - FEM simulation model value)/Experimental Value

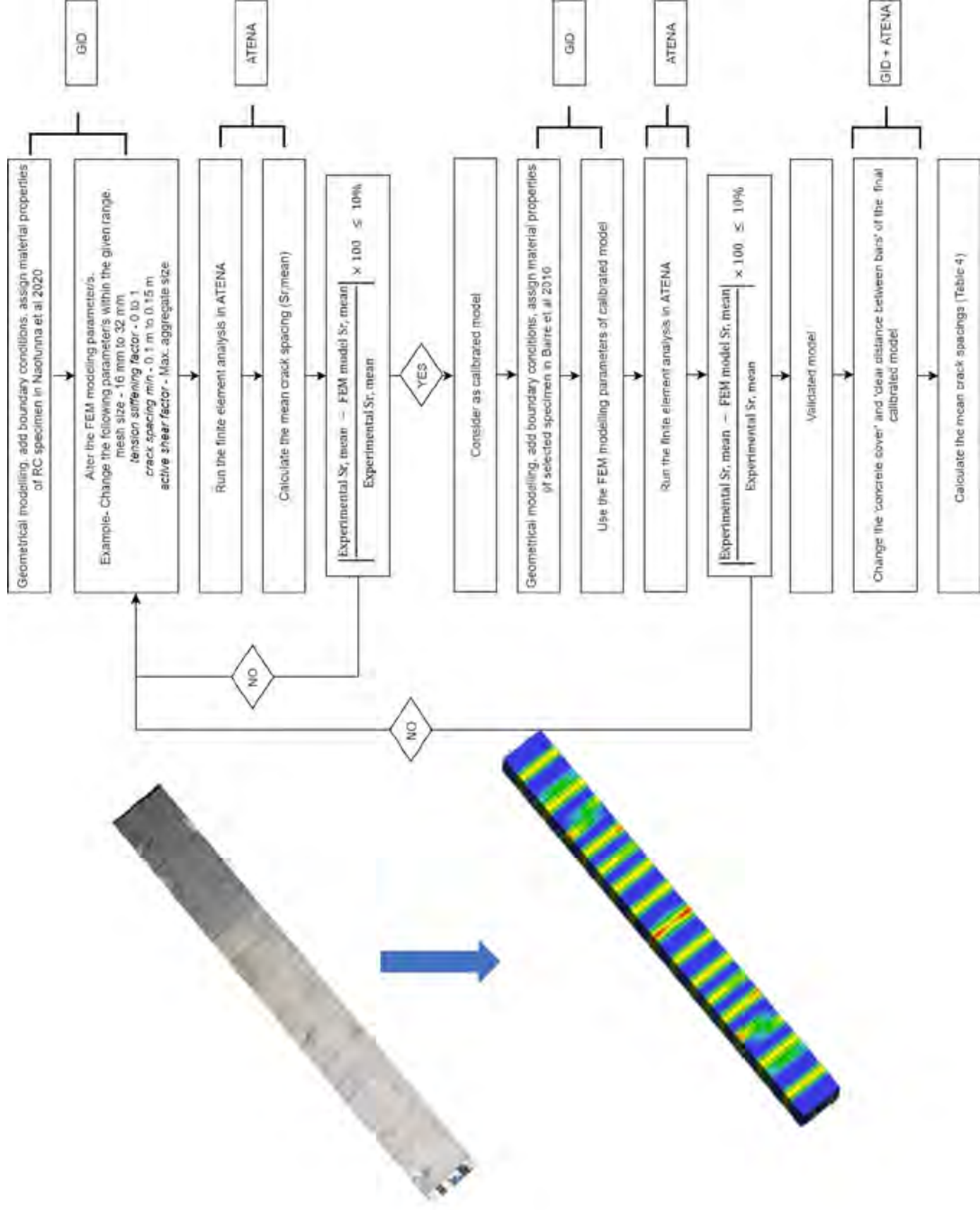


Figure 3. Flow chart of the calibration, validation and the parametric analysis conducted during this study

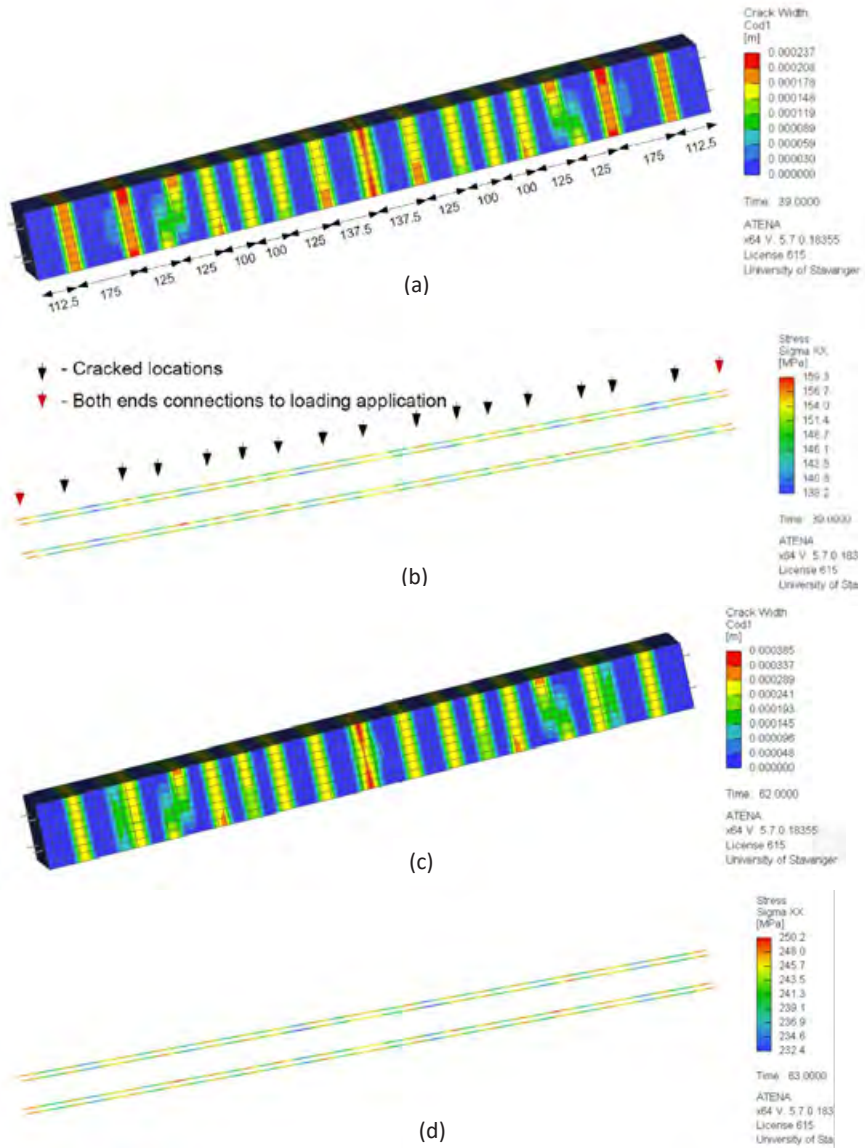


Figure 4. Cracking behavior of the 3D FEM calibrated model (a) cracking behavior of the specimen at the applied tensile load of 500 KN (crack spacing measurements are in mm), (b) stress distribution of reinforcement at the applied tensile load of 500 KN, (c) cracking behavior of the specimen at the applied tensile load of 800 KN, (d) stress distribution of reinforcement at the applied tensile load of 800 KN.

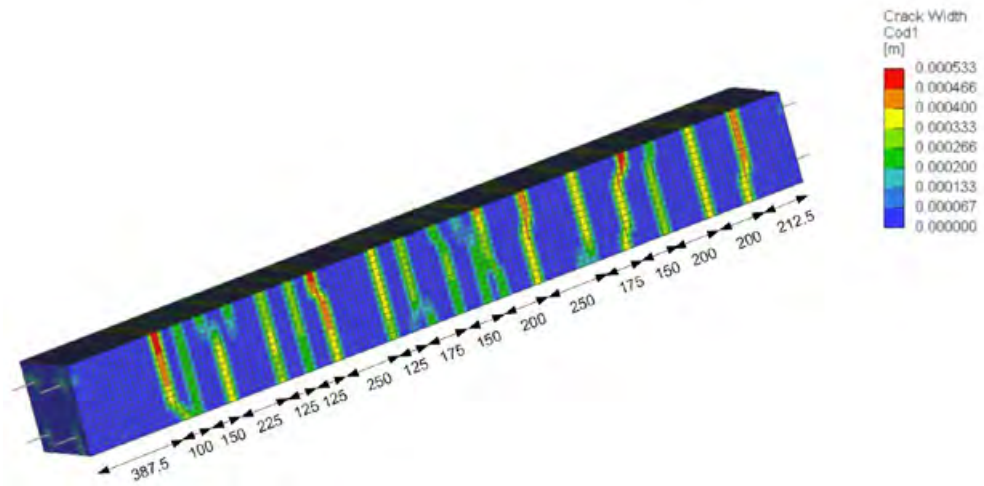


Figure 5. Cracking behavior of the FEM simulation model developed to simulate the mentioned experiment in Barre et al. (2016), the validation model (crack spacing measurements are in mm).

4. Development of new crack spacing model

As mentioned in Section 1, the governing crack spacing parameters for this study have been identified as concrete cover thickness and the clear distance between tensile bars. Therefore, the developed calibration model has been used to study the effect of these two parameters on crack spacing. Since the FEM simulation model is calibrated with a mesh size of 25 mm, the specimen size can be increased in 25-mm steps. With the increase in model size, the number of elements in the FEM models also increases. This leads to a further increase in the computational time and space. When designing a structure for a longer service life, a large concrete cover thickness is required. The current requirement for concrete cover thickness can be as large as 120 mm, according to the Norwegian Public Road Administration guidelines (NPRA, 2009). Therefore, in the parametric analysis, the concrete cover has been changed from 35 mm to 122.5 mm, and the clear distance between tensile bars has been changed from 66 mm to 216 mm, in several steps. Table 3 shows the mean crack spacing values of the developed 3D FEM simulation models, with changed concrete cover thickness and bar spacing. When developing these models, not only the mesh size, material properties and the boundary conditions but also the other FEM modeling parameters are kept the same as in the calibration model.

According to Table 3, the experimental mean crack spacing values are 6% larger than the FEM simulation model predictions. Therefore, the obtained results from the aforementioned FEM simulation models have been increased by 6%. Several models can be identified which do not have a satisfactory convergence criterion. The model is developed to stop the iterations, if the relative error in displacement or force equilibrium is larger than 10% in several steps in a row, since the results tend to be unreliable (Pryl & Cervenka, 2013). In such cases, there are several methods that can be used to improve the model, i.e. reducing the stiffness of the overall specimen, reducing the displacement step, and so on (Pryl & Cervenka, 2013). Since it is not possible to change the calibrated FEM modeling parameters, such models were not improved, and the results of these models were not considered for this analysis (blank spaces in Table 3).

Broms and Lutz (1965) identified that the crack spacing behavior would change when the concrete cover thickness is larger than the clear distance between the tensile bars. The highlighted data in Table 3 are from such cases. Therefore, the first focus is on cases where the concrete cover thickness is less than the clear distance between the tensile bars. In this study, the independent variables are concrete cover thickness and the clear distance between tensile reinforcements, and the dependent variable is the mean crack spacing. The purpose was to obtain a simple equation to predict the mean crack spacing, which can be more practically used in industry. A linear regression analysis can be conducted for the mentioned data in Table 3, to find the best-fitting equation. Since this is a study with two independent variables, the solution of the linear regression analysis will be a plane (surface). As the best fitting surface, a first-degree polynomial equation has been obtained as given in Equation 1. This is the equation for the surface given in Figure 6. Even though a relatively large amount of data points has been used for the analysis (Table 3), the R^2 value is 0.78.

$$S_{r,\text{mean}} = 66 + 0.51 c + 0.6 s \quad (\text{all values in mm}) \quad \text{Equation 1}$$

where $S_{r,\text{mean}}$ is the mean crack spacing, 'c' is the concrete cover thickness, and 's' is the clear distance between tensile reinforcements.

The size effect or the geometric parameters of a RC specimen have been identified as a factor influencing crack spacing (Wang et al., 2017). The virtual experiments conducted using non-linear 3D FEM simulation models are only for those cases where RC specimens have four reinforcements (two tensile bars are close to the surface of each face). When the number of bars close to the specimen surface (n) is two, concrete cover thickness and clear distance between bars gives a good representation of size effect. However, in general, the value of 'n' can vary, and in such cases the concrete cover and bar spacing do not represent the geometric parameters of a specimen (refer to Figure 7, when $n = 3$). Equation 1 is developed for those specimens with two tensile bars close to the surface of each face ($n = 2$). Therefore, to represent the size effect of specimens with different numbers of 'n' values, the term with bar spacing in Equation 1 has been divided by two and multiplied with 'n'. Equation 2 represents the modified crack spacing model with several reinforcement bars close to the surface.



$$S_{r,\text{mean}} = 66 + 0.51 c + 0.6 s \frac{n}{2} \quad (\text{all values in mm}) \quad \text{Equation 2}$$

As mentioned, Equations 1 and 2 have been developed for cases where the value of 's' is larger than 'c'. The highlighted cases in Table 3 are those where 'c' is larger than 's'. For these cases, the effect of parameter 's' can be identified as becoming less important to the crack spacing. Then, it can be seen that, when parameter 's' in Equation 2 is replaced with 'c', it gives better predictions with the highlighted "green" data in Table 3. Equation 3 shows the developed mean crack spacing model for the RC beams, when the concrete cover is larger than the clear distance between the tensile bars.

$$S_{r,\text{mean}} = 66 + c (0.51 + 0.6 \frac{n}{2}) \quad (\text{all values in mm}) \quad \text{Equation 3}$$

Table 3. Obtained mean crack spacing values from the FE analysis.

Clear distance between tensile reinforcement (mm)	Concrete cover thickness (mm)						
	35	60	85	97.5	110	122.5	
66	133	151	146	177	184	173	
91	125	141	151	180	163	173	
116	163	163	177	-	163	177	
141	170	177	212	-	-	-	
166	177	-	236	-	193	-	
191	184	212	-	-	-	-	
216	193	236	265	-	-	-	

¹ convergence limit is larger than 10% in several steps.
 Mean crack spacing values are highlighted for those specimens in which the concrete cover thickness is larger than the clear distance between bars.
 This mark shows the locations of calibrated model.
 This mark shows the approximate location of the validated model (cover is 65 mm and clear distance between bars is 175 mm).

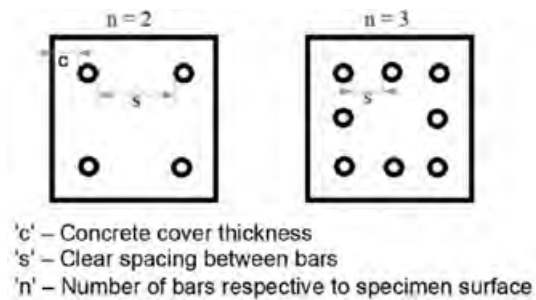


Figure 7. Notations of the proposed equation.

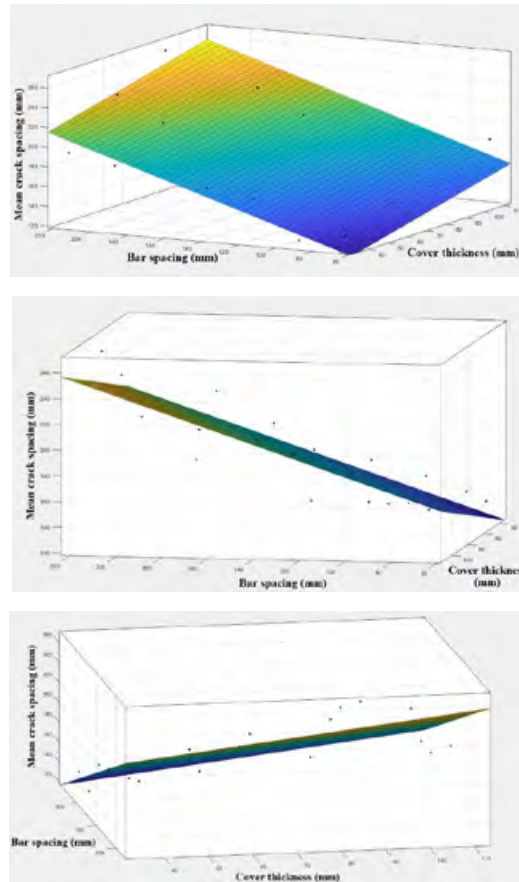


Figure 6. Behavior of the mean crack spacing for specimens with different cover thicknesses and bar spacings in three different rotation angles.

5. Verification of the proposed equations

The equations developed to predict the mean crack spacing of RC beams with multiple reinforcements subjected to axial tension are given in Equations 2 and 3. In order to validate the equations, they have been checked with the results of recent experimental studies. Recent literature has recorded a limited number of axial tensile tests conducted on RC specimens with multiple bars. Cases were selected from Tan et al. (2018), Naotunna et al. (2020a), Barre et al. (2016), Rimkus and Gribniak (2017) and Garcia and Caldentey (2020). Details of the RC specimens of these selected specimens are listed in Table 4. Moreover, Tan et al. (2018) did not apply the tensile load directly to the reinforcement. However, in every other experiment mentioned, the tensile load is directly applied to the reinforcement. Other than the experiment considered to validate the numerical model, another axial tensile test was conducted in Barre et al. (2016) for a specimen with eight reinforcements, and this is mentioned as case 3 in Table 4. Rimkus and Gribniak (2017) studied the effect on crack spacing of different reinforcement layouts. Tested specimens are around 0.5 m long, and it is important to mention that cases 13, 14 and 15 in Table

4 have two reinforcement layers, respective to each concrete surface. Garcia and Caldentey (2020) focused on the effect of the casting position on the cracking behavior. The ‘good bond’ and ‘poor bond’ faces are considered as the bottom and top faces of the specimen, respectively, when it is being cast. Since the developed equations are based on the perfect bond criteria, only the results of ‘good bond’ cases have been considered in this study. Another important fact is that, from these cases in Table 4, the mean compressive strength of concrete varies from 32 MPa to 74 MPa, and different reinforcement layouts have been used.

The experimental mean crack spacing values of the aforementioned experiments have been compared with the proposed models in Broms (1965) and Beeby and Scott (2005), since they are based on the ‘no-slip’ theory. EC2 and MC 2010 have models for calculating the ‘maximum crack spacing’ values. Both the EC2 and MC 2010 models consider the maximum crack spacing to be 1.7 times the mean crack spacing, based on Braam (1992) and CEB design manual (CEB, 1985), respectively. Therefore, Table 4 consists of the mean crack spacing predictions of both EC2 and MC 2010, by dividing their maximum crack spacing predictions by the 1.7 factor. The predictions from the proposed models are based on Equations 2 and 3. In cases 6, 7, 11, 12, 14 and 15, the concrete cover thickness is larger than the clear distance between tensile reinforcements. Therefore, Equation 3 is used for those cases, while Equation 2 is used for the other cases.

When considering the error values in Table 4, the EC2 model predictions are considered to be more on the conservative side. This relatively high overestimation of the EC2 crack spacing model is noted in several studies (Naotunna et al., 2020a; Tan, 2019; Tan et al., 2018). Except for four cases, the MC 2010 predictions are on the conservative side. However, compared to the EC2 predictions, the percentage of overestimations is lower in the MC 2010 estimations. Of all 18 cases, the predictions from Broms (1965) and Beeby and Scott (2005) have underestimated the experimental values in 15 and 13 cases, respectively. These two models are mainly developed for the axial tensile RC specimens consisting of a single embedded reinforcement. When considering the proposed model, four cases underestimate the experimental values. However, these underestimated percentages are still lower than 20%. Of the 18 cases mentioned in Table 4, 12 cases have an ‘absolute error’ value less than 20%. From the cases mentioned in Table 4, five cases have a concrete cover thickness larger than 60 mm (up to 90 mm). For these cases, the predictions of the proposed model give good agreement, where the absolute error values lie below 20%. Furthermore, as highlighted (light green) in Table 4, the proposed model gives the best fit for the majority of cases. When comparing the predictions of the aforementioned models, the relative best agreement for the experimental mean crack spacing values are obtained from the proposed Equations, 2 and 3.

Table 4. Comparison of the experimental mean crack spacing values with the prediction models.

Study	Case no.	Width × Height × Length (m × m × m)	Concrete cover (mm)	Clear distance between bars (mm)	No. of bars close to each surface	Exp. mean crack spacing (mm)	Predicted mean crack spacing (mm)				Error ^a %					
							Proposed Equation [14] ^d	Broms 1965 [14] ^d	Beeby and Scott 2005 [32] ^e	EC2 [39]	MC2010 [40]	Proposed equation	Broms 1965	Beeby and Scott 2005	EC2	MC2010
Naotunna et al 2020 [3]	1	0.2 × 0.2 × 2	35	66	2	133	124	102	107	149	106	6.8	23.3	19.7	-12.0	20.3
Barre et al 2016 [55]	2	0.355 × 0.355 × 3.2	65	175	2	200	204	155	198	391	347	-2.0	22.5	0.9	-95.5	-73.5
	3	0.355 × 0.355 × 3.2	45	108.5	3	174	187	106	137	314	257	-7.5	39.1	21.1	-80.5	-47.7
	4	0.4 × 0.4 × 3	40	130	3	163	203	122	122	335	255	-24.5	25.2	25.2	-105.5	-56.4
Tan et al 2018 [41]	5	0.4 × 0.4 × 3	40	112	3	178	187	122	122	239	177	-5.1	31.5	31.5	-34.3	0.6
	6	0.4 × 0.4 × 3	90	80	3	217	193	274	275	435	314	11.1	-26.3	-26.5	-100.5	-44.7
	7	0.4 × 0.4 × 3	90	62	3	266	216	274	275	339	236	18.8	-3.0	-3.2	-27.4	11.3
Gracia and Caldentey 2020 [70]	8	0.35 × 0.45 × 5.22	32	79.3	4	162	178	76	98	240	182	-9.9	53.1	39.8	-48.1	-12.3
	9	0.35 × 0.45 × 5.22	32	74	4	147	171	80	98	203	151	-16.3	45.6	33.6	-38.1	-2.7
	10	0.35 × 0.45 × 5.22	32	62	4	115	157	89	98	163	119	-36.5	22.6	15.1	-41.7	-3.5
Rimkus and Gribniak 2017 [1]	11	0.15 × 0.15 × 0.5 ^b	82	40.6	4	220	206	180	250	477	352	6.4	18.2	-13.7	-116.8	-60.0
	12	0.15 × 0.15 × 0.5 ^b	82	28.6	4	184	206	189	250	365	260	-12.0	-2.7	-35.9	-98.4	-41.3
	13 ^a	0.15 × 0.15 × 0.5 ^b	30	33	3	100	111	68	92	119	84	-11.0	32.0	8.5	-19.0	16.0
Rimkus and Gribniak 2017 [1]	14 ^a	0.15 × 0.15 × 0.5 ^b	30	22	4	92	117	66	92	119	84	-27.2	28.3	0.5	-29.3	8.7
	15 ^a	0.15 × 0.15 × 0.5 ^b	30	28	4	73	117	65	92	132	94	-60.3	11.0	-25.3	-80.8	-28.8
	16	0.15 × 0.15 × 0.5 ^b	30	62	2	100	119	74	92	162	118	-19.0	26.0	8.5	-62.0	-18.0
Gribniak 2017 [1]	17	0.15 × 0.15 × 0.5 ^b	30	66	2	86	121	72	92	179	133	-40.7	16.3	-6.4	-108.1	-54.7
	18	0.15 × 0.15 × 0.5 ^b	30	70	2	113	123	70	92	204	152	-8.8	38.1	19.0	-80.5	-34.5

^a Specimens consist of several layers of reinforcement.

^b Rimkus & Gribniak's specimens vary in length between 379 mm and 505 mm.

^c Error = (Experimental Value - Predicted Value)/Experimental Value.

^d Broms 1965 Equation $S_{r,mean} = 2(c + \phi/2)$; where ϕ is the diameter of tensile reinforcement.

^e Beeby and Scott 2005 Equation $S_{r,mean} = 3.05c$

In the pink colored cases, the concrete cover is larger than the clear distance between bars. Therefore, Equation (6) is used to predict the mean crack spacing values. The light-green colored cases show the closest value to the experimental mean crack spacing.

6. Conclusion

This paper studies the crack spacing behavior of RC specimens with multiple bars, subjected to axial tension. The main identified crack spacing governing parameters for this study are concrete cover thickness and the clear distance between tensile reinforcements. To reduce the time, labor and cost of laboratory experiments, finite element modeling has been used to study the cracking behavior. From the previous literature, it can be identified that a negligible amount of slip occurs between the reinforcement and concrete in axial tension. Therefore, a finite element model has been developed, considering a perfect bond between reinforcement and concrete. After calibrating and validating the FEM simulation models, they have been used to study the effect of concrete cover thickness and tensile bar spacing on crack spacing. The following are the most important findings identified from this study,

The smeared crack model with perfect bonding criteria in the can predict the crack spacing behavior of an RC specimen with multiple bars subjected to axial tension.

The developed FEM simulation models can predict the crack spacing behavior with different concrete cover thicknesses and changes in the spacing between tensile bars.

With the results of several virtual experiments, a 'mean crack spacing model' could be developed for use in axial tensile specimens with several reinforcements.

This proposed model is developed from the results of 3D non-linear FEM models, up to a concrete cover thickness of 122.5 mm. It has been proved that this model gives good predictions with the experimental results of RC specimens up to 90-mm cover thickness.

7. Future work

The proposed model is developed from the data of FEMs with four reinforcement bars. Then it has been improved for specimens with several bars. However, the effect of several tensile reinforcement layers is not considered for this model. This is a parameter of the Japanese code model, and when the highest overestimated case of the proposed model is considered (case 15 in Table 4 has two layers of tensile reinforcements respective to each face), the necessity of studying this parameter is apparent.

The parameter 'n', which is the number of reinforcements respective to the specimen face, is introduced to make the proposed model more applicable to general beams. However, this parameter makes it difficult to use this model for RC slabs. Therefore, future research is required to make this model more applicable to RC slabs.

Developing a mean crack spacing model is the first step to develop the maximum crack spacing model. Widely used 'maximum crack spacing models' have been developed by multiplying the mean 'crack spacing model' with a factor that represents the ratio of maximum to mean crack spacing. EC2 and MC2010 consider this ratio to be 1.7. By considering the results of several recent axial tensile experiments, Naotunna et al. (2020a) identified that this ratio varies between 1.2 and 1.7. However, Broms and Lutz (1965) and Beeby and Scott (2005) considered this parameter to be 2. Therefore, the next step is to decide on a suitable ratio for the maximum to mean crack spacing and develop an equation for 'maximum crack spacing'.

This study has been conducted by using FEM simulations. Aghajanzadeh et al. (2019), has modeled the concrete fracture process by combining both smeared crack approach with extended finite element (XFEM) method. Therefore, improved simulation models can be developed using XFEM to predict the crack spacings in RC specimens.

Acknowledgment

The authors would like to thank Dr Dobromil Pryl from Cervenka Consulting, for the variety of support given during the numerical simulations.

Conflict of interest

The authors declare no conflict of interest.

Data availability statement

The data that support the findings of this study are available from the corresponding author upon reasonable request.

References

- FIB. (2013). fib Model Code 2010 for concrete structures. In *Structural Concrete*.
- ACI. (1995). *Aci Committee 318: Building Code Requirements for Structural Concrete:(ACI 318-95); and Commentary (ACI 318R-95)*.
- Al-Fayadh, S. (2001). *Cracking behaviour of reinforced concrete tensile members*. Retrieved from Lulea, Sweden:
- Balazs, G. L. (1993). Cracking analysis based on slip and bond stresses. *Materials Journal*, 90(4), 340-348.
- Barre, F., Bisch, P., Chauvel, D., Cortade, J., Coste, J.-F., Dubois, J.-P., . . . Mazars, J. (2016). *Control of cracking in reinforced concrete structures: Research project CEOS. fr*. Great Britain and the United States: John Wiley & Sons.
- Bažant, Z. P., & Oh, B. H. (1983). Spacing of cracks in reinforced concrete. *Journal of structural Engineering*, 109(9), 2066-2085.
- Beconcini, M. L., Croce, P., & Formichi, P. (2008). *Influence of bond-slip on the behaviour of reinforced concrete beam to column joints*. Paper presented at the Proceedings of International fib Symposium "Taylor Made Concrete Structures: New Solutions for our Society", Amsterdam.
- Beeby, A. (2001). Crack control provisions in the new eurocode for the design of concrete structures. *ACI Special Publication*, 204, 57-84.
- Beeby, A., & Scott, R. (2005). Cracking and deformation of axially reinforced members subjected to pure tension. *Magazine of concrete research.*, 57(10), 611-621.
- Beeby, A. W. (2004). The influence of the parameter ϕ/ρ eff on crack widths. *Structural Concrete*, 5(2), 71-83.
- Bernardi, P., Michelini, E., Minelli, F., & Tiberti, G. (2016). Experimental and numerical study on cracking process in RC and R/FRC ties. *Materials and structures*, 49(1-2), 261-277.
- Borges, J. F. (1965). *Cracking and deformability of reinforced concrete beams*: Laboratório Nacional de Engenharia Civil.
- Braam, C. R. (1992). *Control of crack width in deep reinforced concrete beams*. (PhD). Technische Universiteit Delft, Meinema, Hippolytusbuurt 4, Delft, The Netherlands.
- Broms, B. B. (1965). Crack width and crack spacing in reinforced concrete members. *ACI Journal Proceedings*, 62(10), 1237-1256.
- Broms, B. B., & Lutz, L. A. (1965). *Effects of arrangement of reinforcement on crack width and spacing of reinforced concrete members*. Paper presented at the ACI Journal Proceedings.
- BS. (1985). BS 8110: Part 1, Structural use of concrete—code of practice for design and construction. In. London UK.

- CEB-FIP. (1978). CEB-FIP Model code for concrete structures. In *CEB Bulletin d'Information* (pp. 124–125). Paris, France: Comité Euro-International du Béton.
- CEB-FIP. (2010). *fib Bulletin No. 52: Structural Concrete Textbook on behaviour, design and performance, Second edition Volume 2: Basis of design* (Vol. 52). Lausanne, Switzerland: fib.
- CEB. (1985). CEB design manual on cracking and deformations. In: École Polytechnique Fédérale de Lausanne.
- CEN. (2004). EN 1992-1-1 Eurocode 2: Design of concrete structures - Part 1–1: General rules and rules for buildings In: European Committee for Standardization.
- Červenka, J., Červenka, V., & Laserna, S. (2018). On crack band model in finite element analysis of concrete fracture in engineering practice. *Engineering Fracture Mechanics*, *197*, 27-47.
- Červenka, J., & Papanikolaou, V. K. (2008). Three dimensional combined fracture–plastic material model for concrete. *International journal of plasticity*, *24*(12), 2192-2220.
- Cervenka, V., Cervenka, J., & Pukl, R. (2002). ATENA—A tool for engineering analysis of fracture in concrete. *Sadhana*, *27*(4), 485-492.
- Cervenka, V., Jendele, L., & Cervenka, J. (2015). *ATENA program documentation part 1 theory* (Vol. 231). Prague: Cervinka Consulting.
- Cervenka, V., Cervenka, J., Pukl, R. A. & Sajdlova, T. E. (2016) Prediction of shear failure of large beams based on fracture mechanics. In International Conference on Fracture Mechanics of Concrete and Concrete Structures 2016 May (pp. 1-8).
- Ciampi, V., Eligehausen, R., Bertero, V. V., & Popov, E. P. (1981). *Analytical model for deformed bar bond under generalized excitations*. Retrieved from Delft, Zürich.
- Cope, R., Rao, P., Clark, L., & Norris, P. (1980). Modelling of reinforced concrete behaviour for finite element analyses of bridge slabs. Numerical methods for nonlinear problems I. In. New York: Taylor & Francis.
- Dahmani, L., Khennane, A., & Kaci, S. (2010). Crack identification in reinforced concrete beams using ANSYS software. *Strength of materials*, *42*(2), 232-240.
- De Borst, R. (1986). *Non-linear analysis of frictional materials*. (PhD). Delft University of Technology, Netherlands.
- de Saint-Venant, M. (1856). *Mémoire sur la torsion des prismes: avec des considérations sur leur flexion ainsi que sur l'équilibre intérieur des solides élastiques en général: et des formules pratiques pour le calcul de leur résistance à divers efforts s' exerçant simultanément*: Imprimerie Nationale.
- Debernardi, P. G., Guiglia, M., & Taliano, M. (2013). Effect of secondary cracks for cracking analysis of reinforced concrete tie. *ACI Materials Journal*, *110*(2), 207.
- Debernardi, P. G., & Taliano, M. (2016). An improvement to Eurocode 2 and fib Model Code 2010 methods for calculating crack width in RC structures. *Structural Concrete*, *17*(3), 365-376.
- Doerr, K. (1978). *Bond behavior of ribbed reinforcement under transversal pressure*. Paper presented at the Nonlinear behavior of reinforced concrete structures; contributions to IASS symposium.
- Eligehausen, R., Popov, E. P., & Bertero, V. V. (1982). Local bond stress-slip relationships of deformed bars under generalized excitations. *Proceedings of the 7th European Conference on Earthquake Engineering*, *4*, 69-80.
- Fields, K., & Bischoff, P. H. (2004). Tension stiffening and cracking of high-strength reinforced concrete tension members. *ACI Structural Journal*, *101*(4), 447-456.

- García, R., & Caldentey, A. P. (2020). Influence of type of loading (tension or bending) on cracking behaviour of reinforced concrete elements. Experimental study. *Engineering Structures*, 222, 111134.
- Gribniak, V., & Rimkus, A. (2016). Vilnius, Lithuania Patent No. State Patent Bureau of the Republic of Lithuania.
- Gribniak, V., Rimkus, A., Caldentey, A. P., & Sokolov, A. (2020). Cracking of concrete prisms reinforced with multiple bars in tension—the cover effect. *Engineering Structures*, 220, 110979.
- Gupta, A. K., & Akbar, H. (1984). Cracking in reinforced concrete analysis. *Journal of structural Engineering*, 110(8), 1735-1746.
- Hofstetter, G., & Meschke, G. (2011). *Numerical modeling of concrete cracking* (Vol. 532). Bochum, Germany: Springer Science & Business Media.
- Hordijk, D. (1991). *Local approach to fatigue of concrete* (Ph. D. Thesis). (PhD). Delft University, Netherlands.
- Hossin, M., & Marzouk, H. (2008). Crack spacing for offshore structures. *Canadian Journal of Civil Engineering*, 35(12), 1446-1454.
- Ingraffea, A. R., & Saouma, V. (1985). Numerical modeling of discrete crack propagation in reinforced and plain concrete. In *Fracture mechanics of concrete: structural application and numerical calculation* (pp. 171-225). Dordrecht: Springer.
- Jaccoud, J.-P. (1987). *Armature minimale pour le contrôle de la fissuration des structures en béton*. EPFL, Lausanne.
- Janovic, K. (1986). Zur Rissbildung im Stahlbeton-und Spannbetonbau. *Betonwerk und Fertigteil-Technik*, 52(12), 815-823.
- JSCE. (2007). Standard Specifications for Concrete Structures-2007 "Design". In *Japanese Society of Civil Engineers Guidelines for Concrete*.
- Lorrain, M., Maurel, O., & Seffo, M. (1998). Cracking behavior of reinforced high-strength concrete tension ties. *ACI Structural Journal*, 95(5), 626-635.
- Mang, C., Jason, L., & Davenne, L. (2016). Crack opening estimate in reinforced concrete walls using a steel-concrete bond model. *Archives of civil and mechanical engineering*, 16, 422-436.
- McLeod, C. H. (2013). *Investigation into cracking in reinforced concrete water-retaining structures*. (Masters). Stellenbosch University, Stellenbosch.
- Mesureur, B., Bernardi, S., & Rivillon, P. (1999). Study of high-strength concretes reinforced with high-strength reinforcement: Study of bonding laws and cracking in static system. *Materials Journal*, 96(4), 491-499.
- Naotunna, C. N., S.M. Samindi, M. K. S., & Fosså, K. T. (2020a). Experimental and theoretical behavior of crack spacing of specimens subjected to axial tension and bending. *Structural Concrete*, 1-18. doi:<https://doi.org/10.1002/suco.201900587>
- Naotunna, C. N., S.M. Samindi, M. K. S., & Fosså, K. T. (2020b). *Identification of the influence of concrete cover thickness and ϕ/ρ parameter on crack spacing*. Paper presented at the XV International Conference on Durability of Building Materials and Components, Barcelona, Spain.
- Ngo, D., & Scordelis, A. C. (1967). Finite element analysis of reinforced concrete beams. *ACI Journal Proceedings*, 64(3), 152-163.
- Nilson, A. H. (1968). Nonlinear analysis of reinforced concrete by the finite element method. *ACI Journal Proceedings*, 65(9), 757-766.
- NPRA. (2009). Statens Vegvesen, Håndbok N400 Bruprosjektering. In. Oslo: Vegdirektoratet.

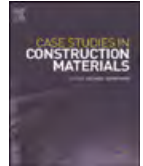
- Oh, B. H., & Kang, Y. J. (1987). New formulas for maximum crack width and crack spacing in reinforced concrete flexural members. *ACI Structural Journal*, 84(2), 103-112.
- Pérez Caldentey, A., Corres Peiretti, H., Peset Iribarren, J., & Giraldo Soto, A. (2013). Cracking of RC members revisited: influence of cover, ϕ/ps , e_f and stirrup spacing—an experimental and theoretical study. *Structural Concrete*, 14(1), 69-78.
- Pryl, D., & Cervenka, J. (2013). *ATENA Program Documentation, Part 11: Troubleshooting Manual*. Prague: Cervenka Consulting Ltd.
- Rashid, Y. R. (1968). Ultimate strength analysis of prestressed concrete pressure vessels. *Nuclear engineering and design*, 7(4), 334-344.
- RILEM. (1983). Bond test for reinforcement steel. 2. In *Pull-out test*.
- Rimkus, A., Cervenka, V., Gribniak, V., & Cervenka, J. (2020). Uncertainty of the smeared crack model applied to RC beams. *Engineering Fracture Mechanics*, 107088.
- Rimkus, A., & Gribniak, V. (2017). Experimental investigation of cracking and deformations of concrete ties reinforced with multiple bars. *Construction and Building Materials*, 148, 49-61.
- Rots, J. G., & Blaauwendraad, J. (1989). Crack models for concrete, discrete or smeared? Fixed, multi-directional or rotating? *Heron*, 34.
- Saliger, R. (1936). *High grade steel in reinforced concrete*. Paper presented at the Second Congress of IABSE, Berlin-Munich.
- Tammo, K., & Thelandersson, S. (2006). Crack opening near reinforcement bars in concrete structures. *Structural Concrete*, 7(4), 137-143.
- Tammo, K., & Thelandersson, S. (2009). Crack behavior near reinforcing bars in concrete structures. *ACI Structural Journal*, 106(3), 259.
- Tan, R. (2019). *Consistent crack width calculation methods for reinforced concrete elements subjected to 1D and 2D stress states A mixed experimental, numerical and analytical approach*. (PhD). Norwegian University of Science and Technology, Trondheim, Norway.
- Tan, R., Eileraas, K., Opkvitne, O., Žirgulis, G., Hendriks, M. A., Geiker, M., . . . Kanstad, T. (2018). Experimental and theoretical investigation of crack width calculation methods for RC ties. *Structural Concrete*, 1436–1447.
- Tan, R., Hendriks, M. A., Geiker, M., & Kanstad, T. (2020). A numerical investigation of the cracking behaviour of reinforced-concrete tie elements. *Magazine of Concrete Research*, 72(3), 109-121.
- Theriault, M., & Benmokrane, B. (1998). Effects of FRP reinforcement ratio and concrete strength on flexural behavior of concrete beams. *Journal of composites for construction*, 2(1), 7-16.
- Vos, E. (1983). *Influence of loading rate and radial pressure on bond in reinforced concrete. A numerical and experimental approach*. Delft University, Delft, Netherlands.
- Wang, J.-J., Tao, M.-X., & Nie, X. (2017). Fracture energy-based model for average crack spacing of reinforced concrete considering size effect and concrete strength variation. *Construction and Building Materials*, 148, 398-410.
- Wu, H., & Gilbert, R. (2009). Modeling short-term tension stiffening in reinforced concrete prisms using a continuum-based finite element model. *Engineering Structures*, 31(10), 2380-2391.
- Yannopoulos, P. (1989). Variation of concrete crack widths through the concrete cover to reinforcement. *Magazine of Concrete Research*, 41(147), 63-68

Paper 7: Experimental investigation of crack width variation along the concrete cover depth in reinforced concrete specimens with ribbed bars and smooth bars.

Naotunna, C.N., Samarakoon, S.M.S.M.K., and Fosså, K.T. (2021)

In: *The Journal of Case Studies in Construction Materials*.

DOI: [10.1016/j.cscm.2021.e00593](https://doi.org/10.1016/j.cscm.2021.e00593).



Experimental investigation of crack width variation along the concrete cover depth in reinforced concrete specimens with ribbed bars and smooth bars

Chavin N. Naotunna^{*}, S.M. Samindi M.K. Samarakoon, Kjell T. Fosså

Department of Mechanical and Structural Engineering and Material Science, Faculty of Science and Technology, University of Stavanger, Stavanger, Norway

ARTICLE INFO

Keywords:

RC specimens
Crack width
Crack pattern
Concrete cover depth
Ribbed reinforcement
Smooth bars
Experiments
Epoxy injection

ABSTRACT

Crack width variation along the concrete cover depth has been studied from the past for better understanding of the cracking phenomenon in reinforced concrete (RC) structures. Previous studies have highlighted important cracking behaviors like internal cracks. The behavior of 'slip' between the reinforcement and concrete and the formation of a nonuniform crack face along the concrete cover depth are still not very clearly understood. An experimental program has been conducted to study the crack width variation along the cover depth in concrete prisms reinforced with a central ribbed bar and smooth bar, by varying the concrete cover depths. Both in specimens with smooth bars (SS) and specimens with ribbed bars (SR), crack width is larger on the concrete surface than at the steel bar surface. The crack width at the reinforcement is considerably larger in the SS than in the SR. In the SR, the crack width increases from the reinforcement along the cover depth bi-linearly, while, in the SS, it increases linearly. For the SR, the aforementioned behavior is due to the occurrence of internal cracks. In the SS, significant slip has been identified at the reinforcement and concrete interface, whereas negligible slip has been observed in the SR. A surface crack width calculation model has been developed, considering both the strain difference and the effect of the nonuniform crack face along the concrete cover depth. Its predictions showed good agreement with the experimental surface crack widths from the conducted study and with the results from the experiments in literature.

1. Introduction

To understand the cracking behavior of RC specimens, crack width variation along the concrete cover depth has been studied and documented since 1968 [1]. Previous studies on crack width variation along the concrete cover depth have mainly employed two different experimental methods. One method is to measure the relative displacement between reinforcement and concrete at the ends of the specimen, using linear variable differential transducer (LVDT) gauges. Such studies are reported in Tammo and Thelandersson [2,3] and in Yannopoulos [4]. However, several difficulties can be identified in this type of experiment. The 'cone failure' that can occur at the end of the specimen can cause readings which are taken at the vicinity of the reinforcement to be misguided. On the other hand, it is difficult to measure the deformation just above the reinforcement, since placing the LVDT gauges consumes several

^{*} Corresponding author.

E-mail address: chavin.guruge@uis.no (C.N. Naotunna).

millimeters. For example, Tammo and Thelandersson [2,3] and Yannopoulos [4] obtained readings closest to the reinforcement at 4.5 mm and 2.2 mm away from the reinforcement, respectively. The other method is to seal the crack with a high strength (to avoid shrinking after load is released) and low viscosity (to penetrate through fine gaps) epoxy and observe the crack after cutting the RC specimen. Husain and Ferguson [1], Beeby [5] and Borosnyoi and Snobli [6] observed the crack width variation along the concrete cover depth by using this method, which involves several cost- and time-consuming activities, compared to the first method. It is necessary to keep the load in the cracked specimen until the injected epoxy is hardened (e.g., 20 h for the conducted test reported in this article). Other than that, it is necessary to cut the RC specimens to obtain the internal crack width measurements. However, the results from both these methods have concluded that, in RC specimens with ribbed bars, the crack width at the reinforcement is significantly smaller than the crack width at the concrete surface.

Analytical [7] or semi-analytical crack width calculation models, as in Eurocode 2 [8] or Model Code 2010 [9], predict the crack width as the extension occurring due to the strain difference between reinforcement and concrete between two cracks. Therefore, the crack width is obtained by multiplying the crack spacing with mean strain difference between reinforcement and concrete. Such models assume a constant crack opening through the cover depth [6,9]. However, according to the results of the aforementioned experiments, a contradictory observation is given that the crack width at the reinforcement is significantly smaller than the crack width at the concrete surface. Borosnyoi and Snobli [6] and Caldentey et al. [10] have explained that this small crack width at the reinforcement is due to the presence of Goto cracks (internal cracks/secondary cracks) [11]. These secondary cracks are mostly formed at the locations of ribs within the concrete, at the vicinity of primary cracks [11–13]. As the concrete strain is accumulated at these secondary cracks, it can be considered that the width of the primary cracks at the reinforcement is reduced. Due to the strong bond between the ribbed reinforcement and concrete, the strain incompatibility which occurs after cracking would accumulate in these internal cracks [14].

Crack spacing calculation models are mainly based on three theories: namely, bond-slip theory, no-slip theory and combined theory. The bond-slip theory assumes that a bond failure would occur at a crack, and therefore a slip would occur between reinforcement and concrete [15]. It is assumed that the slip is at its maximum at the crack and, after a certain distance from the crack, the slip would be zero. By considering the force equilibrium between a crack and a zero-slip location, a crack spacing model can be developed [16]. However, the no-slip theory assumes a perfect bond between reinforcement and concrete, with no possibility of a slip occurring between reinforcement and concrete at the crack [17]. The combined theory [18] considers the effect of slip, as well as the no-slip effect. A detailed study of these theories is mentioned in Naotunna et al. [19]. It is important to identify the crack theory (bond-slip theory or no-slip theory) which is more relevant to the actual cracking behavior of RC specimens, because the crack spacing governing parameters can be identified based on these theories.

Tammo and Thelandersson [3] mentioned that concrete cover depth has two main influences on the crack width. The first influence of concrete cover depth is the effect on the crack spacing. The second is the formation of a non-uniform crack face, which causes the surface crack width to increase. In other words, this effect is discussed as shear lag in several pieces of literature [6,20,21]. The shear-lag effect is not considered or mentioned in any of the widely used crack width calculation models. According to the literature, the effect of shear lag is dominant with the increase in concrete cover depth [6,20,21]. In the first complete draft of Model Code 2010, a formula was given which included the shear-lag effect. However, the effect of shear lag is not taken into account in the final draft, and the proposed crack width calculation model is valid up to a cover depth of 75 mm. It is vital to use large concrete cover depths when structures are located in an adverse environment and have a very long service life (200 or 300 years) [22,23]. According to the Norwegian Public Road Administration guidelines [24], the current requirement for concrete cover depth can be as large as 120 mm. Furthermore, the Hafstrsjord bridge in Norway has been constructed with a 90-mm cover depth [25]. Therefore, it is important to improve the existing crack width calculation models to be used in specimens with large concrete cover depths.

This study of crack width variation along the concrete cover depth has several objectives. One of the main ones is to study the behavior of slip, as the widely used crack spacing models have been developed based on theories considering slip. Another objective is to identify shear-lag effect, which can be more important in specimens with large concrete cover depths. Therefore, an experimental program has been conducted to observe the crack width variation along the concrete cover depth. Concrete prisms reinforced with a



Fig. 1. Reinforcement bars surfaces of 16 mm bars used for the SS and SR.

central bar were tested with different concrete cover depths, varying from 20 mm to 80 mm. For the better understanding and comparison of the cracking behaviors, specimens were cast with both ribbed bars and smooth bars. Then, in order to check whether the surface crack width has an additional effect, other than from the strain difference within the crack spacings, a crack width calculation model was developed by considering the effect of shear lag. A comparison has been made between the experimental surface crack widths and the predictions from the proposed crack widths.

2. Materials and methods

Concrete prisms, with a length of 650 mm and reinforced with a central reinforcing bar, were cast. The central reinforcing bars were 16 mm in diameter, and both ribbed and smooth surface bars were selected. The selected reinforcement bars are shown in Fig. 1. Table 1 gives the specimen sizes and concrete cover depths used in the experiment. For each case, two identical specimens were cast and tested. For the ribbed bar, the reinforcement grade was B500NC according to the NS 3576-3 standard [26], with a characteristic yield strength ($f_{yk, 0.05}$) of 500 MPa and Young's modulus of 200 GPa. For the SS, the smooth bar grade was S355J2 according to the NS 10219 standard [27], with a characteristic yield strength ($f_{yk, 0.05}$) of 355 MPa and Young's modulus of 210 GPa. The focus of the study is to observe the crack width variation along the concrete cover depth. When the crack widths are large, it would make the epoxy injection process to seal the crack easier. For the SS with a cover depth of 20 mm, the crack widths are relatively small due to the lower cover depth. Therefore, in order to ease the epoxy injection, the specimens were loaded up to 400 MPa, after confirming that the yield strength of smooth bars in three samples are above 400 MPa with an average of 425 MPa. The studies conducted by Cadoni et al. [28] and Duarte et al. [29] had obtained the same conclusion from their experiments, that the yield strength of S355J2 steel is above 400 MPa.

The mean $\phi 150 \times 300$ mm cylindrical compressive strength of concrete after 28 days of casting was 24.3 MPa, and the mean splitting tensile strength was 2.2 MPa. The top surface of the specimens (the surface which has not touched the formwork) was covered with polyethene on the first day, just after casting. The specimens were unmolded on the next day, and necessary measures were taken to cure the specimens, to control shrinkage. Next, the specimens were tested in axial tension with a monotonical loading rate of 0.5 mm/min, using the 'Instron 5985' machine. The specimens with ribbed reinforcement were loaded up to 100 kN, and the specimens with smooth bars were loaded up to 80 kN, to prevent yielding of the reinforcement. The specimens were loaded up to this value, since the crack sealing process would be easier with larger crack widths. This would make the crack sealant epoxy penetrate completely throughout the crack. The specimens were axially loaded with a 0.5-mm/min rate, after reaching the aforementioned maximum value, the load was kept constant for 24 h. This time lapse was required for the sealing of the crack, including the hardening of the crack sealant epoxy.

The loading procedure is allocated by the managing software of the loading machine, 'Instron Bluehill'. As mentioned, the specimens were loaded by means of the displacement control method. Then the displacement was kept constant for 24 h, until the applied load had reached the aforementioned threshold values (100 kN for specimens with ribbed bars and 80 kN for specimens with smooth bars). During this period, the cracks that appeared were sealed with a crack sealant epoxy. Sealing a crack was conducted in two main steps. In the first step, surface packers were pasted in the four faces, and the surfaces of the cracks on the four sides of the specimen were sealed with a rapidly hardening epoxy. Surface packers of the necessary size were produced by 3D printing in the University of Stavanger laboratory. Fig. 2 shows the surface packers used for the experimental program. By conducting a trial test, an epoxy named 'super lima' was selected as the surface sealant rapid hardening epoxy. After applying this surface sealant epoxy, nearly 45 minutes were required for hardening. Fig. 3 shows the loaded RC tie with the fixed surface packers. After hardening the surface sealant epoxy with the surface packers, the second step begins. The cracked concrete particles and the dust inside the crack were removed with a portable air pump. Then the cracks were sealed by injecting a crack sealant epoxy through the surface packers. For this purpose, an epoxy named 'Mapepoxy BI-IMP', which has been certified by the European concrete repair standard EN 1504-5 [30], was used. This epoxy consisted of two components, which had to be mixed in the prescribed ratio (component A: component B, mixing ratio 7:3). The mixture had a viscosity of nearly 110 mPa.s; after hardening, it had a compressive strength of 65 MPa. The next important property of this product is that it polymerizes without shrinkage. After mixing, the epoxy was injected into the cracks with a syringe through the previously fixed surface packers. Fig. 4 shows how the epoxy was inserted into the crack. From the trial test, it was identified that it takes around 20 h to harden the epoxy. After hardening the epoxy, the load in the testing apparatus was released and specimens were removed from the apparatus. No difference could be observed in the surface crack widths before and after releasing the applied load. Therefore, it can be assumed that, after the cracks had been sealed using this method, the crack widths did not change after the load was released. When cutting the sealed specimen, the epoxy could be confirmed to have penetrated throughout the whole crack.

Table 1
Sizes of the specimens and concrete cover depths.

Specimen	Concrete cover (mm)	Specimen width \times height \times length (mm \times mm \times mm)
Specimens with ribbed bars (SR)	40	96 \times 96 \times 650
	60	136 \times 136 \times 650
	80	176 \times 176 \times 650
Specimens with smooth bars (SS)	20	56 \times 56 \times 650
	40	96 \times 96 \times 650
	60	136 \times 136 \times 650

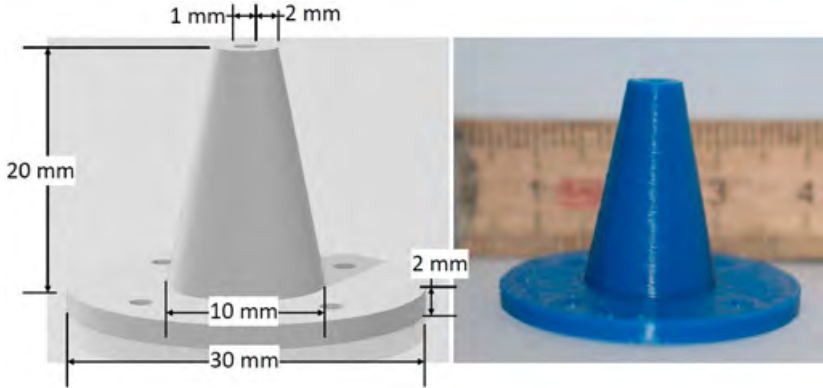


Fig. 2. Surface packers used to inject epoxy.



Fig. 3. Loaded RC tie after fixing the surface packers.

The next step was to cut the specimens, to observe how the crack width varied throughout the concrete cover depth. Specimens were cut, using a ‘Diamant-Cedima’ concrete cutter, with a cutting blade thickness of nearly 1 mm. Fig. 5 shows how the specimens were cut to observe the crack width propagation along the concrete cover. One sealed crack consists of eight cutting surfaces. Since there are several numbers of cutting surfaces, each cutting surface was coded. Fig. 6 shows the codes used to identify the cutting surface. In the specimens with ribbed bars (SR), two cracks per specimen from r.40.1 and r.40.2 and one crack per specimen from r.60.1, r.60.2 and r.80.2 were sealed and observed. In the specimens with smooth bars (SS), two cracks per specimen from r.20.1 and r.20.2 and one crack per specimen from s.40.1 and s.40.2 were sealed and observed. No cracks could be generated from s.60.1 and s.60.2, since the specimen lengths were not sufficient to generate cracks.



Fig. 4. Inserting the Mapepoxy BI-IMP to the crack through the surface packers.

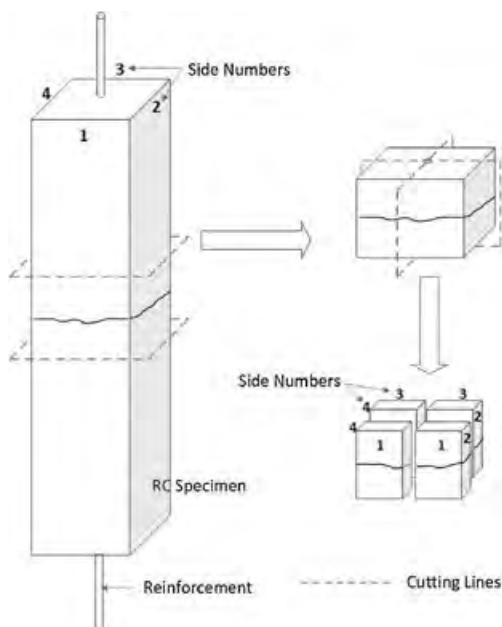


Fig. 5. Cutting of RC ties to observe the crack width propagation along the concrete cover.

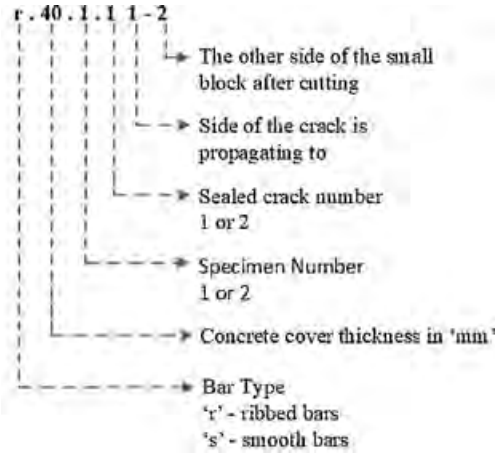


Fig. 6. Identification of the cutting surface.

3. Crack width measurements

In each cutting surface, crack widths were measured along the concrete cover depth at 2-mm intervals. The measurements were obtained using two methods. In the first method, initially photos of the cracks in the cutting surface were taken from a digital single-lens reflex camera (DSLR camera) with a 50-mm macro lens. Then the images were analyzed, using a computer program named 'Fiji ImageJ' [31]. The measurements taken from this method have an accuracy of 1 μm. From this program, the images can be calibrated and meshed with 2-mm grid sizes, to ease the measuring of crack widths. Fig. 7(a) shows an example of how the crack width measurements were taken with the Fiji ImageJ software. These obtained measurements were further confirmed by comparison with the measurements obtained with the 'Dino-Lite' digital microscope [32]. Fig. 7(b) shows the crack width measurements with the Dino-Lite digital microscope. As can be observed in Fig. 7(b), since the field of view of the Dino-Lite digital microscope is small, it is mainly used to confirm the measurements obtained from the first method. The measurements obtained from the Dino-Lite digital microscope have an accuracy of 1 μm.

As shown in Figs. 5 and 6, cutting surfaces 1-2 and 1-4 of a crack denote the same crack position, which is propagating to side 1. Similarly, cutting faces 2-1/2-3, 3-2/3-4 and 4-1/4-3 of a crack denote the same positions which are propagating to sides 2, 3 and 4, respectively. However, slight changes can be observed between the crack width measurements, even obtaining the readings of two cutting surfaces of the same crack, which are propagating to the same side (e.g., crack width measurements of cutting surfaces 1-2 and 1-4). One reason for this is that the position of the measurement point (2-mm steps) is not similar in both cutting faces. The other reason can be the 1-mm width of the cutting blade, which is wearing from the specimen while cutting. For example, there is a 1-mm gap between cutting faces 1-2 and 1-4 of a sealed crack. For this reason, the crack width measurements of two cutting faces which are propagating to the same side have been averaged (e.g., cutting phases 1-2 and 1-4 are averaged to represent the crack propagation to side 1). Therefore, as shown in Figs. 8 and 9, each sealed crack has four sets of readings, corresponding to each side of the face. In some

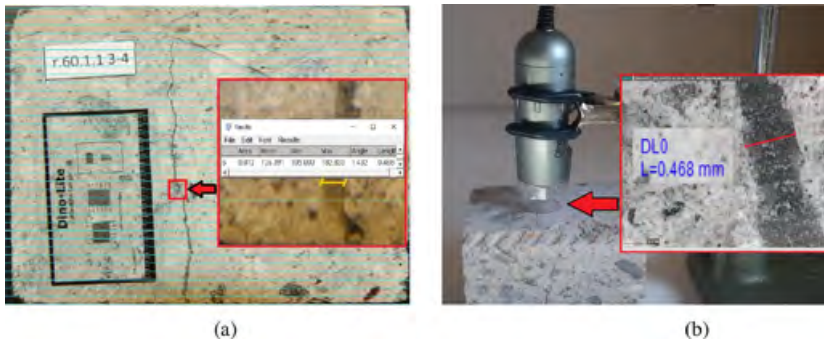


Fig. 7. Measurement of crack widths using (a) DSLR camera photo with Fiji ImageJ program interface; (b) Direct observation with Dino-Lite digital microscope.

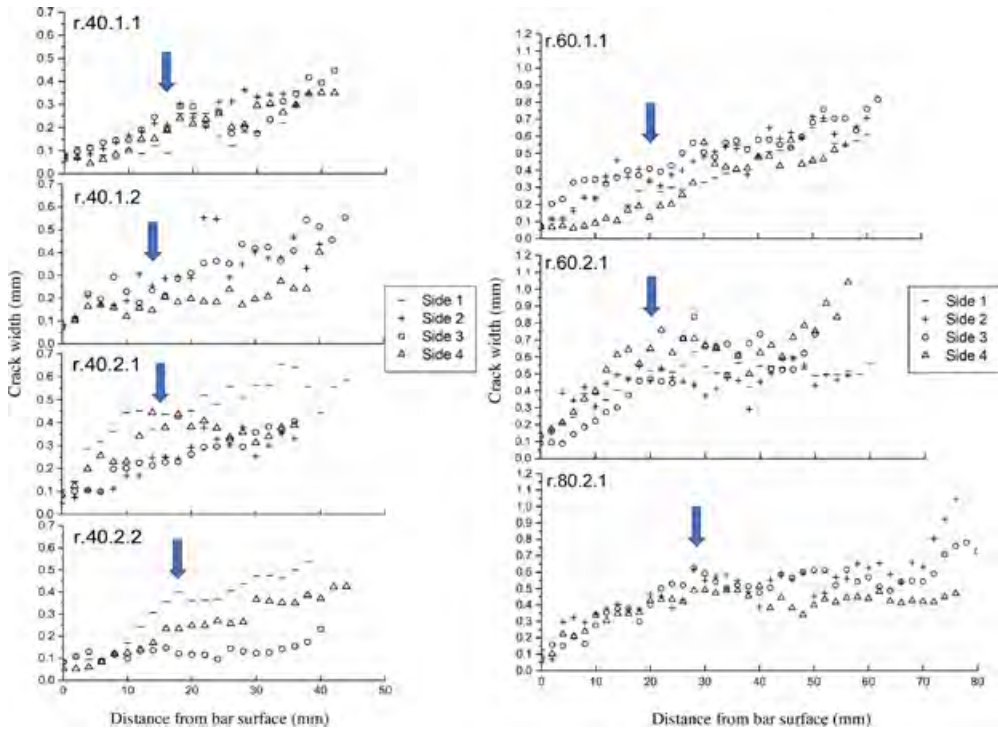


Fig. 8. Crack width variation along the concrete cover depth of the specimens with ribbed reinforcement.

cases, when more than one crack was generated in the tested specimen, two cracks were sealed. For example, in specimens r.40.1, r.40.2, s.20.1 and s.20.2, two cracks were sealed. Furthermore, specimen r.80.1 could not generate a crack, even when it was loaded up to the threshold value. Therefore, in the r.80.2 specimen, a 20-mm deep notch was made in side 1. Since the focus is to observe the crack width propagation along the concrete cover depth, crack width measurements were obtained from sides 2, 3 and 4. Further, in the specimens with smooth bars s.60.1 and s.60.2, no cracks could be obtained, as the specimens were not long enough. As can be observed in Figs. 8 and 9, it was not possible to obtain some measurements. In most of such cases, the specimen had been damaged while cutting. When the specimens are damaged, it is not possible to obtain a flat surface to measure the crack widths. This issue occurred more frequently in specimens with 20-mm cover depth. The measured crack width readings along the concrete cover depths are given in the Table A in attachment (Supplementary material).

4. Crack width variation along the concrete cover depth

Fig. 8 shows the crack width variation along the concrete cover depth of the SR. According to this figure, the crack width at the reinforcement is significantly smaller than the crack widths at the concrete surface. This observation is similar to the findings in the previously mentioned experiments reported in Tammo and Thelandersson [2,3], Yannopoulos [4], Husain and Ferguson [1], Beeby [5] and Borosnyoi and Snobli [6]. The crack width at the reinforcement is independent of the concrete cover depth, and, in all the cases, the crack width at the reinforcement showed a value below 0.1 mm. When considering the cases in Fig. 8, the rate of change in crack width, up to 10–30 mm from the reinforcement, is considerably higher than the rate of change in crack width beyond this limit. Borosnyoi and Snobli [6] and Caldentey et al. [10] have mentioned that this is due to the internal cracks (Goto cracks [11]), which are propagating up to this 10- to 30-mm limit. This limit of these internal cracks has been identified experimentally in Goto [11], and later considered in several studies like those of Debernardi et al. [12] and Debernardi and Taliano [13].

When primary cracks are developing, the tensile strain in reinforcement exceeds the ultimate tensile strain of the surrounding concrete [14]. This strain difference between the steel and concrete is referred to as ‘strain incompatibility’ in Beeby et al. [14]. Due to the good bond between the ribbed reinforcement and surrounding concrete, this strain incompatibility has been accumulated in the internal cracks. Further, it has been observed that this gradient changing point (arrow mark shown in Fig. 8) is moving slightly away from the reinforcement, with the increase in concrete cover depth. For specimens with 40-mm cover, this location lies within 10–18 mm; for specimens with 60-mm cover, this location lies around 20 mm; and, for specimens with 80-mm cover, this position lies around

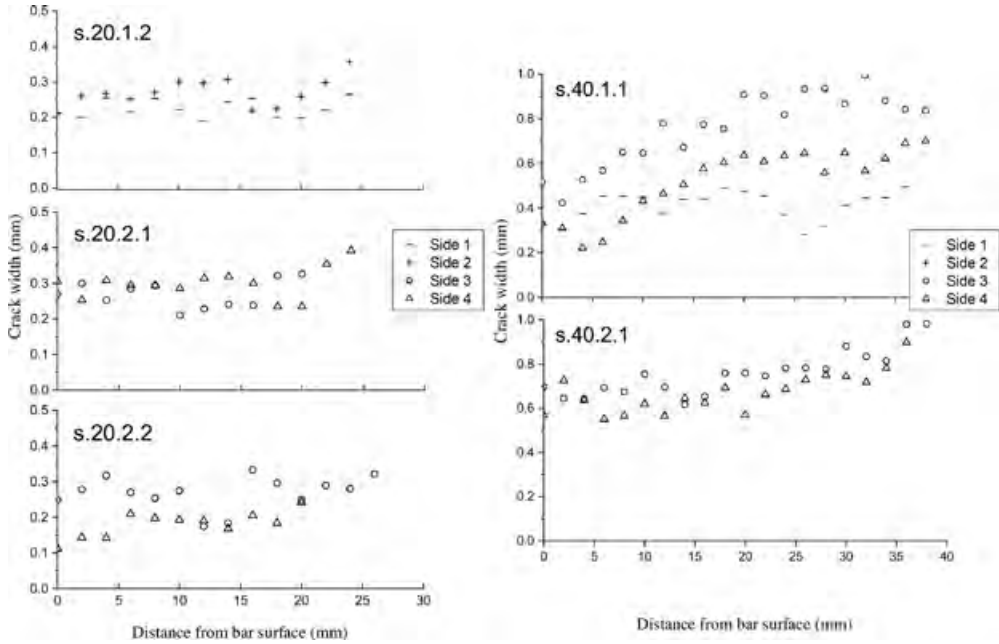


Fig. 9. Crack width variation along the concrete cover depth of specimens with smooth bars.

30 mm from the reinforcement. According to this discussion, which assumes that the internal cracks stop at the gradient changing point, the crack width at this gradient changing point can be considered to be due to the strain difference between reinforcement and concrete. When RC specimens are loaded from the reinforcement, the concrete within the cover depth (concrete between the bar and the concrete surface) is subjected to shear stress [20]. This shear stress would cause a shear deformation, which is referred to as 'shear lag'. According to Fig. 8, the crack widths are still increasing with a low gradient after the gradient changing point, and this can be considered to be due to this shear lag effect, as specified in several items of the literature [3,20,21].

The crack width variation of the SS differs considerably from that of the SR (Fig. 9). As shown in Fig. 9, crack width at the reinforcement is considerably larger than in the SR. The ratio between the surface crack widths and the crack width at the reinforcement of the SS varies from 1.2 to 2.2. On the other hand, unlike in the specimens with ribbed reinforcement, the rate of change in crack width at distance from the reinforcement is nearly the same throughout the concrete cover. Fig. 10 shows the actual view of crack width variation along the concrete cover depth of SR and SS of the specimens with 40-mm concrete cover depth. This implies that, as there are no ribs in the smooth bars, internal cracks are not dominant in these specimens (since the Goto cracks have initiated from the reinforcement ribs). Furthermore, as the crack width at the reinforcement is larger than in SR and the bond between smooth bars and surrounding concrete is comparatively low, it can be assumed that the strain incompatibility is accumulated by the occurrence of a slip [14].

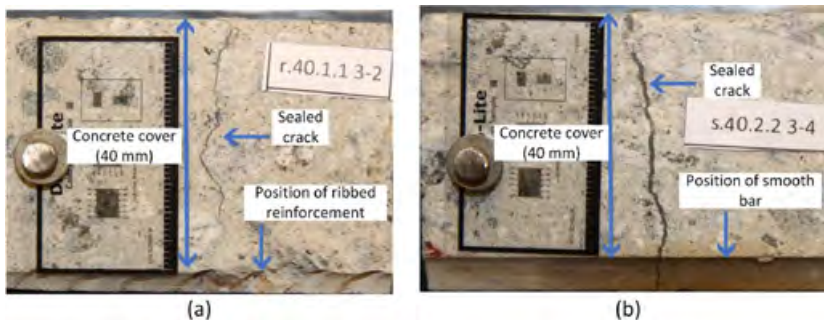


Fig. 10. Crack width variation along the concrete cover depth in specimens with 40-mm cover (a) with ribbed bars; (b) with smooth bars.

Crack width is considered to be the extension accumulated due to the strain difference between reinforcement and concrete within the crack spacing [7]. When considering the surface crack widths, the SS have larger surface crack widths than the SR (consider the specimens with 40-mm cover). This could be due to the SS consisting of larger crack spacings than the SR. Fig. 11 shows the crack position of each face of the tested RC specimens. It can be observed that the crack spacings of the specimens with smooth bars are larger than the crack spacings of the specimens with ribbed bars. This can be compared with the crack spacing results of the specimens with 40-mm cover depth. However, before comparing the crack spacing values in the SS and SR, it is important to mention that the loading conditions are not same in both type of specimens (Bar types are different and SS have loaded up to 80 kN and SR have loaded up to 100 kN). In the two specimens with ribbed bars, three cracks were obtained, while, in the two specimens with smooth bars, only a single crack was obtained. Similar behavior could be seen in the experiments reported in Randic and Markota [33]. Furthermore, many of the widely used crack width calculation models, like Eurocode 2 [8] and the JSCE model [34], predict that specimens with smooth bars

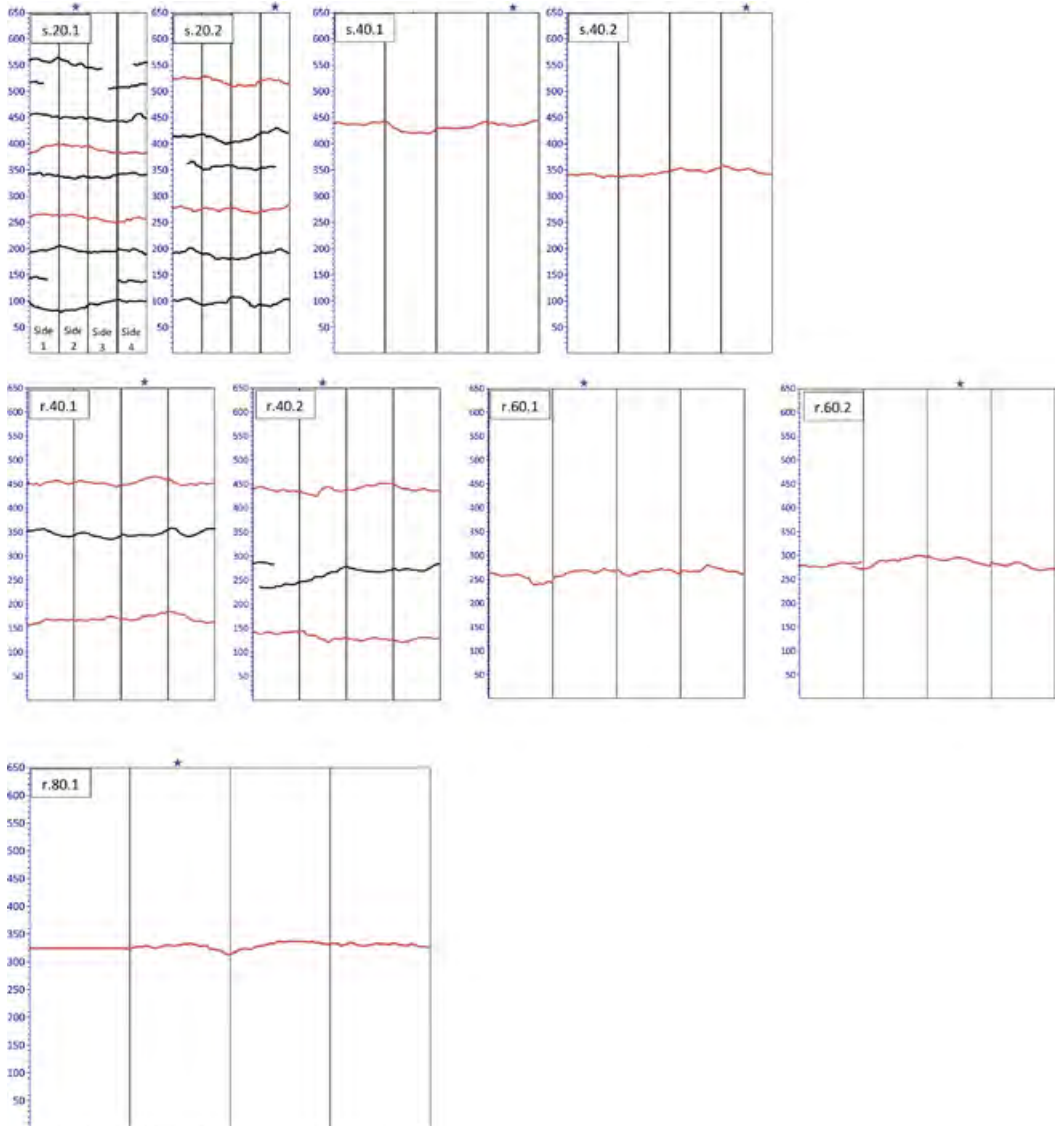


Fig. 11. Crack positions of the four sides of the tested RC specimens (sealed cracks are marked in red) and “star mark” shows the top surface during the concrete pouring.

have larger crack spacings than specimens with ribbed bars. Jakubovskis et al. [35] and Garcia et al. [36] studied the effect of concrete pouring directions on the cracking behavior. The top surface during the concrete pouring is marked with a * (star mark), in Fig. 11. Since it is not a primary objective of this study, the number of top surface during the concrete pouring differs in each specimen. When considering the results in Figs. 8, 9 and 11, no considerable influence could be observed on the crack widths and crack positions in the top surface during the concrete pouring of these tested specimens.

5. Applicability of bond-slip and no-slip theories for SR and SS

The no-slip theory assumes that the reinforcement and surrounding concrete are bonded perfectly [17]. Therefore, at the crack or at the ends of RC specimens, the stress is transferred to the surrounding concrete, according to St. Venant's principle [37]. According to St. Venant's principle, the next crack would occur after a certain distance ($k \times c$ distance; where 'k' is a constant and 'c' is concrete cover depth), when the stress in the concrete specimen is distributed uniformly along the cross section (Fig. 12(a)). The no-slip theory can explain the internal cracks, as they occur due to the strain incompatibility between reinforcement and concrete. When the surrounding concrete is strongly bonded with the reinforcement, and when applied tensile strain in the reinforcement exceeds the ultimate tensile strain of concrete, internal cracks can occur. On the other hand, if a slip occurs, internal cracks cannot be dominant.

According to Fig. 8, in almost all the SR, the crack widths at the reinforcement bar surface are less than 0.1 mm. This means that a negligible amount of slip has occurred between reinforcement and concrete. Therefore, in the SR, as a considerable amount of slip could not be observed, it can be assumed that the cracking behavior of the SR is more related to the no-slip theory. These negligible slip values in SR are evidently proved in the experimental studies focused on the bond-slip behaviors of axial tensile RC specimens, in Beconcini et al. [38], Doerr [39] and Bado et al. [40].

The bond-slip theory considers that a slip would occur between reinforcement and concrete. It is assumed that the slip is at its maximum at the crack and, after a certain distance, would become zero. Due to the slip, the concrete strain is not similar to the reinforcement strain. When the slip becomes zero, concrete strain is considered similar to the reinforcement strain [15] (Fig. 12(b)). When considering the force equilibrium for the concrete block between the crack and the zero slip section, the transfer length can be identified [12,16]. When considering the crack width variation of the SS, the crack width at the reinforcement bar surface is larger than that of the SR (Figs. 9 and 10(b)). The ratio of the average crack widths at the reinforcement bar surface of the SS to the SR is 3.8. Therefore, it can be assumed that a considerable amount of slip has occurred between reinforcement and concrete in the SS, comparatively to the SR. Further, unlike in the SR, during the experiment, a slip was clearly visible at the end of loaded specimens with smooth bars. Fig. 13 shows the reinforcement-concrete interface at the end of the SS, when it is loaded and unloaded. Therefore, the SS can be considered to behave more similarly to the bond-slip theory.

The importance of identifying the crack theory (no-slip or bond-slip theory) which is most related to the actual cracking behavior is that the crack spacing governing parameters are theoretically identified based on this theory. According to the no-slip theory, the governing crack spacing parameters can be considered to be concrete cover depth and the distance between tensile reinforcement (thickness of the surrounding concrete of the tensile reinforcement) [17,41]. For bond-slip theory, the governing crack spacing parameter can be considered to be bond parameter (ϕ/ρ ; where ' ϕ ' is the bar diameter and ' ρ ' is the ratio between reinforcement area and concrete area) [12,16].

The conducted experimental program is focused on examining the crack widths. To study the crack spacings, relatively large specimen lengths are required, to avoid the end-effect encountered in short-length RC specimens [42]. However, Table 2 shows experimentally identified average crack spacings and the Eurocode 2 predictions. For this comparison, r.40, r.60, s.20 and s.40 specimens have been considered, since, in the r.80 specimens, the cracks have been induced. The experimental average crack spacing has been identified, by considering the specimen length and the number of cracks. The ratio of maximum crack spacing to average crack spacing considered in Eurocode 2 is 1.7 [43]. This ratio has been considered, to obtain the Eurocode 2 predicted average crack spacing values. For the SR and SS, the ' k_1 ' parameters in the Eurocode 2 crack spacing model have been considered as 0.8 and 1.6, respectively. In the specimens used for this study, when the concrete cover depth increases, the value of the bond parameter (ϕ/ρ) also

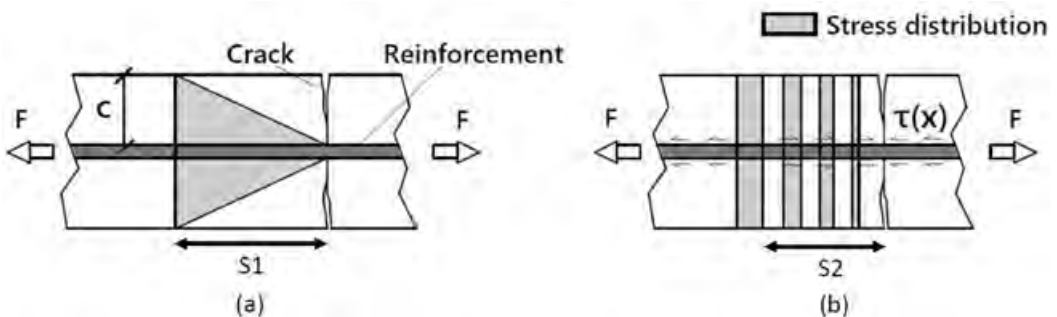


Fig. 12. Stress distribution in the concrete of a RC tie subjected to tension, according to (a) no-slip approach; (b) bond-slip approach.

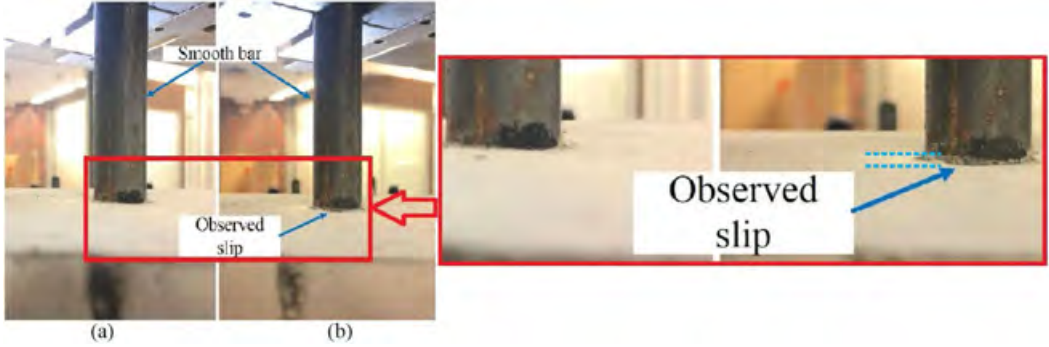


Fig. 13. Reinforcement-concrete interface at the end of the s.40.1 specimen (a) before; (b) after loading.

Table 2
Experimental and Eurocode 2 predicted average crack spacings.

Specimen	Cover (mm)	ϕ/ρ (mm)	Number of cracks	Average crack spacing (mm)	Eurocode 2 average crack spacing (mm)
r.40	40	733.8	3	163	227
r.60	60	1472.6	1	325	415
s.20	20	249.7	6	93	140
s.40	40	733.8	1	325	374

increases. As shown in Table 2, both experimental and Eurocode 2 predicted average crack spacings increased with the increase in concrete cover depth.

6. Derivation of the surface crack width calculation model for SR

Crack width calculation models, including Eurocode 2 and Model Code 2010, consider crack width as the extension accumulated due to the strain difference between reinforcement and concrete within the crack spacing [44]. Such models calculate the crack width by multiplying the crack spacing with the mean strain difference between reinforcement and concrete. These models assume a constant crack opening through the cover depth [6,9]. This implies that this method does not consider the effect of shear lag, which was discussed in Section 4. To identify whether the shear lag has an influence on surface crack width, the results of the conducted experimental program can be used. For this study, the crack spacing values can be directly obtained from the cracked specimens shown

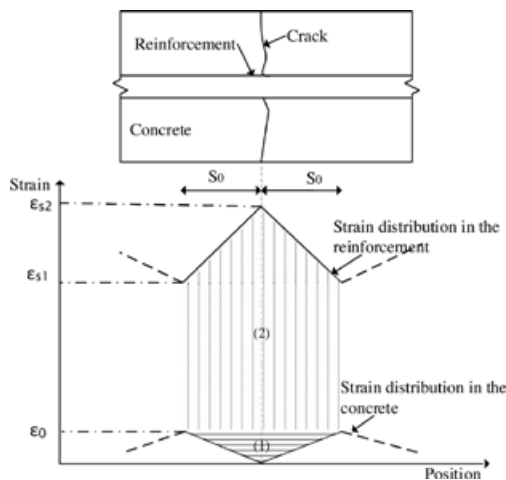


Fig. 14. Strain distribution of reinforcement and concrete at a crack in the stabilized cracking stage.

in Fig. 11. Strain difference between reinforcement and concrete can be calculated from Eurocode 2 or Model Code 2010 models. However, such models consist of several empirical coefficients. Therefore, for the purpose of this study, a crack width calculation model has been derived for the stabilized cracking stage, considering the results of previous experiments studying the strain in cracked RC specimens.

Beeby and Scott [14,45] have identified that the strain variation in steel on both sides of cracks is linear. In this series of experiments mentioned in Beeby and Scott [14,45], the steel strains were measured in 10-mm gaps. Since a linear strain distribution has been observed in every tested specimen, this behavior is considered in the development of the crack width calculation model. Similar observations (linear strain distribution in reinforcement on both sides of the crack) could be observed in the experiments in Kankam [46] and Imai et al. [47]. Since the reinforcement strain is linear, by considering the force equilibrium, it has been assumed that the concrete strain is also linear on both sides of cracks [14]. Fig. 14 shows the strain distribution of reinforcement and concrete in both sides of a crack at the stabilized cracking stage, based on the results of the aforementioned literature.

Crack width can be considered the summation of the contraction of concrete and the extension of the reinforcement in the region of the crack [14]. For the purpose of calculation, it is assumed that the region of the crack is the region within S_0 distance from both sides of the crack (Fig. 14).

Extension of the reinforcement within the region of the crack, due to the increment of reinforcement stress (Area (2) in Fig. 14):

$$\Delta_s = \frac{1}{2} [(\epsilon_{s1} - \epsilon_0) + (\epsilon_{s2} - \epsilon_0)] S_0 \cdot 2 \quad (1)$$

where ϵ_{s1} is the steel strain at the end of the transfer length in the stabilized cracking stage, ϵ_{s2} is the steel strain at the crack in the stabilized cracking stage, ϵ_0 is the concrete strain at the end of the transfer length, and S_0 is the transfer length.

Theoretically, ϵ_{s1} can be written as ' $\epsilon_{s2} - \alpha_e \epsilon_0$ ' [48]. Therefore, Eq. (1) can be rearranged as:

$$\Delta_s = [2 \cdot \epsilon_{s2} - \epsilon_0 (2 + \alpha_e)] S_0 \quad (2)$$

where α_e is the modular ratio.

Contraction of the concrete (Δ_c) within the region of the crack due to the reduction of concrete stress in the crack (Area (1) in Fig. 14):

$$\Delta_c = S_0 \epsilon_0 \quad (3)$$

Crack width (w) is the summation of the contraction of concrete (Δ_c) and the extension of the reinforcement (Δ_s) in the region of the crack. Therefore, crack width at the stabilized cracking stage can be obtained from:

$$w = \Delta_c + \Delta_s \quad (4)$$

$$w = 2 S_0 \left[\epsilon_{s2} - \frac{\epsilon_0 (1 + \alpha_e)}{2} \right] \quad (5)$$

where ' $2 S_0$ ' can be considered the crack spacing and α_e is the modular ratio.

$$\epsilon_{s2} = \sigma_s / E_s \quad (5-a)$$

where σ_s is the steel stress, and E_s is the Young's modulus of steel.

$$\epsilon_0 = \frac{N_{cr}}{E_c A_{c,eff} (1 + \alpha_e \rho)} \quad (5-b)$$

where N_{cr} is the cracking force, E_c is the Young's modulus of concrete, $A_{c,eff}$ is the effective concrete area, α_e is the modular ratio, and ρ is the ratio of reinforcement area to effective concrete area.

$$N_{cr} = \sigma_{sr} A_s \quad (5-c)$$

where σ_{sr} is the maximum steel stress at cracking force, and A_s is the reinforcement area.

When the cracked section is considered, concrete cannot resist tensile stresses at the crack (neglecting the cracked concrete softening effect). Therefore, the maximum steel stress at the cracking force can be obtained from the following equation:

$$\sigma_{sr} = f_{ctm} \left(A_{c,eff} / A_s \right) + f_{ctm} \left(E_s / E_c \right) \quad (5-d)$$

where f_{ctm} is the mean tensile strength of concrete.

Eq. (5-d) can be rearranged according to Eq. (5-e), with familiar notations as represented in Model code 2010.

$$\sigma_{sr} = \frac{f_{ctm}}{\rho_{p,eff}} (1 + \alpha_e \rho_{p,eff}) \quad (5-e)$$

where $\rho_{p,eff}$ is the effective reinforcement ratio ($\rho_{p,eff} = A_s/A_{c,eff}$)

Eq. (5) is developed assuming the concrete strain is distributed uniformly along the concrete cover depth. However, in order to obtain the surface crack widths, the effect of shear-lag can be considered [3,14,21]. Therefore, in order to quantify this effect, the calculation model given in the 'fib Model Code first complete draft' [21] has been considered, following a modification, as shown in Eq. (6).

$$w = \left[S + 1.7 (c - a) \right] \left[\varepsilon_{s2} - \frac{\varepsilon_0(1 + \alpha_e)}{2} \right] \quad (6)$$

where 'S' is the crack spacing value, 'c' is the concrete cover depth and 'a' is the distance to the gradient changing point from the reinforcement surface (15, 20 and 30 mm for cover depths of 40, 60 and 80 mm, respectively).

It has introduced a parameter, 'a', which is the distance to the gradient changing point from the reinforcement surface, instead of the 25-mm value which was originally in the model. According to this study, the distance, 'a', depends on the concrete cover depth (the arrow marked in Fig. 8). For calculation purposes, in specimens with cover depths of 40, 60 and 80 mm, the 'a' value can be considered as 15, 20 and 30 mm, respectively. For those cases where the concrete cover depth is other than the mentioned values, the 'a' distance can be considered by interpolation.

7. Comparison of surface crack widths with the calculated crack widths of the SR

The surface crack width is considered the crack width at the concrete surface over the axis of the reinforcement [9]. As shown in Fig. 5, the crack width variation along the concrete cover depth is also considered along the reinforcement axis. Therefore, the measured surface crack width can be obtained as the concrete surface readings from Fig. 8. For better comparison, the crack width predictions of both Eurocode 2 and Model Code 2010 have been considered. Crack width calculation models in these two codes calculate the crack width by multiplying the crack spacing with the mean strain difference. At the stabilized cracking stage, both standards calculate the mean strain difference according to Eq. (7) (without considering the shrinkage strain term mentioned in Model Code 2010). Both the mean strain difference in Eq. (7) and the strain term in Eqs. (5) and (6) can be calculated with the data from the experiment. For the calculated crack widths from Eq. (8), the parameter k_t , which is used for the duration of load, is considered as 0.4, as suggested by both codes for short-term loadings.

$$\varepsilon_{sm} - \varepsilon_{cm} = \frac{\sigma_s - k_t \left(f_{ct,eff} / \rho_{p,eff} \right) (1 + \alpha_e \rho_{p,eff})}{E_s} \quad (7)$$

$$w = S \cdot (\varepsilon_{sm} - \varepsilon_{cm}) \quad (8)$$

where ' $\varepsilon_{sm} - \varepsilon_{cm}$ ' is the mean strain difference between reinforcement and concrete; ' $f_{ct,eff}$ ' is the mean tensile strength of concrete, effective at the time when the test is performed; ' $\rho_{p,eff}$ ' is the effective reinforcement ratio; 'w' is the crack width; and 's' is the crack spacing value.

The experimental surface crack widths have been compared with the predictions of Eqs. (5), (6) and (8). Eqs. (5) and (8) are developed without considering the effect of shear lag, while Eq. (6) considers the effect of shear lag. For this study, the necessary crack spacing values required for the crack width prediction equations were directly obtained by measuring from the cracked specimens (refer to Fig. 9). The crack spacing value corresponding to a specific crack can be considered as the summation of halves of crack distances to both sides of the cracks (refer to Fig. 14) [44]. It is important to mention that this method of measuring crack spacing is considered only for this study, where the focus is on the width of a specific crack. On the other hand, when developing the basic crack width calculation models in Eurocode 2 and Model Code 2010, the cracking region of a specific crack was identified, based on this method [44]. In the SR, a total number of seven cracks were sealed. For each crack, the surface crack widths and crack positions corresponding to the four surfaces are different from each other (refer to Figs. 8 and 9). Therefore, altogether there is data on 28 (7×4) surface crack widths. However, as some specimens were damaged while cutting the specimens, 26 surface crack widths were considered for this comparison.

The graph of the measured surface crack width versus calculated crack width, using Eqs. (5) and (8), is shown in Fig. 15. The code models are used to verify whether the values of the theoretical crack widths are safe or not, and their purpose is to not to predict exact crack widths. The predictions of Eq. (8) have been considered for this study only as a reference to the predictions of Eq. (5). The mean absolute error (the average of the absolute difference between the measured value and the predicted value) of the predictions from Eqs. (5) and (8) is 0.12 and 0.11, respectively. Fig. 15 shows that there are several calculated crack widths consistent with a constant value. This is because, according to the aforementioned crack spacing measuring method, the crack spacing values of the specimens with a single crack will be 325 mm for every case (half of the specimen size). This figure shows that, for the majority of cases, the predictions of Eqs. (5) and (8) are underestimating the experimental surface crack width. From a total of 26 cases, 16 cases from both Eqs. (5) and (8) predict underestimated crack width values, compared to the experimental observations. Eq. (8) is the crack width prediction model in Eurocode 2. Therefore, in order to predict conservative crack width values, this can be the reason that the Eurocode 2 crack spacing model predicts significantly overestimated crack spacing values to calculate the crack widths [19,48,49]. Fig. 16 shows the comparison of the measured surface crack widths with the predictions from Eq. (6), which have considered the effect of shear lag. The mean absolute error of the predictions from Eq. (6) is 0.15. According to these Eq. (6) predictions, only 8 out of 26 cases underestimate the

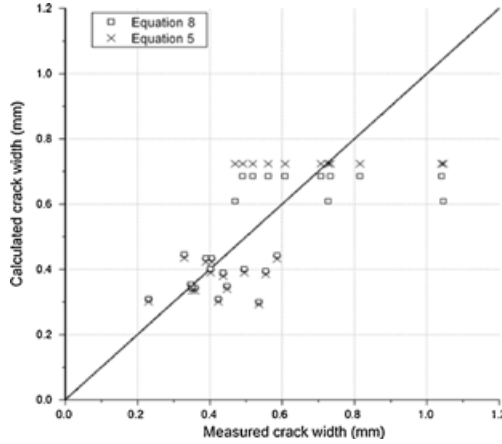


Fig. 15. Comparison of the measured surface crack widths of SR with Eqs. (5) and (8) (models do not consider the shear lag effect).

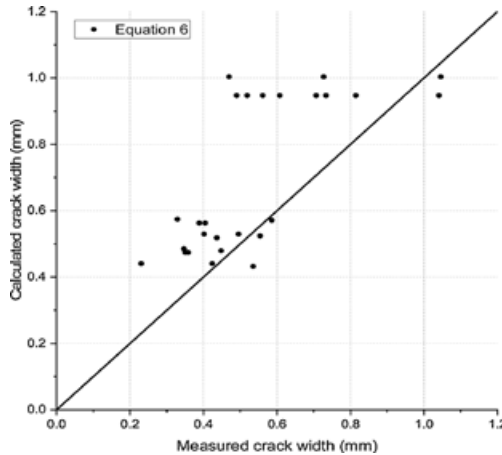


Fig. 16. Comparison of the measured surface crack widths of SR with Eq. (6) (equation with the shear lag effect).

experimental crack widths.

This comparison shows the importance of the effect of shear lag on the surface crack widths. However, this study has been conducted for a limited number of results. Therefore, this must be further verified with RC specimens with different types of concrete, sizes of bar diameters and cover depths. For that, exact crack widths (not average values), and the exact crack spacing values correspond to each crack, are required. Therefore, despite the large body of literature available on crack width studies, the experimental program mentioned in Gribniak et al. [50], which includes the aforementioned data, was selected. Further, it is important to mention that this ‘a’ value is obtained only for short-length concrete prisms reinforced with a central bar (the conducted experimental program). However, these values must be further verified with the practical size members, due to the identified end-effect encountered in short-length RC specimens [42]. To verify the proposed equations, the results in Gribniak et al. [50] were compared with the predictions of the proposed models (Eqs. (5) and (6)). For this comparison, the results of 1210-mm-long RC specimens with identical 150 × 150-mm cross sections were considered. The cover depths of the selected RC specimens were 30 mm, 40 mm and 50 mm, and they were reinforced with four 10-mm bars. Depending on the availability of data, the results of 3, 2 and 2 specimens, with concrete cover depths of 50 mm, 40 mm and 30 mm, respectively, were selected. In this experiment, the crack widths were measured at the concrete surface above the positions of the reinforcement bars. For this study, the crack widths when the applied load is 100.4 K N were considered. These crack widths were measured using the DIC (Digital Image Correlation) system. As specified in Section 6, the ‘a’ values have considered to be 17.5 mm, 15 mm and 12.5 mm for specimens with 50 mm, 40 mm and 30 mm covers, respectively. Fig. 17 shows the graph of the measured surface crack width versus calculated crack width, using Eqs. (5) and (6), and the Table B in

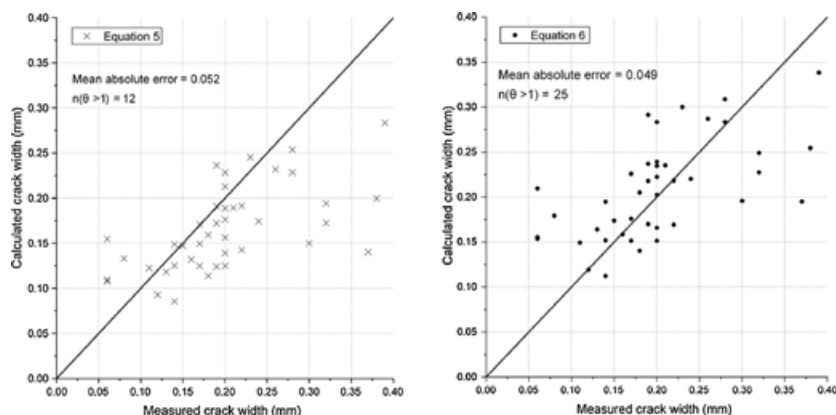


Fig. 17. Comparison of the measured surface crack widths in Gribniak et al [50] with the predictions from (a) Eq. (5), and (b) Eq. (6). ' $n(\theta > 1)$ ' notation represent the number of conservative predictions out of 42 cases, where calculated crack width is greater than the measured crack width.

Attachment (Supplementary material) shows the calculated and measured crack width values. The mean absolute error values for the predictions of Eqs. (5) and (6) are 0.052 and 0.049, respectively. When considering the 42 cases mentioned in Fig. 17, according to the Eq. (5), only 12 cases and according to the Eq. (6), 25 cases give conservative predictions (calculated crack width is greater than the measured crack width). Therefore, the proposed Eq. (6), which includes the shear-lag effect, gives better agreement with the experimental results than Eq. (5) does.

8. Conclusions

To understand the cracking behavior of RC specimens, crack width variation along the concrete cover depth was studied. An experimental program was conducted, using concrete prisms reinforced with a central bar. RC specimens were cast with both ribbed bars and smooth bars and with different concrete cover depths. These specimens were tested by applying an axial tensile load, and the generated cracks were sealed by using a high-strength and low viscosity epoxy. After the epoxy had hardened, the cracked specimens were cut and the crack width propagation along the concrete cover depth observed. The following observations and understandings can be obtained from this study.

- When considering the specimens with ribbed bars (SR), the ratios of average surface crack width to average crack width, at the reinforcement surface in each crack, vary from five to ten. The crack width difference between reinforcement bar surface and concrete surface can be identified as being due to the internal cracks which occur at the vicinity of the primary crack. In SR, the strain incompatibility that occurs between reinforcement and concrete accumulates in the internal cracks. On the other hand, a negligible amount of slip could be observed between these ribbed bars and the surrounding concrete. This can be considered to be due to the good bond between the ribbed reinforcement and the concrete.
- In the specimens with smooth bars (SS), the average crack width at the reinforcement bar surface is almost four times larger than that of the specimens with ribbed bars. Since the crack width varies linearly along the cover depth, it is assumed that there is no significant effect from the internal cracks. Therefore, in the SS, it can be assumed that the strain incompatibility between reinforcement and concrete has been accommodated by a slip.
- It is important to identify the crack theory (bond-slip theory or no-slip theory) which is more relevant to the actual cracking behavior of the RC specimens, because the crack spacing governing parameters are mainly identified based on these theories. Therefore, according to the experimental results, it can be stated that specimens with ribbed bars behave in a way more related to the no-slip theory, while specimens with smooth bars behave in a manner more related to the bond-slip theory.
- A surface crack width prediction model has been developed by considering the effect of shear lag. A simple study has been conducted, to compare the experimental surface crack widths with the predictions from models which do consider and do not consider the shear-lag effect. The end results have shown that the shear-lag effect has an influence on surface crack widths. However, this study must be further verified for RC specimens with different concrete properties, bar diameters and concrete covers.

Declaration of Competing Interest

The authors report no declarations of interest.

Acknowledgements

The authors would like to thank the University of Stavanger laboratory manager, John C. Grønli, laboratory engineers, Jarle Berge and Samdar Kakay, as well as Johannes Jensen, for the variety of support given during the experiments. Further, the authors would like to thank Mikko Mathias, Espen Sorensen and William Bui for the variety of support given regarding specimen preparations.

Appendix A. Supplementary data

Supplementary material related to this article can be found, in the online version, at doi:<https://doi.org/10.1016/j.cscm.2021.e00593>.

References

- [1] S.I. Husain, P.M. Ferguson, Flexural Crack Width at the Bars in Reinforced Concrete Beams, The University of Texas at Austin, Center for Highway research, 1968.
- [2] K. Tammo, S. Thelandersson, Crack opening near reinforcement bars in concrete structures, *Struct. Concr.* 7 (4) (2006) 137–143.
- [3] K. Tammo, S. Thelandersson, Crack behavior near reinforcing bars in concrete structures, *ACI Struct. J.* 106 (3) (2009) 259.
- [4] P. Yannopoulos, Variation of concrete crack widths through the concrete cover to reinforcement, *Mag. Concr. Res.* 41 (147) (1989) 63–68.
- [5] A. Beeby, Corrosion of reinforcing steel in concrete and its relation to cracking, *Struct. Eng.* 56 (3) (1978).
- [6] A. Borosnyói, I. Snóhli, Crack width variation within the concrete cover of reinforced concrete members, *Építőanyag* 62 (3) (2010) 70–74.
- [7] G.L. Balazs, Cracking analysis based on slip and bond stresses, *Mater. J.* 90 (4) (1993) 340–348.
- [8] E.C.f. Standardization, Eurocode 2: Design of Concrete Structures - Part 1–1: General Rules and Rules for Buildings, 2004.
- [9] I.F.f.S.C. (fib), fib Model Code for concrete structures. *Structural Concrete*, 2010.
- [10] A. Pérez Caldentey, H. Corres Peiretti, J. Peset Iribarren, A. Giraldo Soto, Cracking of RC members revisited: influence of cover, ϕ/ψ , e_f and stirrup spacing—an experimental and theoretical study, *Struct. Concr.* 14 (1) (2013) 69–78.
- [11] Y. Goto, Cracks formed in concrete around deformed tension bars, *ACI J. Proc.* (1971) 244–251.
- [12] P.G. Debernardi, M. Guiglia, M. Taliano, Effect of secondary cracks for cracking analysis of reinforced concrete tie, *ACI Mater. J.* 110 (2) (2013) 207.
- [13] P.G. Debernardi, M. Taliano, An improvement to Eurocode 2 and fib Model Code 2010 methods for calculating crack width in RC structures, *Struct. Concr.* 17 (3) (2016) 365–376.
- [14] A. Beeby, R. Scott, Cracking and deformation of axially reinforced members subjected to pure tension, *Mag. Concr. Res.* 57 (10) (2005) 611–621.
- [15] R. Saliger, High grade steel in reinforced concrete, Second Congress of IABSE (1936). IABSE Publications, Berlin-Munich.
- [16] M. Taliano, Cracking analysis of concrete tie reinforced with two diameter bars accounting for the effect of secondary cracks, *Eng. Struct.* 144 (2017) 107–119.
- [17] B.B. Broms, Crack width and crack spacing in reinforced concrete members, *ACI J. Proc.* 62 (10) (1965) 1237–1256.
- [18] J.F. Borges, Cracking and Deformability of Reinforced Concrete Beams, Laboratório Nacional de Engenharia Civil, 1965.
- [19] C.N. Naotunna, M.K.S.S.M. Samindi, K.T. Fosså, Experimental and theoretical behavior of crack spacing of specimens subjected to axial tension and bending, *Struct. Concr.* 1 (18) (2020).
- [20] A. Beeby, C. Alander, E. Giuriani, G. Plizzari, S. Pantazopoulou, The influence of the parameter ϕ/ρ_{eff} on crack widths. Author's reply and discussion, *Struct. Concr.* (Lond. 1999) 6 (4) (2005) 155–165.
- [21] J. Walraven, Model Code 2010-First Complete Draft-Volume 2: Model Code, fib Fédération Internationale du Béton, 2010.
- [22] G. Marques, M. Kiousmarsi, Need for further development in service life modelling of concrete structures in chloride environment, *Procedia Eng.* 171 (2017) 549–556.
- [23] J. Connal, M. Berndt, Sustainable bridges: 300 year design life for Second Gateway Bridge, in: 7th Austroads Bridge Conference, Auckland, New Zealand, 2009.
- [24] NPRA, Statens Vegvesen. Håndbok N400 Bruprosjektering, Vegdirektoratet, Oslo, 2009.
- [25] M. Basteskár, M. Engen, T. Kanstad, K.T. Fosså, A review of literature and code requirements for the crack width limitations for design of concrete structures in serviceability limit states, *Structural Concrete* 20 (2) (2019) 678–688.
- [26] NS, EN 3576-3, Steel for the Reinforcement of Concrete - Dimensions and Properties - Part 3: Ribbed Steel B500NC, 2012.
- [27] NS, EN 10219, Cold Formed Welded Structural Hollow Sections of Non-Alloy and Fine Grain Steels, Part 1: Technical Delivery Conditions, 2006.
- [28] E. Cadoni, D. Forni, R. Gioletta, L. Kruszka, Tensile and compressive behaviour of S355 mild steel in a wide range of strain rates, *Eur. Phys. J. Spec. Top.* 227 (1) (2018) 29–43.
- [29] A. Duarte, B. Silva, N. Silvestre, J. De Brito, E. Júlio, J. Castro, Tests and design of short steel tubes filled with rubberised concrete, *Eng. Struct.* 112 (2016) 274–286.
- [30] EN, 1504-5: 2004, Products and Systems for the Protection and Repair of Concrete Structures, Definitions, Requirements, Quality Control and Evaluation of Conformity. Concrete Injection, 2004.
- [31] C.A. Schneider, W.S. Rasband, K.W. Eliceiri, NIH Image to ImageJ: 25 years of Image analysis, *Nat. Methods* 9 (7) (2012) 671–675.
- [32] M. Amato, F. Lupo, G. Bitella, R. Bochicchio, M.A. Aziz, G. Celano, A high quality low-cost digital microscope minirhizotron system, *Comput. Electron. Agric.* 80 (2012) 50–53.
- [33] J. Radnić, L. Markota, Experimental verification of engineering procedures for calculation of crack width in concrete elements, *Int. J. Eng. Model.* 16 (2003) 63–69.
- [34] JSCE, Standard Specifications for Concrete Structures-2007, Design, Japanese Society of Civil Engineers Guidelines for Concrete, 2007.
- [35] R. Jakubovskis, R. Kupliauskas, A. Rimkus, V. Gribniak, Application of FE approach to deformation analysis of RC elements under direct tension, *Struct. Eng. Mech.* 68 (3) (2018) 345–358.
- [36] R. García, A.P. Caldentey, Influence of type of loading (tension or bending) on cracking behaviour of reinforced concrete elements. Experimental study, *Eng. Struct.* 222 (2020), 111134.
- [37] M. de Saint-Venant, Mémoire sur la torsion des prismes: avec des considérations sur leur flexion ainsi que sur l'équilibre intérieur des solides élastiques en général: et des formules pratiques pour le calcul de leur résistance à divers efforts s' exerçant simultanément, Imprimerie National, 1856.
- [38] M.L. Beconcini, P. Croce, P. Formichi, Influence of bond-slip on the behaviour of reinforced concrete beam to column joints, *Proceedings of International fib Symposium* (2008) 19–21. Taylor Made Concrete Structures: New Solutions for our Society, Amsterdam.
- [39] K. Doerr, Bond behavior of ribbed reinforcement under transversal pressure, *Nonlinear Behavior of Reinforced Concrete Structures; Contributions to IASS Symposium* (1978) 3–7.
- [40] M.F. Bado, J.R. Casas, G. Kaklauskas, Distributed Sensing (DOFS) in reinforced concrete members for reinforcement strain monitoring, crack detection and bond-slip calculation, *Eng. Struct.* 226 (2020), 111385.
- [41] B.B. Broms, L.A. Lutz, Effects of arrangement of reinforcement on crack width and spacing of reinforced concrete members, *ACI J. Proc.* (1965) 1395–1410.
- [42] V. Gribniak, A. Rimkus, L. Torres, R. Jakstaite, Deformation analysis of reinforced concrete ties: representative geometry, *Struct. Concr.* 18 (4) (2017) 634–647.

- [43] C. Braam, Control of Crack Width in Deep Reinforced Concrete Beams [Dissertation], Delft University of Technology, Netherlands, 1990.
- [44] A. Beeby, Crack control provisions in the new eurocode for the design of concrete structures, *ACI Spec. Publ.* 204 (2001) 57–84.
- [45] A.W. Beeby, R.H. Scott, Influence of Tension Stiffening on Deflection of Reinforced Concrete Structures: Report of a Concrete Society Concrete Society Technical Report, Camberley, 2003.
- [46] C.K. Kankam, Relationship of bond stress, steel stress, and slip in reinforced concrete, *J. Struct. Eng.* 123 (1) (1997) 79–85.
- [47] M. Imai, R. Nakano, T. Kono, T. Ichinomiya, S. Miura, M. Mure, Crack detection application for fiber reinforced concrete using BOCDA-based optical fiber strain sensor, *J. Struct. Eng.* 136 (8) (2010) 1001–1008.
- [48] R. Tan, K. Eileraas, O. Opkvitne, G. Zirgulis, M.A. Hendriks, M. Geiker, D.E. Brekke, T. Kanstad, Experimental and theoretical investigation of crack width calculation methods for RC ties, *Struct. Concr.* (2018) 1436–1447.
- [49] R. Tan, Consistent Crack Width Calculation Methods for Reinforced Concrete Elements Subjected to 1D and 2D Stress States A Mixed Experimental, Numerical and Analytical Approach, Norwegian University of Science and Technology, Trondheim, Norway, 2019.
- [50] V. Gribniak, A. Rimkus, A.P. Caldentey, A. Sokolov, Cracking of concrete prisms reinforced with multiple bars in tension—the cover effect, *Eng. Struct.* 220 (2020), 110979.

Appendices

Supplementary documents of Paper 7 can be found in the online version at [doi:https://doi.org/10.1016/j.cscm.2021.e00593](https://doi.org/10.1016/j.cscm.2021.e00593).

